JAERI-M
82-008

ANALYSIS OF LOFT SMALL BREAK EXPERIMENT L3-1 WITH THYDE-P CODE (CSNI INTERNATIONAL STANDARD PROBLEM NO. 9 AND THYDE-P SAMPLE CALCULATION RUN 50)

February 1982

Masashi HIRANO, Takashi SHIMIZU* and Yoshiro ASAHI

日本原子力研究所
Japan Atomic Energy Research Institute

JAERI-Mレポートは，日本原子力研究所が不定期に公刊している研究報告書です。
入手の問合わせは，日本原子力研究所技術情報部情報資料課（〒319-11茨城県那珂郡東海村）あて，お申しこしください。なお，このほかに財団法人原子力弘済会資料センター（〒319-11 茨城県那珂郡東海村日本原子力研究所内）で複写による実費頒布をおこなっております。

JAERI-M reports are issued irregularly.
Inquiries about availability of the reports should be addressed to Information Section, Division of Technical Information, Japan Atomic Energy Research Institute, Tokai-mura, Naka-gun, Ibaraki-ken 319-11, Japan.

編集兼発行　日本原子力研究所
印　　刷　㈱高野高速印刷

Analysis of LOFT Small Break Experiment L3-1 with THYDE-P Code

(CSNI International Standard Problem No. 9
and THYDE-P Sample Calculation Run 50)

Masashi HIRANO, Takashi SHIMIZU* and
Yoshiro ASAHI

Division of Reactor Safety Evaluation,
Tokai Research Establishment, JAERI

(Recieved January 30, 1982)

Experiment L3-1 was the first small break loss-of-coolant experiment conducted at the Loss-of-Fluid Test (LOFT) facility with the nuclear core at 48.9±1.0 MW, which is about 98% of the LOFT rated thermal power of 50 MW. The break size was equivalent to a 4-inch pipe rupture, or a 2.5% break, in a commerecial plant, scaled on a break area basis. This experiment was selected as OECD-CSNI International Standard Problem No. 9.

The THYDE-P code is a computer code to analyze both the blowdown and refill-reflood phases of loss-of-coolant accidents (LOCAs) of pressurized water reactors (PWRs) without a change in the models and the methods and is now under verification and modification study. The present calculation was the first verification study applied to a small break LOCA and was performed as Sample Calculation Run 50 which is part of a series of THYDE-P sample calculations. The calculation was carried out from test initiation to 2000 sec after rupture since it was the period of interest in the present work. The discharge coefficient for the Moody correlation was assumed to be 0.8. The overall trend of the experiment was well simulated by THYDE-P.

Keywords : LOFT, Experiment L3-1, Small Break, LOCA, THYDE-P Code, CSNI International Standard Problem No. 9

---

* On leave from Japan Information Survice, Ltd.

THYDE－P コードによる LOFT小破断実験 L 3－1の解析
(CSNI 国際標準問題No.9及び THYDE－P サンプル計算 Run 50)

日本原子力研究所東海研究所安全解析部
平野 雅司・志水 孝司*・朝日 義郎

(1982年1月30日受理)

L 3－1実験は LOFT で行われた最初の小破断冷却材喪失実験で，初期出力48.9±1MWで行われた。これは，LOFT定格熱出力50MWの98%に当る。破断口径は，商用原子炉の4インチ配管破断，又は2.5%破断に相当する。この実験は OECD－CSNI 国際標準問題No.9に指定された。

THYDE－P コードは，加圧水型軽水炉（PWR）の冷却材喪失事故（LOCA)時に於けるブローダウン及び再冠水過程をモデル及び手法の変更なしに一貫して解析する計算コードであり，現在，検証計算及び修正を行っている。本計算は，小破断 LOCA に適用した最初の検証計算であり，一連の THYDE－P サンプル計算の一環であるサンプル計算 Run 50として行ったものである。計算は，2000秒まで行った。ムーディの相関式に対する放出係数は，0.8とした。実験の全体的挙動は，THYDE－P によって良く模擬された。

---

*業務協力員；日本情報サービス（株）

Contents

Contents(continued)

目　　次

List of Figures

List of Figures (continued)

List of Tables

1. Introduction

This report contains results from the best estimate post test calculation of LOFT Small Break Experiment L3-1[6][20] using the THYDE-P code[1]-[5].

Experiment L3-1 was performed as part of the Loss-of-Fluid Test (LOFT) program conducted by EG&G Idaho, Ing., for U. S. Nuclear Regulatory Commission (NRC). This experiment is part of the LOFT Small Break Experiment Series L3 which was designed to investigate the thermal-hydraulic response of LOFT reactor system to small primary system rupture. Experiment L3-1 was conducted at initial power level of 48.9±1 MW (yielding a maximum linear heat generation rate of 51.7±1 kW/m, which is about 98% of the LOFT rated thermal power of 50 MW. The experiment simulatef a postulated loss-of-coolant accident (LOCA) caused by a small break in the primary coolant system cold leg in a commercial PWR (about 1000 MWe). The break size was equivalent to a 4-inch pipe rupture, or a 2.5% break, in a commercial plant, scaled on a break area to system volume basis. The LOFT emergency core cooling system (ECCS) simulates the ECCS of a commercial PWR. The accumulator (ACC), the high pressure injection system (HPIS) and the low-pressure injection system (LPIS) were used during the experiment. Each system was arranged to inject scaled flow rates into the primary system cold leg. Electrical power to the primary coolant pump motor generator sets were terminated at blowdown initiation and the primary coolant pumps began to coast down under the influence of a flywheel system. Throughout the experiment, DNB at the cladding surface was not observed.

In the present calculation, the LOFT system was nodalized into 43 nodes and 37 junctions. The active core was simulated by 4 nodes and the downcomer was nodalized into a single node. A hot channel analysis was not performed but an average channel analysis was done. The discharge coefficient for the Moody correlation[7] was assumed to be a value of 0.8. The ACC water temperature was set by an input to be 307 K on the basis of the experimrnt. In order to avoid unrealistically large pressure decrease due to cold water injection, a time delay mode for density change[3][4], which takes non-equilibrium effects into account phenomenologically, was applied. Since a model for auxiliary feed water injection to SG secondary system is not implemented in the present version of the THYDE-P, a simple model was tentatively applied to auxiliarly feed water injection.

The calculation proceeded until 2000 sec after rupture, when the ACC injection was cmpleted and the system pressure became stabilized. The calculated system pressure was in good agreement with the experimental data. One of the most prominent phenomena calculated was that the ACC check valve was calculated to open intermittently, where the time average injection flow rate is seemingly in good agreement with the experimental data. DNB was calculated to occur at the cladding surface in conjunction with low enthalpy ACC water injection not for a long period but for a very short period.

2. Description of LOFT L3-1

2.1 Primary Objectives

The primary objectives of Experiment L3-1 were to obtain data for analytical code assessment and to further understand the thermal-hydraulic behavier which occurs during a postulated loss-of-coolant accident in a pressurized water reactor. Other objectives of the experiment were to determine any unexpected thresholds or events, determine how effectively typical process instrumentation indicated the true system condition, and define variations in system design or plant operation that could mitigate small break transient phenomena.

2.2 System Description

The LOFT major components are schematically shown in Fig. 2.1. The core contains 1300 unpressurized nuclear fuel rods arranged five square and four triangular (corner) fuel modules as shown in Fig. 2.2. The center assembly is highly instrumented. Two of the corner and one of the square (15x15) assemblies are not instrumented. The fuel rods have active length of 1.67 m and an outside diameter of 10.72 mm. Cladding material is zircaloy-4. Cladding inside and outside diameters are 9.49 and 10.72 mm, respectively.

2.3 Experiment Procedures

The experiment was initiated by opening the broken loop cold leg quick-opening blowdown valve (QOBV). The flow area (205.9 mm^2) of the small break orifice, which is schematically shown in Fig. 2.3, corresponded to the flow area of a 4-inch Schedule 160 (0.10-m OD) pipe in a commercial PWR. The pressurizer and broken loop hot leg heaters were turned off prior to blowdown.

Electrical power to the primary system motor generator sets was terminated at blowdown initiation and the primary coolant pumps began to coast down under the influence of a flywheel system (316.0 kg-m).

Emergency core coolant injection was directed to the intact loop cold leg during blowdown. The HPIS flow was initiated automatically 4.6±0.5 sec after blowdown initiation. The injection flow rate was held constant until the pressure reached 8.36 MPa, at which point the HPIS flow was increased with decreasing system pressure by operator action. Accumulator ACC-A injection at a system pressure of 4.37±0.06 MPa began 633.6±0.5 sec after the initiation of the blowdown.

3. Analytical Models in Present Calculation

The methods and the models in THYDE-P are described in detail in Ref. (1), some of which have been revised. The version of THYDE-P used in the present calculation is called "SV01L16".

2. Description of LOFT L3-1

2.1 Primary Objectives

The primary objectives of Experiment L3-1 were to obtain data for analytical code assessment and to further understand the thermal-hydraulic behavier which occurs during a postulated loss-of-coolant accident in a pressurized water reactor. Other objectives of the experiment were to determine any unexpected thresholds or events, determine how effectively typical process instrumentation indicated the true system condition, and define variations in system design or plant operation that could mitigate small break transient phenomena.

2.2 System Description

The LOFT major components are schematically shown in Fig. 2.1. The core contains 1300 unpressurized nuclear fuel rods arranged five square and four triangular (corner) fuel modules as shown in Fig. 2.2. The center assembly is highly instrumented. Two of the corner and one of the square (15x15) assemblies are not instrumented. The fuel rods have active length of 1.67 m and an outside diameter of 10.72 mm. Cladding material is zircaloy-4. Cladding inside and outside diameters are 9.49 and 10.72 mm, respectively.

2.3 Experiment Procedures

The experiment was initiated by opening the broken loop cold leg quick-opening blowdown valve (QOBV). The flow area (205.9 mm^2) of the small break orifice, which is schematically shown in Fig. 2.3, corresponded to the flow area of a 4-inch Schedule 160 (0.10-m OD) pipe in a commercial PWR. The pressurizer and broken loop hot leg heaters were turned off prior to blowdown.

Electrical power to the primary system motor generator sets was terminated at blowdown initiation and the primary coolant pumps began to coast down under the influence of a flywheel system (316.0 kg-m).

Emergency core coolant injection was directed to the intact loop cold leg during blowdown. The HPIS flow was initiated automatically 4.6±0.5 sec after blowdown initiation. The injection flow rate was held constant until the pressure reached 8.36 MPa, at which point the HPIS flow was increased with decreasing system pressure by operator action. Accumulator ACC-A injection at a system pressure of 4.37±0.06 MPa began 633.6±0.5 sec after the initiation of the blowdown.

3. Analytical Models in Present Calculation

The methods and the models in THYDE-P are described in detail in Ref. (1), some of which have been revised. The version of THYDE-P used in the present calculation is called "SV01L16".

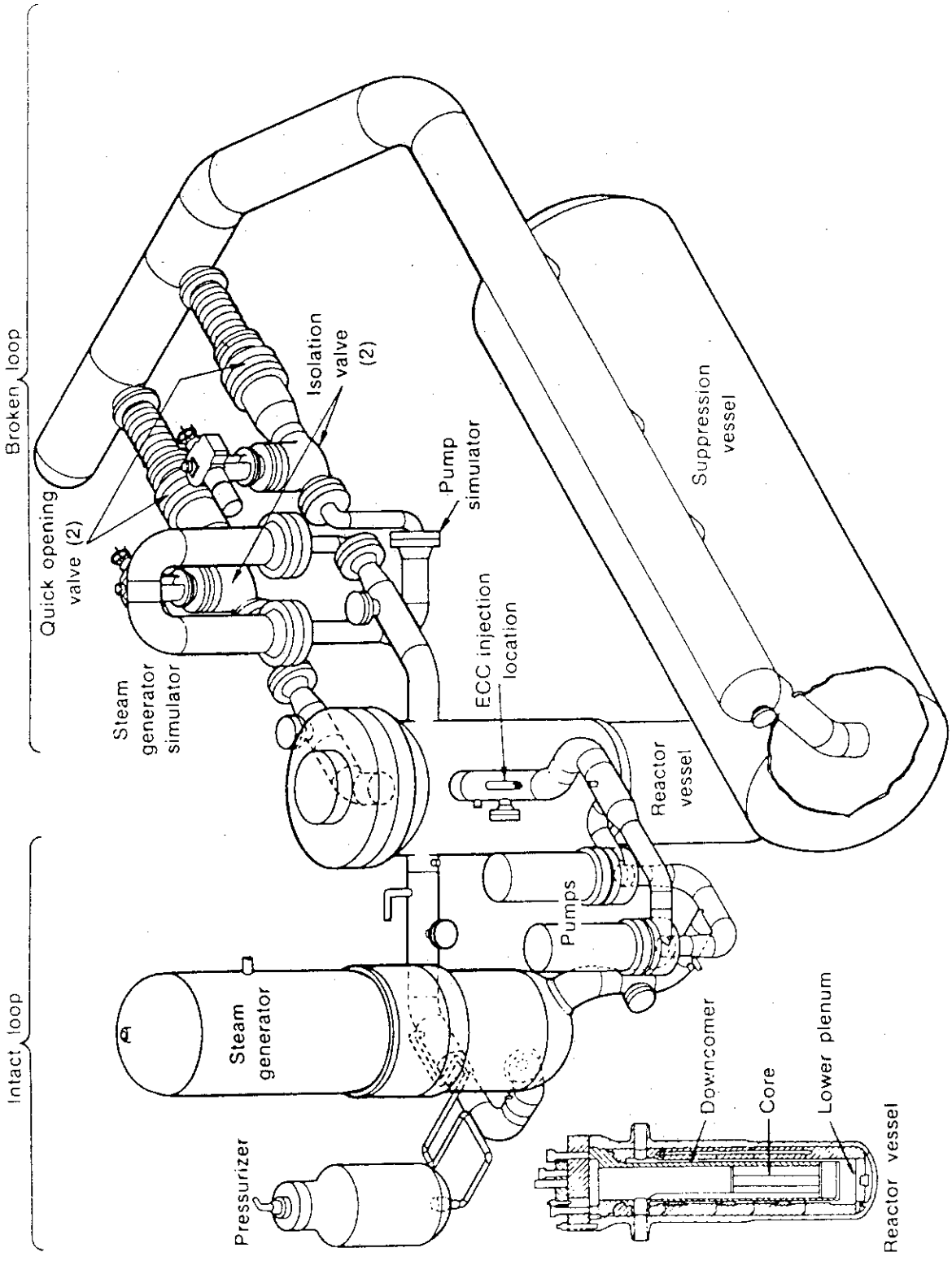

Fig.2.1 LOFT major components

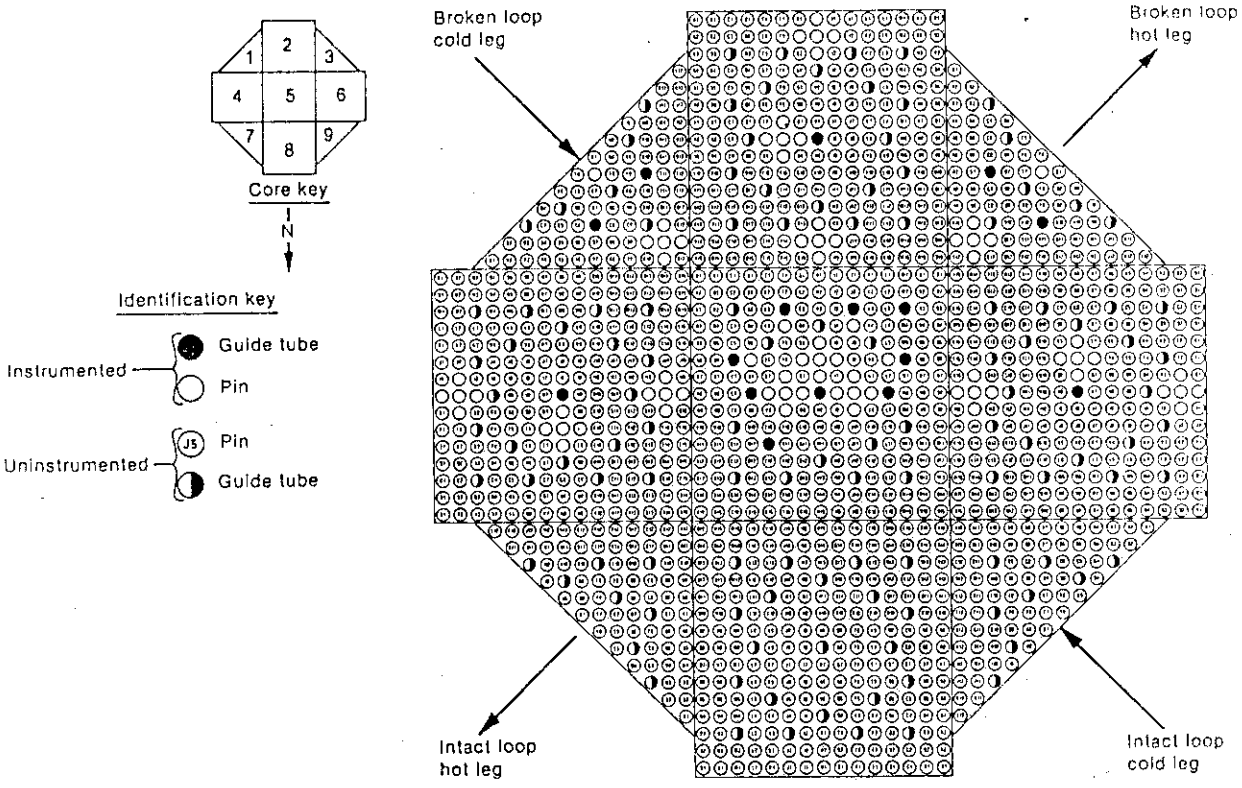

Fig.2.2 LOFT Core 1 Configuration showing rod designations

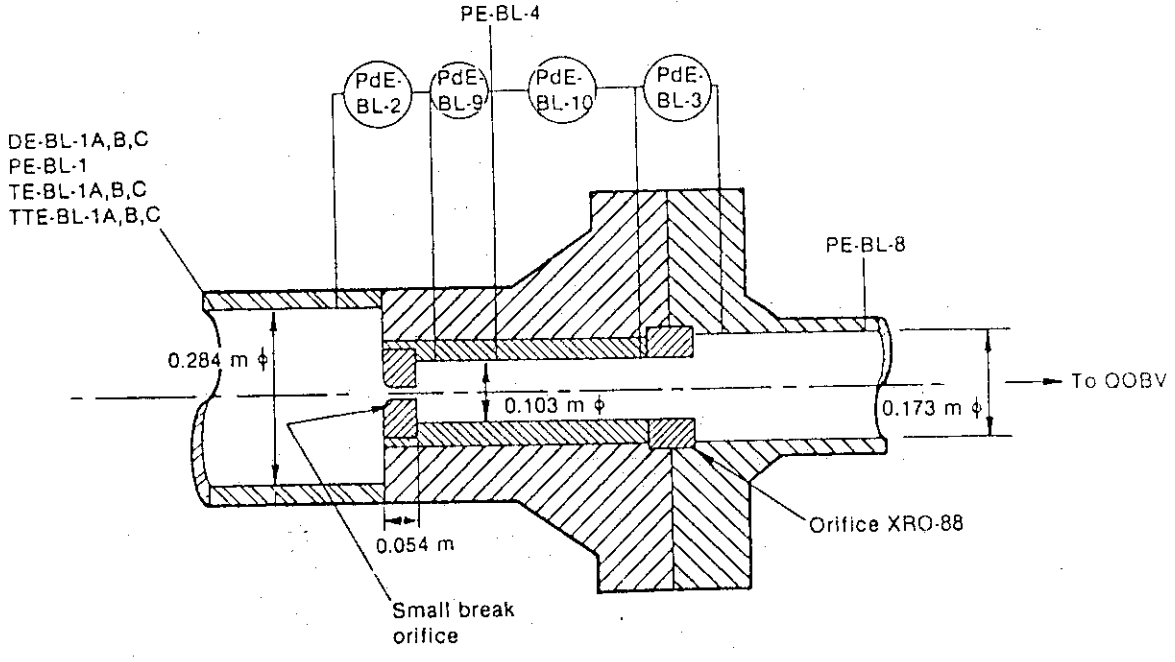

Fig.2.3 LOFT small break orifice area and instrumentation

Several models which are most relevant to the present calculation are briefly presented in this section.

3.1 Pump Model

In the present version of THYDE-P, two options are implemented to calculate pump speed. One is to simulate locked rotor and the other is to simulate pump coastdown due to loss of electrical power. In both cases, the pump speed is set a constant value at the steady state before the pump tripped off. When the former option is selected, the pump speed is not calculated by solving a time-dependent pump equation[1] but calculated by the following equation.

$$a(t) = a(t_{trip})\exp(-(t-t_{trip})/\tau_{pump}) \qquad (3.1.1)$$

where

t	Current time (sec)
t_{trip}	Trip time (sec)
τ_{pump}	Time constant for pump rotor lock (sec)

In the present calculation, the pump coastdown was simulated by using the locked rotor option and the time constant was chosen to be 12 sec from the experimental data.

3.2 Accumulator Check Valve

As will be shown later, the accumulator check valve played an important role in the present calculation. The model for the check valve is shown as follows.

When the pressure at the outlet point (Point E) of ACC duct node n, i.e. p_n^E, is higher than the initial ACC pressure $p_{ACC}(0)$, the check valve is calculated to be closed. This simulates the time period before ACC injection initiation. Then, the following boundary condition is assumed at point E of node n.

$$G_n^E = 0 \qquad \text{for } p_n^E(t) > p_{ACC}(0) \qquad (3.2.1)$$

When p_n^E decreases and becomes less than p_{ACC}, the accumulator injection is initiated. Then the following boundary condition is assumed.

$$p_n^E(t) = p_{ACC}(t^{old}) \qquad (3.2.2)$$

where t^{old} represents the time which is one time step before the current time. With this boundary condition, the flow equations are solved on the basis of a non-linear implicit method and as a result G_n^E, which is the injection flow rate, is obtained. And then the current value of the ACC pressure $p_{ACC}(t)$ is calculated by using the injection mass flow rate. This procedure is

repeated. This model may be enough to analyze large break LOCAs since the system depressurization is much faster than that of the accumulator. In the caces of slow transients such as small break LOCAs, the depressurization in the accumulator might be calculated faster than the system depresurization. In such a case, a reverse flow may be calculated for the boundary condition shown in Eq. (3.2.2). Then, if the reverse flow into the the accumulator is calculated to occur, a recalculation must be performed with the same boundary condition except for

$$G_n^E(t) = 0 \qquad (3.2.3)$$

at the AC injection point. Obviously, in the new model for the ACC check valve, a physical model to describe closing or opening of a valve is not taken into consideration. Modifications will be done in the future version.

3.3 Time Delay Model for Density Change

A time delay model for density change[3][4], which takes non-equilibrium effects into account phenomenologically, is implemented in THYDE-P in order to avoid unrealistically large pressure decrease due to cold water injection. What is the most difficult is to determine the time constant of the delay realistically. A physical model to evaluate it is yet to be developed. In the present calculation, the time constants for the nodes are assumed to be proportional to the node volume with 1 sec for the core nodes. They are assumed to be bounded from below by 1 sec. In sample calculations 30[3] and 40[4], for LOFT large break experiment L2-2 and L2-3, the time constants were similarly determined.

4. Modification to Original Version

In the course of the present calculation, several modifications to the original version (SV01L16) were needed to perform the calculation. In the following subsections, they are briefly described.

4.1 CHF and Heat Transfer Correlations

The Biasi correlation[9] and the modified Zuber correlation[10] were used to predict CHF values for a forced flow condition ($G > G_{min}$) and a pool flow condition ($G \leq G_{min}$), respectively, where G_{min} = 273 kg/m^{2}s. The heat transfer correlations applied are shown in Tables 4.1.1 and 4.1.2. This set of the CHF and heat transfer correlations are the same as that tentatively applied in the analyses of LOFT L2-2[3] and L2-3[4] with THYDE-P.

4.2 Break Flow Simulation Model

The slightly modified[1] Zaloudek correlation[8] and the Moody correlation[7] are implemented in the present version of THYDE-P. The discharge coefficient for the Moody correlation is assumed to be 0.8, which is the same as that in the analyses of LOFT L2-2[3] and L2-3[4]. The sensitivity study for the discharge coefficient was not performed in the present work.

In order to simulate the small break orifice, a node with a very small flow area or a orifice node must be placed at the break point. Therefore, the following model was tentatively applied in the present calculation.

(a) Inertial Flow Calculation Just after Rupture

For the time period from break initiation until a critical flow is calculated to occur, an inertial flow calculation[1] is performed in THYDE-P. The pressure drop across an orifice Δp could be evaluated by the following equation[18].

$$G_b = C_d \sqrt{\frac{2\rho\Delta P}{1+a^2}} \qquad (4.2.1)$$

where

$a = A_0/A_b$,

$C_d = 0.61$,

A_0 : Orifice flow area, and

A_b : Flow area of break node.

Then the boundary condition at the outlet point of the break node during the period of the inertial flow is assumed to be as follows:

Table 4.1.1 Heat Transfer Correlations

Mode		Conditions		Correlations
Core	SG	Coolant Condition	Other conditions	
1	1	Subcooled water	$T_{wall} < T_{sat}$	Dittus-Boelter[11]
2	2	Subcooled water	$T_{wall} > T_{sat}$	Interpolation between D-B and J-L
3	3	Saturated state	$\phi < \phi_{CHF}$	Jens and Lottes[12]
4	/	Saturated state	$\phi > \phi_{CHF}$	(see Table 4.1.2)
5	5	Superheated steam	$Re < 3000$	Forced convection[1]
6	6	Superheated steam	$3000 < Re < 5000$	Interpolation
7	7	Superheated steam	$Re > 5000$	McEligot[15]
/	8	Saturated state	$T_{coolant} > T_{wall}$	Condensation[18]

Table 4.1.2 Heat Transfer Correlations in Mode 4

Mode	Conditions	Correlations
4-1	$G > Gmin$, $\phi_{4-1} > \phi_{4-2}$	McDonough, Milich and King[19]
4-2	$G > Gmin$, $\phi_{4-1} < \phi_{4-2}$	Groenevelt[13]
4-3	$G < Gmin$, $\Delta T_s < \Delta T_{min}$	Pool transition boiling correlation[17]
4-4	$G < Gmin$, $\Delta T_s > \Delta T_{min}$	Berenson[14]
4-5	$G < Gmin$, $x < x_c$	Pool transition boiling[4]

$$P_b = P_t + G_b\left(\frac{1}{a^2}-1\right)/2\ \rho\ C_d \qquad (4.2.2)$$

where

P_t = $\beta\ P_b(t=t_b) + (1-\beta)\ P_{ref}(t)$

β = $\exp[-(t-t_b)/\tau_b]$

P_{ref} ; Reference pressure

τ_b ; Time constant (= 2.0 sec)

P_b ; Break node pressure at $t=t_b$

t_b ; Rupture time

(b) Critical Flow Calculation

Since an orifice node was not placed at the break, the following care had to be taken. The flow area of the small break orifice was taken into consideration in the following manner, when a critical flow was calculated to occur.

$$G_b = aG_c(P_b, h_b) \qquad (4.2.3)$$

where

G_c; Critical flow

4.3 Drift Flux Model

In analysis of small break LOCAs, models to account for a relative velocity between two phases may play an important role since flows tend to be stagnant. In the present version of THYDE-P, however, only a single correlation for a drift velocity is implemented. That is:

$$V_{gj} = 1.41\left\{\frac{g\sigma(\rho_{fs}-\rho_{gs})}{\rho_{fs}^2}\right\}^{\frac{1}{4}} \qquad (4.3.1)$$

which takes gravity induced velocity difference in a churn turbulent bubbly flow. Moreover, in the energy conservation equation at a junction, the term to take into account the relative velocity was neglected. Therefore, two kinds of modifications have been done in the cource of the present work:

(1) Since the correlation in Eq. (4.3.1) is not applicable for a large void fraction, v_{gj} is made to vanish for $\alpha > 0.8$, for simplicity,

(2) The energy conservation at the junction equation with respect to relative velocity was taken into consideration.

4.4 SG Secondary System Auxiliary Feed Water Simulation

In the present version of THYDE-P, mass accumulation in a SG secondary system is not taken into consideration. Therefore, the auxiliary feed water injection could not be simulated. At the early portion of the calculation until 400 sec after rupture, the effects of auxiliary feed water were neglected. Since the SG secondary pressure was considerablly overestimated by the time, the effects were taken into account after 400 sec. in such a manner that the out-surge flow of the saturated steam from the steam outlet was the same mass flow rate as that of the auxiliary feed water. As expected, the calculated SG secondary pressure was considerably underestimated by 1000 sec after rupture, so that both the auxiliary feed water injection and the out-surge flow were made to stop at the time.

4.5 Numerical Solution Method of Thermal Conduction Equation within Fuel Rod

In the THYDE-P code, a non-linear implicit method is applied to solve the one-dimensional node-and-junction equations on the basis of the Newton method. On the other hand, an explicit integration method is used to solve the thermal conduction equation within a fuel rod in the present version of THYDE-P (SV01L16). In the cource of the present work, i.e. at about 300 sec after rupture, the numerical solusion method was revised from the explicit method to a liner implicit method in order mainly to elongate the time step width.

4.6 Heat Transfer between Coolant and Structure

In the present version of THYDE-P, a model to simulate heat transfer between coolant and structure is not yet implemented. Since heat addition to coolant from structure may play an important role especially at a sudden decrease in pressure, it was taken into consideration by a simple model generally referred to as "lump model" in the present calculation. The model was applied after ACC injection initiation along the ACC water flow path. Only nucleate boiling was assumed to occur at the structure surface and the Jens and Lottes correlation[12] was used to evaluate the heat flux from the structure to coolant. Heat loss to environment was not modeled. The model is described as follows.

$$Q^* = r_1 h_{tc}(T_k - T_n) \qquad (4.6.1)$$

$$(\rho\, c_p)_k dT_k/dt = -r_2 Q^*$$

where

$$r_1 = A_k/V_n$$

$$r_2 = V_n/V_k$$

and

T_n	Coolant temperature
T_k	Structure temperature
$(\rho\ c_p)_k$	Volumetric heat capacity of structure
A_k	Heat transfer area
V_n	Node volume
V_k	Volume of structure
Q^*	Heat input to coolant per unit volume
h_{tc}	Heat transfer coefficient

The volumetric heat capacity $(\rho\ c_p)_k$ for SUS 304 is approximated by a constant value of 720.8 kcal/m^3°C. In the present calculation, heat flow from coolant to structure was not considered for simplicity. This model was applied to nodes 9, 10, 29, 21, 22 and 23 (see Fig. 5.1 and Table 5.2), and the values of r_1 and r_2, which express the geometry of the structure, are as follows.

Node No.	Description	r_1 (1/m)	r_2
9 and 10	Intact loop cold leg	14.1	1.97
20 and 21	Broken loop cold leg	14.1	1.97
22	Downcomer	9.08	0.479
23	Lower plenum	4.96	4.02

5. Input Data and Results of Steady State Adjustment

The input data in the present calculation are shown in App. A. The initial conditions for the calculation are compared with those for the experiment in Table 5.1. The input data and the results of steady state adjustment[1),(2)] are summarized in this section.

5.1 Nodalization

The nodalization in the present calculation is shown in Fig. 5.1. The node geometrical data are shown in Table 5.2 with their descriptions. The pressure vessel was expressed by an assembly of nodes from 22 to 33. Node 33 simulated part of the upper plenum. The downcomer was simulated by a single node, whose number is 22. The active core was nodalized into 4 nodes, i.e. nodes from 26 to 29. The small break was assumed to occur at the cold leg side of junction 6. The hot leg side of junction 6 was a dead end. The reflood assist line was nodalized into nodes 34 and 35. The pressurizer surge line was simulated by nodes 36 and 37. The recirculation lines, which establish a small flow from the broken leg to the intact loop to maintain approximately equal temperatures and are isolated from the the system prior to blowdown initiation, were not simulated in the present calculation. Also, the core bypass from the downcomer top to the upper plenum was not taken into consideration.

5.2 Trip Data

The following trip actions were taken by inputs.

SG secondary feed water injection teminated	0.0 sec
Reactor tripped	0.0 sec
HPIS injection initiated	4.5 sec .

5.3 Core Data

The initial heat fluxes at the core nodes were given by inputs on the basis of the experimental data as listed below.

Node No.	Initial heat flux ($kcal/m^2s$)
25	148.06
26	249.64
27	190.32
28	62.88

The input data for the nuclear fuel rods are summarized as follows:

Number of fuel rods	1300
Cladding outer diameter	1.072×10^{-2} m
Cladding thickness	6.172×10^{-4} m
Fuel pelet diameter	8.934×10^{-3} m

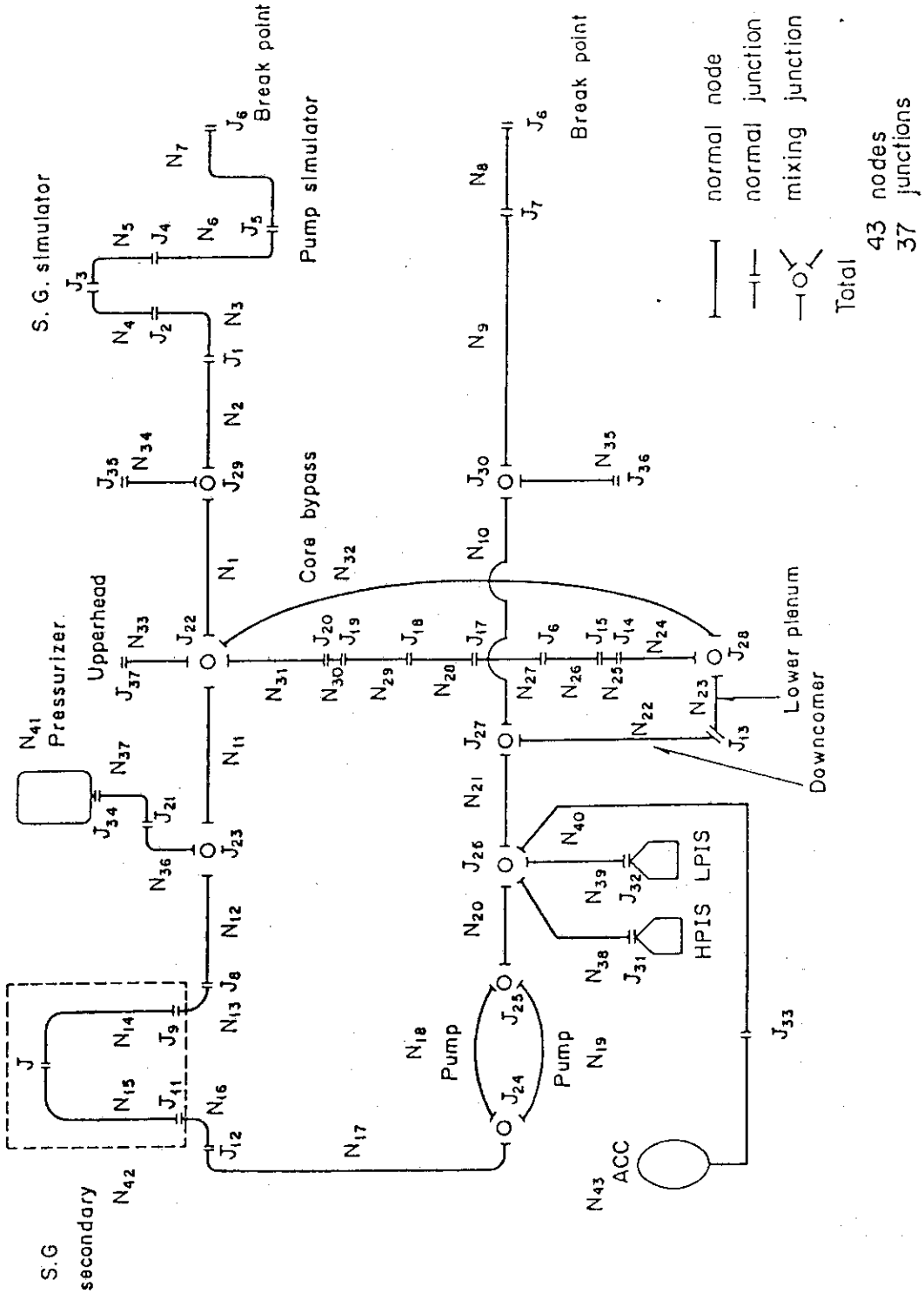

Fig.5.1 Nodalization for LOFT L3-1

Table 5.1 Initial Conditions for Test L3-1

	Experiment[4]	Present Analysis
Primary Coolant System		
Intact Loop		
Mass Flow Rate (kg/s)	484.0 ± 6.3	484.
Hot Leg Pressure (MPa)	14.85 ± 0.04	14.8
Cold Leg Temperature (K)	554.0 ± 3	554.
Hot Leg Temperature (K)	574.0 ± 1	573.
Pressure Vessel		
Power Level (MW)	48.9 ± 1	50.0
Pressurizer		
Steam Volume (m^3)	0.343 ± 0.008	0.343
Liquid Volume (m^3)	0.620 ± 0.008	0.616
Water Temperature (K)	617.0 ± 3	613. and 573.[a]
Pressure (MPa)	14.81 ± 0.04	14.8
Liquid Level (m)	1.10 ± 0.01	1.11[b]
Broken Loop		
Cold Leg Temperature (K)	557.3 ± 5.0	553.
Hot Leg Temperature (K)	562.0 ± 5.0	573.
SG Secondary System		
Water Level (m)	3.15 ± 0.03	3.15[b]
Water Temperature (K)	536.0 ± 3.9	542. and 527.[a]
Pressure (MPa)	5.43 ± 0.11	5.43
Mass Flow Rate (kg/s)	25.0 ± 0.4	25.0
Accumulator		
Liquid Level (m)	1.71 ± 0.01	1.71
Gas Volume (m^3)	1.39 ± 0.03	1.39
Pressure (MPa)	4.37 ± 0.06	4.37

Table 5.1 Initial Conditions for Test L3-1 (Continued)

	Experiment[4]	Present Analysis
Temperature (K)	304.7 ± 3	305.
High Pressure Injection System		
Initial Mass Flow Rate (kg/s)	0.33 ± 0.02	0.33
Temperature (K)		297.

(a) Water temperatures at saturated and subcooled regions, respectively
(b) What is called "collapsed level"

Table 5.2 Node Geometrical Data

Node No.	Description	Flow Area A (m^2)	Node Length L (m)	Node Height H_L (m)
1	Broken loop hot leg	0.06344	1.332	0.0
2	Broken loop hot leg	0.06344	0.6965	0.0
3	Broken loop hot leg	0.00836	1.517	0.7174
4	Broken loop hot leg	0.09539	3.228	2.705
5	Broken loop hot leg	0.09539	3.228	-2.705
6	Broken loop hot leg	0.01271	2.423	-2.039
7	Broken loop hot leg	0.008365	1.883	1.322
8	Broken loop cold leg	0.008365	0.4877	0.0
9	Broken loop cold leg	0.06344	0.6965	0.0
10	Broken loop cold leg	0.06344	0.9510	0.0
11	Intact loop hot leg	0.06344	2.6160	0.0
12	Intact loop hot leg	0.06299	2.643	0.2423
13	SG inlet plenum	0.6481	0.5175	0.5175
14	SG U-tube	8.187 E-5	2.568	2.483
15	SG U-tube	8.187 E-5	2.568	-2.483
16	SG outlet plenum	0.6481	0.5175	-0.5175
17	Crossover leg	0.06793	2.429	-1.523
18	Pump	0.09446	1.867	1.281
19	Pump	0.07273	3.111	1.281
20	Intact loop cold leg	0.0597	1.399	0.0
21	Intact loop cold leg	0.06343	0.5313	0.0
22	Downcomer	0.1604	4.256	-4.256
23	Lower plenum	0.7917	0.7318	0.0
24	Mixing box	0.1532	0.4285	0.4285
25	Non-active core	1.143 E-4	0.09423	0.09423
26	Active core	1.143 E-4	0.4191	0.4191
27	Active core	1.143 E-4	0.4191	0.4191
28	Active core	1.143 E-4	0.4191	0.4191
29	Active core	1.143 E-4	0.4191	0.4191
30	Non-active core	1.143 E-4	0.01753	0.01753
31	Upper core structures	0.2387	1.668	1.668

(continued)

32	Core bypass	4.766 E-3	4.146	4.146
33	Upper head	0.2306	0.9144	0.9144
34	Reflood assist line	0.03871	4.048	0.8620
35	Reflood assist line	0.03871	4.840	0.6075
36	Pressurizer surge line	1.452 E-3	4.592	0.4255
37	Pressurizer surge line	1.452 E-3	4.767	0.7678
38	ECCS piping	6.221 E-3	5.5	0.0
39	ECCS piping	6.221 E-3	5.5	0.0
40	ECCS piping	6.221 E-3	58.0	0.0

Table 5.3 Loss coefficients of nodes

Node No	k	k_A^f	k_A^r	k_E^f	k_E^r
1	0.0422	0.400	0.800	0.000	0.000
2	0.0327	0.000	0.000	0.000	0.000
3	0.0201	0.391	0.754	1.520	1.090
4	0.0723	0.000	0.000	189.0	189.0
5	0.0308	0.000	0.000	142.0	198.0
6	0.0249	0.000	0.000	20.00	20.00
7	0.0203	0.000	0.000	0.000	0.000
8	0.0528	0.000	0.000	0.753	0.390
9	0.0093	0.000	0.000	0.000	0.000
10	0.0232	0.000	0.000	3.580	3.000
11	0.0200	0.400	0.800	0.000	0.000
12	0.0201	0.000	0.000	0.815	0.406
13	0.0097	0.000	0.000	0.000	0.000
14	0.0464	0.345	0.588	0.000	0.000
15	0.0198	0.000	0.000	0.588	0.345
16	0.0210	0.000	0.000	0.000	0.000
17	0.0167	0.403	0.801	0.000	0.000
18	0.1058	0.000	0.000	0.000	0.000
19	0.0233	0.400	0.800	0.000	0.000
20	0.0201	0.400	0.800	0.000	0.000
21	0.0213	0.000	0.000	3.580	3.000
22	0.0241	0.620	0.620	3.500	3.500
23	0.0155	0.000	0.000	0.000	0.000
24	1.03E1	0.000	0.000	0.000	0.000
25	3.6699	0.014	9.E-4	0.000	0.000
26	3.4118	0.000	0.000	0.000	0.000
27	3.3290	0.000	0.000	0.000	0.000
28	3.2882	0.000	0.000	0.000	0.000
29	3.2922	0.000	0.000	0.000	0.000
30	4.1027	0.000	0.000	0.143	0.170
31	1.46E1	0.000	0.000	0.000	0.000
32	4.15E1	0.000	0.000	0.000	0.000
33	0.1000	0.000	0.000	0.000	0.000
34	0.1000	0.400	0.800	0.000	0.000
35	0.1000	0.400	0.800	0.000	0.000
36	1.00E1	0.400	0.800	9.000	9.000
37	1.00E1	0.000	0.000	0.000	0.000
38	1.00E1	0.400	0.800	0.000	0.000
39	1.00E1	0.400	0.800	0.000	0.000
40	1.00E1	0.400	0.800	0.000	0.000

Rod pitch	1.430×10^{-2} m
Plenum gas volume	5.493×10^{-6} m^3
Plenum gas mole number	5.70×10^{-4} mole

The gap gas molecular fractions were given by inputs as listed below.

Gas	Gas molecular fraction (-)
He	0.887
Xe	0.0355
Kr	0.0063
N_2	0.0712

The initial power level calculated using these input data is 11941 kcal/sec (50MW). As a result of steady state adjustment, the following values were calculated.

Steady state gap pressure 2.9×10^5 Pa

Node No.	Fuel centre temp. (°C)	Fuel surface temp. (°C)
25	967.0	305.6
26	1561.5	326.7
27	1210.0	324.3
28	569.8	309.1

Node No.	Heat transfer coefficient (kcal/m^2.s.°C)	
	Cladding surface	Gap
25	7.33	0.52
26	7.41	0.58
27	7.45	0.55
28	7.47	0.48

It should be noted that the input data for the fuel rod geometries are supposed to be those at the steady state, i.e. "hot dimensions", in the pesent version of THYDE-P. The input data in the present analysis, which are taken from the experimental specifications[2], however, are so called "cold dimensions". Therefore, the calculated gap pressure, for example, might be overestimated.

5.4 Steam Generator Data

The primary and secondary systems of the steam generator were simulated by nodes 13 to 16 and node 42, respectively. The U-tubes were simulated by nodes 14 and 15. The SG inlet and outlet plenums were simulated by nodes 13 and 16, respectively. The input data for these nodes are summarized as follows.

Plenums	
Volume	0.353 m^3
Hydraulic diameter	0.908 m
Height	0.518 m
U-tubes	

Number	1845
Outer diameter	1.021×10^{-2} m
Height	2.483 m
Pitch	1.905×10^{-2} m

SG secondary system

Steady state pressure	53.6 atm
Feed water enthalpy	190 kcal/kg
Feed water mass flow rate	25 kg/s
Flow area	1.589 m^2
Height	4.188 m
Initial subcooled water level	0.24 m
Initial void fraction of saturated region	0.27

The initial liquid enthalpy of the subcooled region, h_2, was calculated by the following equation.

$$h_2 = h_{surge} + b(h_{fs} - h_{surge}) \quad (5.1)$$

where the constant b, which takes a recirculation flow into account, was given by an input to be 0.8 in the present calculation. The initial heat flux ratios of the SG primary nodes were given by inputs as follows.

Node No.	Initial heat flux ratio(-)
14	0.714
15	0.286

The results of steady state adjustment concerning the steam generator are summarized as follows.

Region	Average enthalpy (kcal/kg)	Total mass (kg)	Bulk temp. (℃)
1 (saturated)	286.9	356.9	269.0
2 (subcooled)	263.5	303.3	253.5

Node No.	HTC (kcal/m^2.s.℃)		Wall temp. (℃)	
	primary	seconary	primary	secondary
14	7.86	9.77	279.2	273.1
15	7.81	6.36	277.7	270.9

5.5 Pressurizer Data

The pressurizer was simulated by node 41. The input data for the pressurizer are summarized as follows.

Flow area	0.557 m^2
Height	1.7235 m
Initial subcooled water level	1.1 m
Initial void fraction of saturated region	0.99

Standpipe length	0.01 m

In the present calculation, the effects of the standpipe was neglected for lack of the data and a small value of 0.01 m was set by an input for its length.

The following values were obtained as a result of steady state adjustment.

Pressure	14.9 MPa
Enthalpy of subcooled region	320.0 kcal/kg
Enthalpy of saturated region	610.8 kcal/kg
Total mass of subcooled region	444.0 kg
Total mass of saturated region	34.9 kg

The geometrical data and the loss coefficients at the pressurizer surge line (nodes 36 and 37) are shown in Table 5.3.

5.6 Pump Data

The primary coolant pumps were simulated by nodes 18 and 19. The input data for the pumps are listed below.

Rated speed	3530 rpm
Rated flow	0.3155 m^3/s
Rated head	108.1 m
Rated torque	500.24 J/rad
Rated density	613.73 kg/m^3
Moment of inertia	1.4382$kg/m^2/rad^2$
Time constant for pump rotor lock (see Subsec. 3.1)	12 sec

As for the single-phase and two-phase pump characteristic curves, reference should be made to Ref. (3).

5.7 ECCS Data

The input data for the accumulator are listed below.

Pressure	41.13 atm
Liquid volume	1.39 m^3
Liquid enthalpy	30 kcal/kg

The total mass of the accumulator was calculated to be 1.706×10^3 kg. The accumulator standpipe was not taken into account in the present calculation, so the amount of liquid mass injected into the system was overestimated as will be shown in the next section.

The initial liquid enthalpy of the HPIS and the LPIS were given by inputs to be 24 kcal/kg. The injected mass flow rates from the HPIS and the LPIS were set by inputs as time tables on the basis of the experiment (see Fig. 6.32).

5.8 Simulated SG and Pump Data

The simulated pump and simulated SG in the broken loop hot leg were nodalized into nodes 3 to 7. The loss coefficients for the nodes are listed in Table 5.3.

6. Calculated Results and Discussion

6.1 Chronology of Events

The chronology of events for the present calculation is compared with that for the experiment[5] in Table 6.1. As shown in the table, the reactor scram signal was recieved 2.15 sec prior to rupture. In the present calculation, however, the reactor scram was assumed to occur simultaneously with rupture for simplicity. For each item in Table 6.1, discussion will be done in the following subsections. It should be noted that the calculated timing of ACC injection initiation is in good agreement with the experimental data. The fact implies that the calculated temporal behavier of the system pressure was well simulated by the present calculation.

6.2 Temporal Behaviors until 200 sec

6.2.1 Pressure

The pressures calculated until 200 sec at the four legs, i.e. the intact loop hot and cold legs, and the broken loop hot and cold legs, are shown in Figs. 6.1, 6.2, 6.3 and 6.4, respectively, along with the experimental data. The calculated pressures in the figures were underestimated until about 20 sec after rupture. The major reason was that the initial liquid enthalpy of the pressurizer in the calculation was considerably lower than that in the experiment as shown in Table 5.1. In the present version of THYDE-P, an initial subcooled water level is given by an input and the subcooled liquid enthalpy is set to be the same as that at the surge line. Since the flow at the surge line is assumed to be initially stagnant, the coolant enthalpy at the surge line is set to the same as that at the intact loop hot leg. Therefore, the pressurizer liquid enthalpy is considerablly underestimated and voiding inception at the pressurizer surge line and the intact loop hot leg was delayed in comparison with the experiment. Consequently, the depressurization until about 20 sec was much faster than that in the experiment. The calculated pressurizer pressure is shown in Fig. 6.5, along with the experimental data. Resuling from the faster system depressurization than the experimental data, the time when the upper plenum pressure reached the saturation pressure was calculated to be about 16 sec earlier than that in the experiment as shown in Table 6.1.

6.2.2 Density

The calculated coolant densities until 200 sec after rupture are shown in Figs. 6.6 through 6.9, along with the experimental data. In the experiment, the fluid densities were measured by gamma ray densiometers, each of which consisted of a source and several detectors. These detectors (A, B and C) were aligned with collimated gamma ray beams passing through the pipe as shown in Fig. 6.10. The experimental curves in Figs. 6.6 and 6.7 clearly

Table 6.1 Chronology of Events

Events	Time after LOCE Initiation (sec)	
	Experiment[4]	Analysis
Reactor scramed	-2.15	0.[a]
Primary coolant pumps tripped	0.04 ± 0.01	0.04[a]
HPIS injection initiated	4.6 ± 0.5	4.6[a]
Pressurizer emptied	17.0 ± 1	not clear
PCP coastdown completed	19.0 ± 1	20.[a]
Upper plenum reached saturation pressure	24.4 ± 0.5	8.0[b]
SCS auxiliary feed water pump started	75.0 ± 1	400.[c]
ACC injection initiated	633.6 ± 0.5	687.
ACC liquid level below stand pipe	1570.0 ± 1	1620.
SCS auxiliary feed water pump tripped	1875.0 ± 0.5	1000.[c]

(a) Given by the input data

(b) See Subsec. 6.2.1

(c) Artificially changed from the experimental value . (see Subsec. 4.4)

show the flows were stratified. On the other hand in the calculation, only overall trends were simulated since basically a homogeneous model is applied in THYDE-P.

6.2.3 Pump Speed

The calculated pump speed at pump node 18 is shown in Fig. 6.11, along with the experimental data. As presented in Subsec. 3.1, the time constant τ_{pump} was determined by curve-fitting to the experimental data shown in this figure.

6.3 Temporal Behavior until 2000 sec

6.3.1 Pressure

The pressures calculated at the four legs are shown in Figs. 6.12 through 6.15, along with the experimental data. The trends of the calculated results are in good agreement with those of the experimental data. It is shown in these figures, several sharp pressure decreases were calculated to occur after about 700 sec until about 1700 sec. These presure decreases were brought about by cold water injection from the accumulator. As will be shown in the subsequent section, the accumulator check valve was calculated to open intermittently.

6.3.2 Accumulator Injection

The pressure and the water level calculated at the accumulator are shown in Figs. 6.16 and 6.17, respectively, along with the experimental data. The calculated mass flow rate at the accumulator duct node is shown in Fig. 6.18. The present model for the accumulator check valve has already been presented in Subsec. 3.2.

One of the most prominent phenomena in the present calculation was that the accumulator check valve was calculated to open intermittently. When the check valve opened, rapid condensation due to low enthalpy ACC water started and the system pressure decreased. This depressurization brought about increase in the injection flow rate, so it accelerates the depressurization in the accumulator. As explained in Subsec. 3.2, when the ACC pressure became less than the system pressure, the check valve was calculated to close and, thereby system pressure recovery started mainly due to increase in heat addition to coolant. These processes were repeated. In the experiment, the ACC pressure was always a little higher than the system pressure and the injection flow rate was relatively low. The reason why the depressurization rate of the accumulator became larger than that of the system may be as follows. One of the reasons comes from the model for the check valve. The mechanical movement of the check valve may have to be taken into consideration. Another reason, which might be the most crucial, comes from the condensation model, i.e. the time delay model for density change (see Subsec. 3.3). Without the time delay model, the system depressurization rate is unrealistically large after ACC

injection initiation. Consequently the injection flow rate becomes much larger than the experimental data and finally the calculation fails. In such a way, the injection mass flow rate and the depressurization of the accumulator are highly dependent on the condensation model applied. It might to be possible that the calculated results are hopefully improved by improving the time delay model.

In Fig. 6.19, the calculated coolant temperature at the intact loop cold leg near the ECC injection point is compared with the expeimental data. The observed data were obtained by using a measurement device called "ECC Rake", whose description is shown in Fig. 6.20. In this figure, the measured coolant temperatures near the top and bottom of the horizontal duct are shown, where it is shown that the observed subcooling of the coolant near the bottom of the duct was as high as 100°C. This means thermal non-equilibrium effects were considerablly large and the condensation rates may seriously be overestimated by using equilibrium models.

The calculated heat inputs from the SG secondary system to the primary nodes 14 and 15 are shown in Figs. 6.21(a) and (b), respectively. The heat inputs to coolant from the structure walls calculated at the downcomer and the lower plenum, i.e. nodes 22 and 23, are shown in Figs. 6.22 and 6.23, respectively. As shown in these figures, heat inputs to coolant considerablly increased at the sudden decreses in the system pressure and contributed to the pressure recovery after the sudden decreases in pressure.

6.3.3 Coolant Density

The coolant density calculated at the intact loop cold leg is shown in Fig. 6.24, along with the experimental data. The observed density gradually increased after about 800 sec until 1800 sec because of ACC injection. In the calculation, however, the effects of injected ACC water appeared intermittently.

The coolant density calculated at the intact loop hot leg downstream of the ECC injection point is compared with the experimental data in Fig. 6.25, which clearly showed the flow was stratified in the experiment. The calculated coolant density tended to be underestimated since the node located upstream of the ECC injection point and therefore the coolant enthalpy was calculated high as long as the flow was foward because of the heat inputs from the SG secondary system. The reason for the sharp peak at about 1700 sec was that a reverse flow was calculated to occur and low enthalpy ACC water flew into the node.

In Figs. 6.26 and 6.27, the coolant densities at the broken loop hot and cold legs are shown. Bypassing water from the intact loop hot leg to the broken loop cold leg across the downcomer became subcooled several times corresponding to ACC water injection as shown in Fig. 6.27.

6.3.4 Mass Flow Rate

The calculated mass flow rate at the four legs are shown in Figs. 6.28 to 6.31. The mass flow rate at the intact loop hot leg(see Fig. 6.28) suddenly decreased just after the pumps

tripped off and became oscillatory around zero point after about 200 sec. At the intact loop cold leg, the flow was also oscillatory but almost a forward flow direction was established because of the effects of ECC water from the HPIS. The injection mass flow rate from the HPIS was about 1.6 kg/s as shown in Fig. 6.32.

The calculated mass flow rates at the downcomer inlet and the pressurizer surge line are shown in Fig. 6.33 and 6.34, respectively, while the corresponding experimental data were not available.

6.3.5 Break Flow

The calculated break flow is shown in Fig. 6.35, along with the experimental curve, which was transfered from Ref. (5). The coolant enthalpy calculated also at the break point is shown in Fig. 6.36. Overall trend of the experimental break flow was well simulated by the present analysis. As shown in Fig. 6.36, bypassing coolant across the downcomer top became subcooled several times after ACC injection initiation. Consequently, several peaks appeared in the calculated break flow curve (see Fig 6.35). In the nodalization applied, where the downcomer was nodalized into a single node, the break enthalpy might be underestimated especially after ACC injection initiated, since the two-dimensional effects of the downcomer was not taken into account. In fact, the break flow was overestimated after about 400 sec, and therefore the the mass inventory was underestimated. This is one of the reasons why DNBs were calculated to occure on the contrary to the experimental data, which will be discussed later.

6.3.6 Thermal-Hydraulic Behavior in Core

The cladding surface temperatures calculated at the active core, i.e. nodes 26, 27, 28 and 29, are shown in Figs. 6.37(a), (b), (c) and (d), respectively, alog with the experimental data. The calculated heat transfer coefficients at the core nodes are shown in Figs. 6.38(a) through (d). It is clearly shown in these figures that the DNBs were calculated to occur at about 1550 sec after rupture. In the calculation, as shown in Figs. 6.16 to 6.18, the ACC injection was terminated after about 1050 sec untill about 1550 sec and therfore the core inlet and outlet flows were seriously decreased (see Figs. 6.39 and 6.40). Subsequently, the calculated coolant qualities at the core nodes gradually increased during the time period (see Figs. 6.41(a) to (d)) and finally DNBs were calculated to occur. But quenching was also calculated to occur soon after the DNB due to the core recovery following ACC injection.

6.3.7 SG Secondary System

The pressure calculated at the SG secondary system is shown in Fig. 6.42, along with the experimental data. The agreement of the calculated results to the experimental data was poor. As for

the overestimation until auxilially feed water injection initiatin, i.e. 75 sec after rupture, the effects of the leakage flow from the main steam control valve might be effective. In the Experiment L3-6, the valve was cycled due to electronic noise imposed on the transducer signal. There was possibility that the same situation happened in the Experiment L3-1 since the observed SG secondary pressure started to decrease before 100 sec although the primary system pressure stayed higher than the secondary pressure until about 400 sec.

The reason why the calculated depressurization rate after 400 sec to 1000 sec was larger than that in the experiment was, as presented in Subsec. 4.4, that the leakage flow from the steam outlet at the same mass flow rate as that of auxiliary feed water was assumed. Since in analyses of small break LOCAs, the auxiliary feed water injection plays an important role, a model to describe low enthalpy auxiliary feed water injection should be implemented in THYDE-P.

6.3.8 Coolant Temperature

The coolant temperatures at the intact loop hot and cold legs, the broken loop hot and cold legs, and the upper plenum are shown in Figs. 6.43, 6.19, 6.44, 6.45 and 6.46, respectively, along with the experimental data. The calculated coolant temperatures in the figures are almost at the coolant saturation temperatures. It should be noted that superheated steam was not observed at the upper plenum (see Fig. 6.46) but was observed at the intact loop and broken loop hot legs (see Figs. 6.43 and 6.44). One of the reasons was surmised to be that the flows were stratified and the steam temperatures near the duct walls might be measured. In the calculation, however, the coolant temperature stayed at the saturation temperature during this period since only the node average properties are calculated.

7. CPU Time and Time Step Width

The CPU time required for the present calculation by a FACOM M-200 computer was about 5 hours. The ratio of the CPU time to the problem time was about 9. The computer core strage requirment was 1200 kB. The maximum time step width allowed by an input in the present calculation was shown as follows.

$$\Delta t = \begin{cases} 0.008 \text{ sec} & \text{for } 0 < t < 12 \text{ sec} \\ 0.016 \text{ sec} & \text{for } 12 < t < 49 \text{ sec} \\ 0.032 \text{ sec} & \text{for } 49 < t < 300 \text{ sec} \\ 0.064 \text{ sec} & \text{for } 300 < t < 3000 \text{ sec} \end{cases}$$

8. Conclusion

The main purpose of the present calculation were to investigate the system performance of THYDE-P to small break LOCAs and to verify the applicability of THYDE-P to small break LOCAs. Since the overall trends of the experimental data were successfully reproduced by the present calculation, the applicability of THYDE-P to small break LOCAs was verified, although several problems still remained. The problems, which have been pointed out in the course of the present calculation could be summarized as follows.

(1) The present model for the SG secondary system should be improved, as it has already been pointed out. Capability to analyze spacial non-equilibrium effects within the SG secondary system, especially during auxiliary feed water injection, should be implemented,

(2) Since it is important to describe phase separation in analyses of small break LOCAs, improvements with respect to the present drift flux model should be performed, and

(3) The time delay model for density change has large effects on the system thermal-hydraulics during ECC water injection, so that a model to evaluate the delay parameter realistically must be needed.

Acknowledgement

The authors would like to express their thanks to Mr. K. Sato, Chief of Reactor Safety Code Development Laboratory, and the members of the laboratory for their useful discussions.

7. CPU Time and Time Step Width

The CPU time required for the present calculation by a FACOM M-200 computer was about 5 hours. The ratio of the CPU time to the problem time was about 9. The computer core strage requirment was 1200 kB. The maximum time step width allowed by an input in the present calculation was shown as follows.

$$\Delta t = \begin{cases} 0.008 \text{ sec} & \text{for } 0 < t < 12 \text{ sec} \\ 0.016 \text{ sec} & \text{for } 12 < t < 49 \text{ sec} \\ 0.032 \text{ sec} & \text{for } 49 < t < 300 \text{ sec} \\ 0.064 \text{ sec} & \text{for } 300 < t < 3000 \text{ sec} \end{cases}$$

8. Conclusion

The main purpose of the present calculation were to investigate the system performance of THYDE-P to small break LOCAs and to verify the applicability of THYDE-P to small break LOCAs. Since the overall trends of the experimental data were successfully reproduced by the present calculation, the applicability of THYDE-P to small break LOCAs was verified, although several problems still remained. The problems, which have been pointed out in the course of the present calculation could be summarized as follows.

(1) The present model for the SG secondary system should be improved, as it has already been pointed out. Capability to analyze spacial non-equilibrium effects within the SG secondary system, especially during auxiliary feed water injection, should be implemented,

(2) Since it is important to describe phase separation in analyses of small break LOCAs, improvements with respect to the present drift flux model should be performed, and

(3) The time delay model for density change has large effects on the system thermal-hydraulics during ECC water injection, so that a model to evaluate the delay parameter realistically must be needed.

Acknowledgement

The authors would like to express their thanks to Mr. K. Sato, Chief of Reactor Safety Code Development Laboratory, and the members of the laboratory for their useful discussions.

7. CPU Time and Time Step Width

The CPU time required for the present calculation by a FACOM M-200 computer was about 5 hours. The ratio of the CPU time to the problem time was about 9. The computer core strage requirment was 1200 kB. The maximum time step width allowed by an input in the present calculation was shown as follows.

$$\Delta t = \begin{cases} 0.008 \text{ sec} & \text{for } 0 < t < 12 \text{ sec} \\ 0.016 \text{ sec} & \text{for } 12 < t < 49 \text{ sec} \\ 0.032 \text{ sec} & \text{for } 49 < t < 300 \text{ sec} \\ 0.064 \text{ sec} & \text{for } 300 < t < 3000 \text{ sec} \end{cases}$$

8. Conclusion

The main purpose of the present calculation were to investigate the system performance of THYDE-P to small break LOCAs and to verify the applicability of THYDE-P to small break LOCAs. Since the overall trends of the experimental data were successfully reproduced by the present calculation, the applicability of THYDE-P to small break LOCAs was verified, although several problems still remained. The problems, which have been pointed out in the course of the present calculation could be summarized as follows.

(1) The present model for the SG secondary system should be improved, as it has already been pointed out. Capability to analyze spacial non-equilibrium effects within the SG secondary system, especially during auxiliary feed water injection, should be implemented,

(2) Since it is important to describe phase separation in analyses of small break LOCAs, improvements with respect to the present drift flux model should be performed, and

(3) The time delay model for density change has large effects on the system thermal-hydraulics during ECC water injection, so that a model to evaluate the delay parameter realistically must be needed.

Acknowledgement

The authors would like to express their thanks to Mr. K. Sato, Chief of Reactor Safety Code Development Laboratory, and the members of the laboratory for their useful discussions.

Reference

(1) Asahi, Y., "Description of THYDE-P Code (Preliminary Report of Methods and Models)", JAERI-M7751, 1978.

(2) Asahi, Y. and Hirano, M., "Verification Study of LOCA Analysis Code THYDE-P (Sample Calculation Run 10)", JAERI-M8560, 1979.

(3) Hirano, M. and Asahi, Y., "Through Analysis of LOFT L2-2 by THYDE-P Code (I) (Sample Calculation Run 30)", JAERI-M9535, 1981.

(4) Hirano, M., "Through Analysis of LOFT L2-3 by THYDE-P Code (Sample Calculation Run 40)", JAERI-M9765, 1981.

(5) Shimizu, T. and Asahi, Y., "Through Calculation of 1,100 MWe PWR Large Break LOCA by THYDE-P (Sample Calculation Run 20)", JAERI-M9819, 1981.

(6) Reeder, D. L., "LOFT SYSTEM AND TEST DESCRIPTION (5.5FT CORE1 LOCES)", NUREG/CR-0247, July 1978.

(7) Moody, F. J., "Maximum Flow Rate of Single Phase and Two-Phase Mixture", Heat Trans.-Trans. ASME, 87 nl, pp 134-142, 1965.

(8) Zaloudek, F. R., "Steam-Water Critical Flow from High Pressure Systems", HW-68936, Hanford works, 1963.

(9) Biasi, L., et. al, "Studies on Burnout : Part 3", Energia Nucleare, 550-536, 1967.

(10) Zuber, N., Tribus, M. and Westwater, J. W., "The Hydrodynamic Crisis in Pool Boiling of Saturated and Subcooled Liquids", International Developments in Heat Transfer, Part II, pp 230-236, 1961.

(11) Dittus, F. W., and Boelter, L. M. K., "Heat Transfer in Automobile Radiators of The Tubular Tube", 2, No. 13, pp 334-461, 1930.

(12) Jens, W. H. and Lottes, P. A., "Analysis of Heat transfer, Burnout, Pressure Drop and Density for High-Pressure Water", ANL-4627, 1951.

(13) Groenevelt, D. C., "An Investigation of Heat Transfer in The Liquid Deficient Regime", Report AECL-3281, Chalk Rever, Ontario, Dec. 1968.

(14) Berenson, P. J., "Film-Boiling Heat Transfer from A Horizontal Surface", J. of Heat Transfer, Vol. 83, pp 351-358, Aug. 1961.

(15) McEligot, D. M., Ormand, L. W. and Perkins, H. C., J. Trans. Amer. Soc. Mech. Engrs., 88, Series C, pp 239-245, May 1966.

(16) Dougal, R. L and Rohsenow, W. M., "Film Boilin on the Inside of Vertical Tubes With Upward Flow of the Fluid at Low Qualities", MIT-TR-9079-26, 1963.

(17) Moore, K. V., "RELAP-4-A Computer Program for Transient Thermal-Hydraulic Analysis", ANCR-1127, Dec. 1973.

(18) McAdams, W. H., "Heat Transmission", 3rd Ed., pp 337, McGrow-Hill, 1954.

(19) McDonough, J. B., Milich, W. and King, E. C., "Partial Film Boiling with Water at 2000 psig in a Round Vertical Tube", MSA Research Corp., Technical Report 62(NP-6976), 1958.

(20) Bayless, P. D and Carpenter, J. M., "Experimental Data Report for LOFT Nuclear Small Break Experiment L3-1", NUREG/CR-1145,1980.

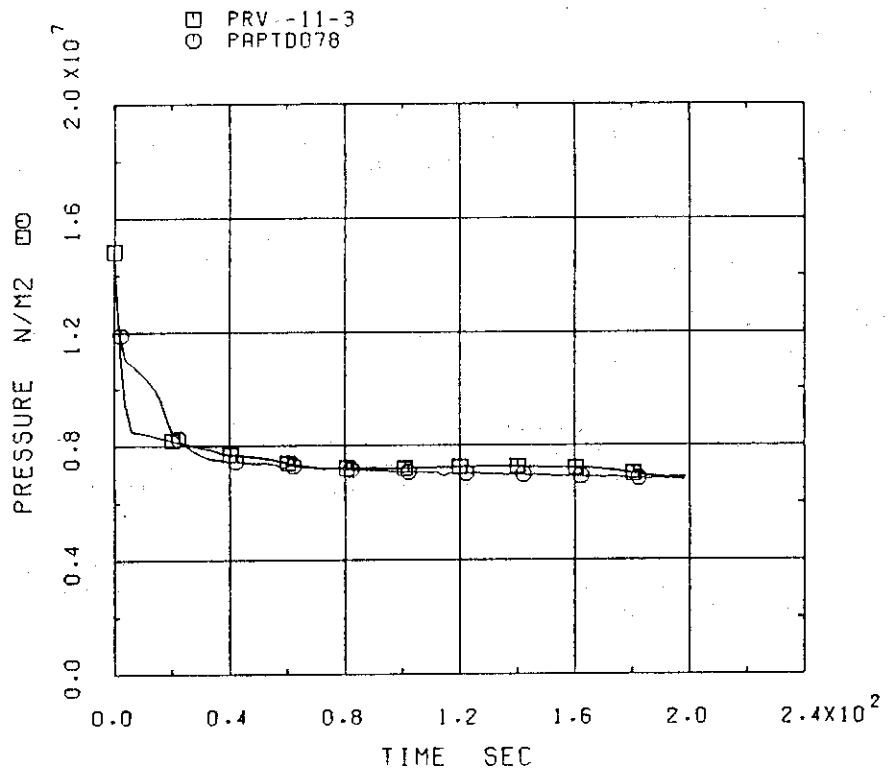

Fig.6.1 Intact loop hot leg pressure (short range)

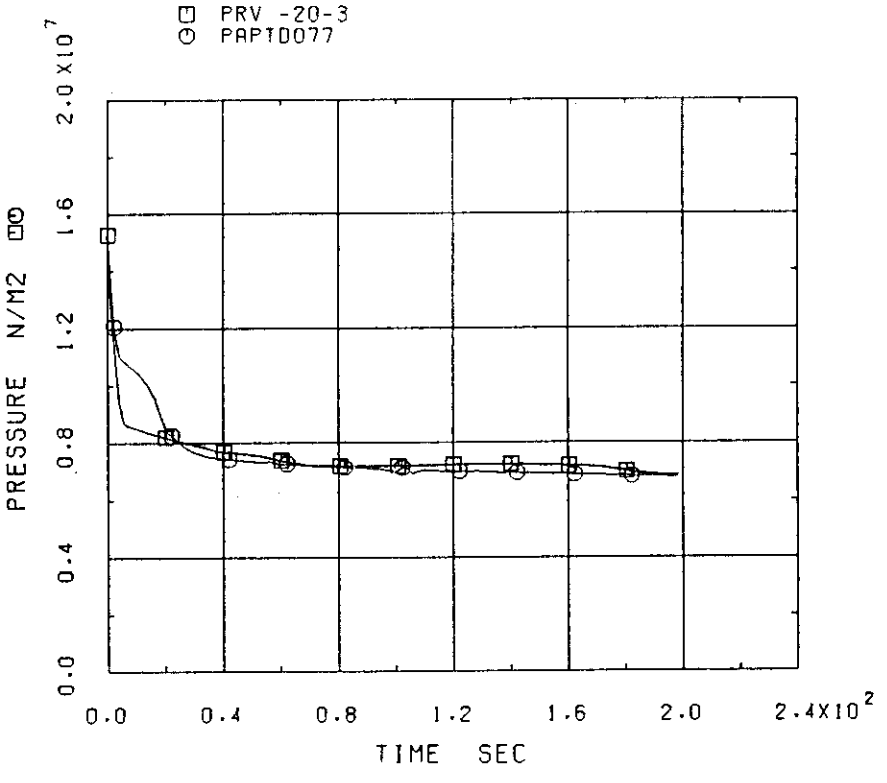

Fig.6.2 Intact loop cold leg pressure (short range)

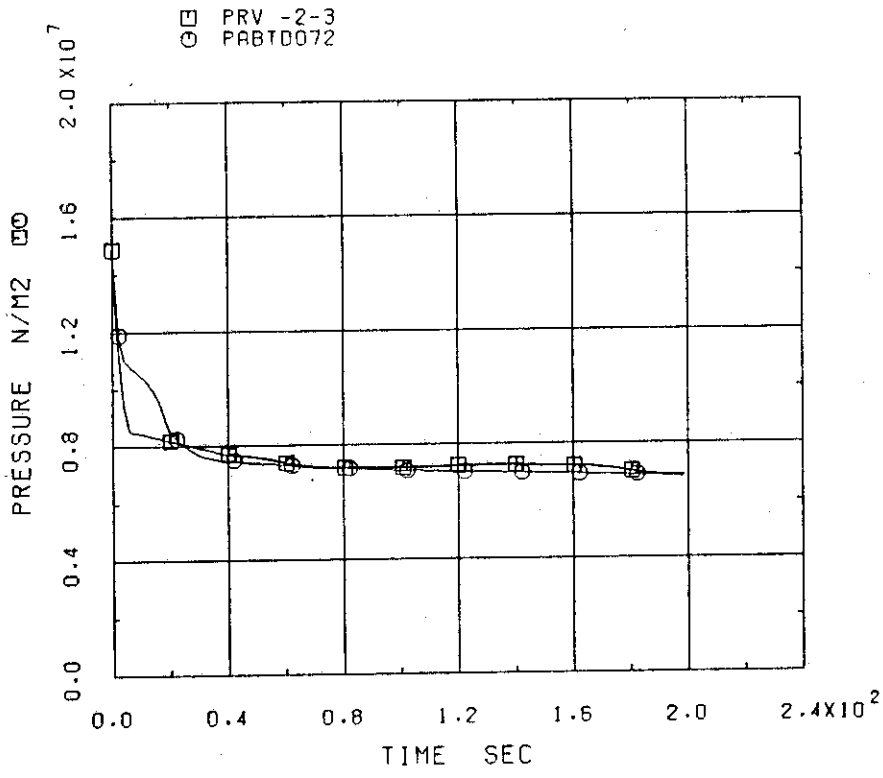

Fig.6.3 Broken loop hot leg pressure (short range)

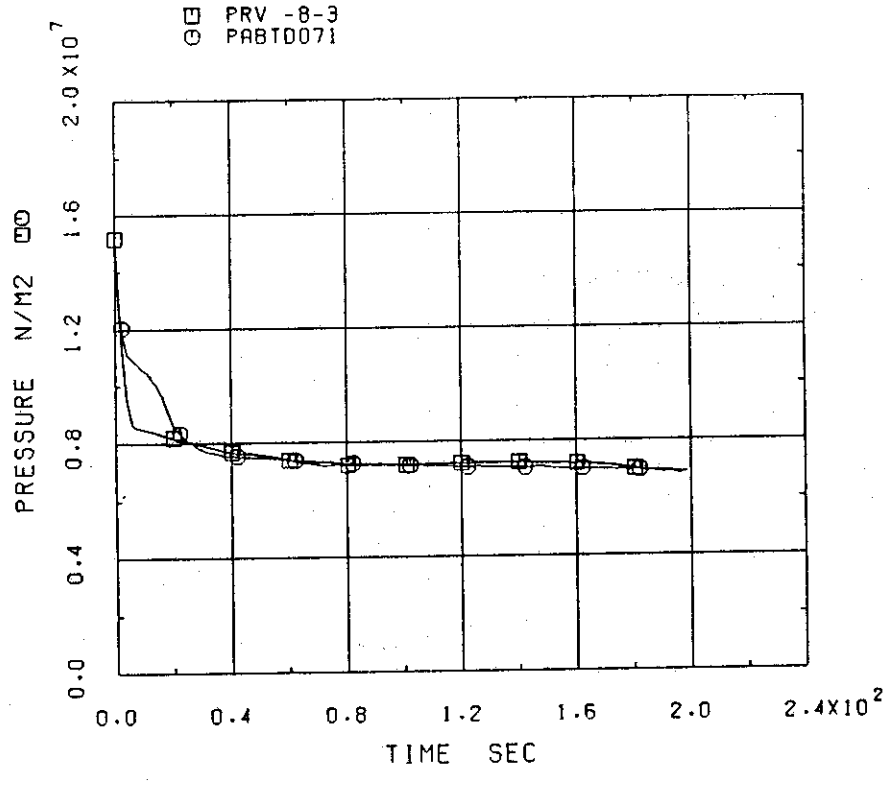

Fig.6.4 Broken loop cold leg pressure (short range)

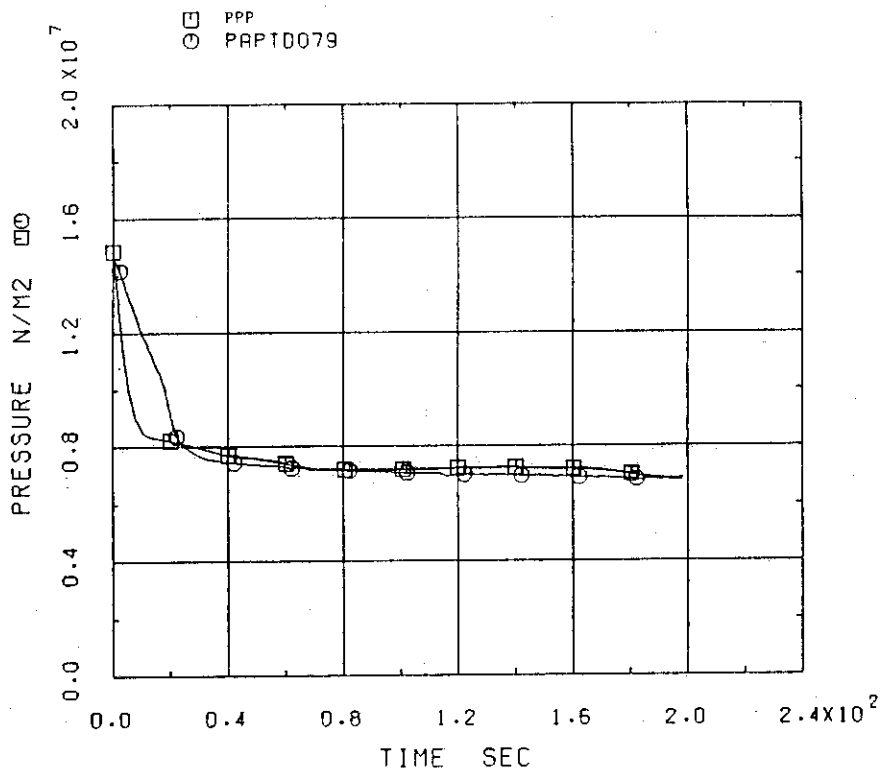

Fig.6.5 Pressurizer pressure (short range)

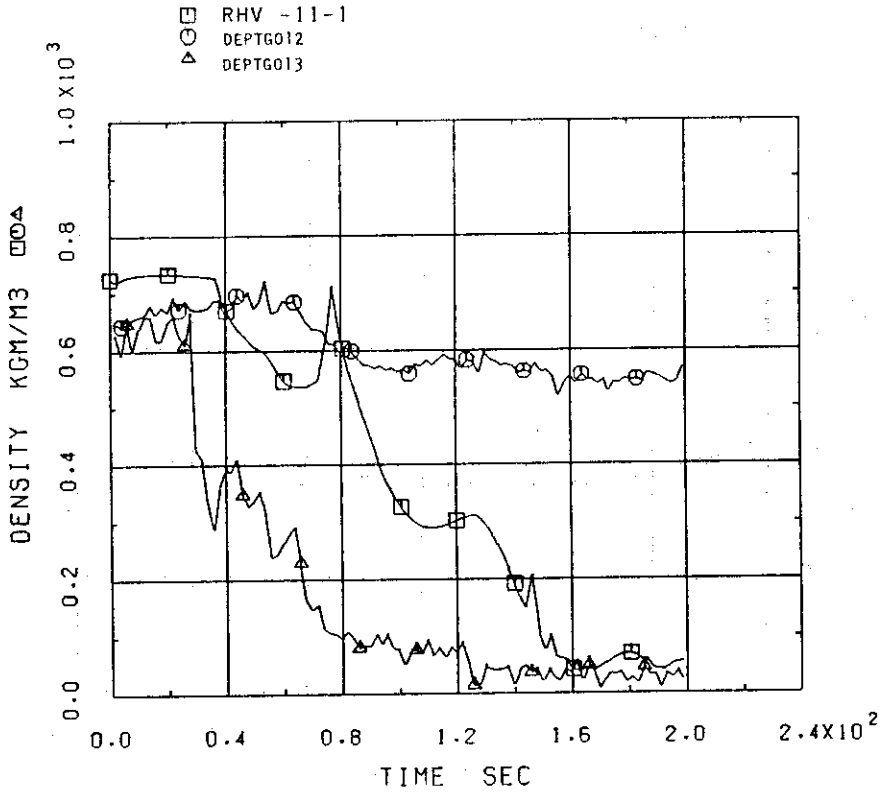

Fig.6.6 Coolant density at intact loop hot leg (short range)

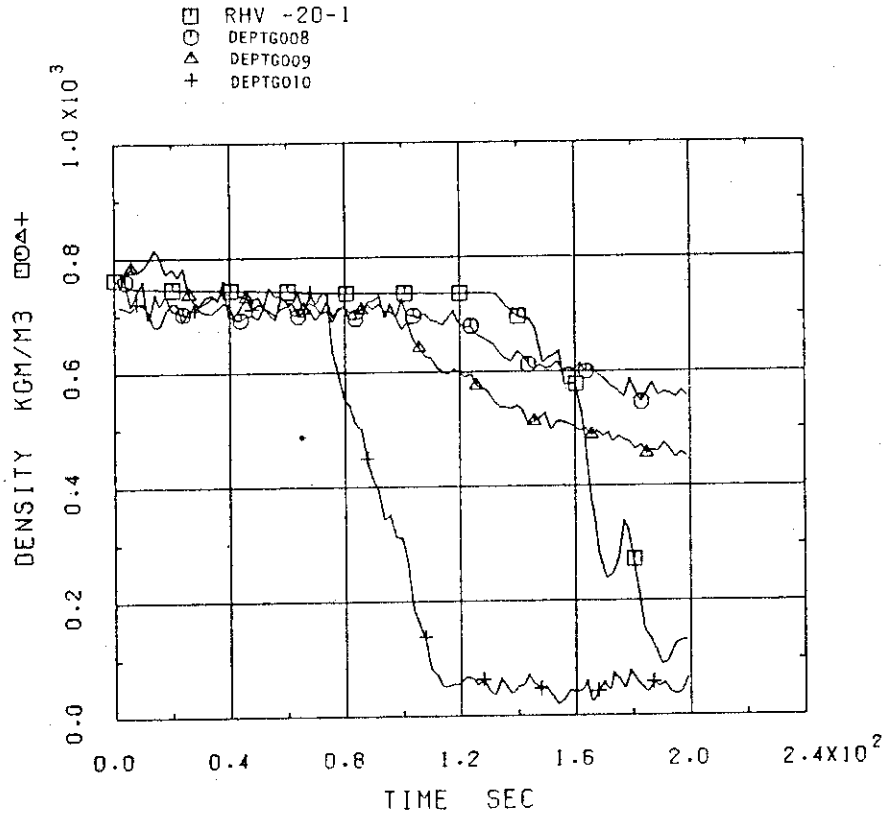

Fig.6.7 Coolant density at intact loop cold leg (short range)

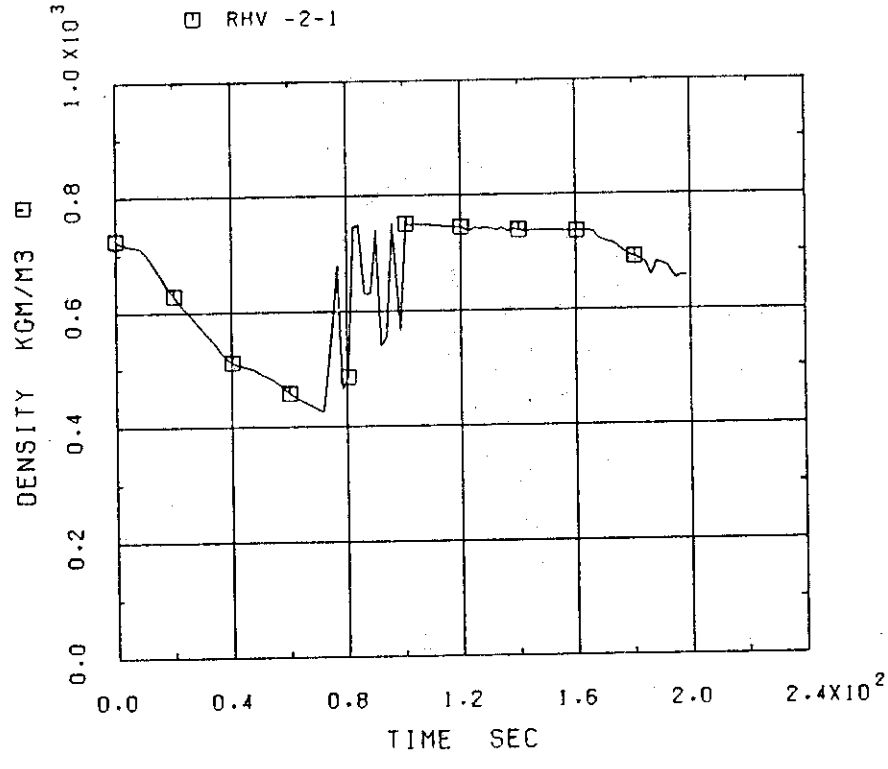

Fig.6.8 Coolant density at broken loop hot leg (short range)

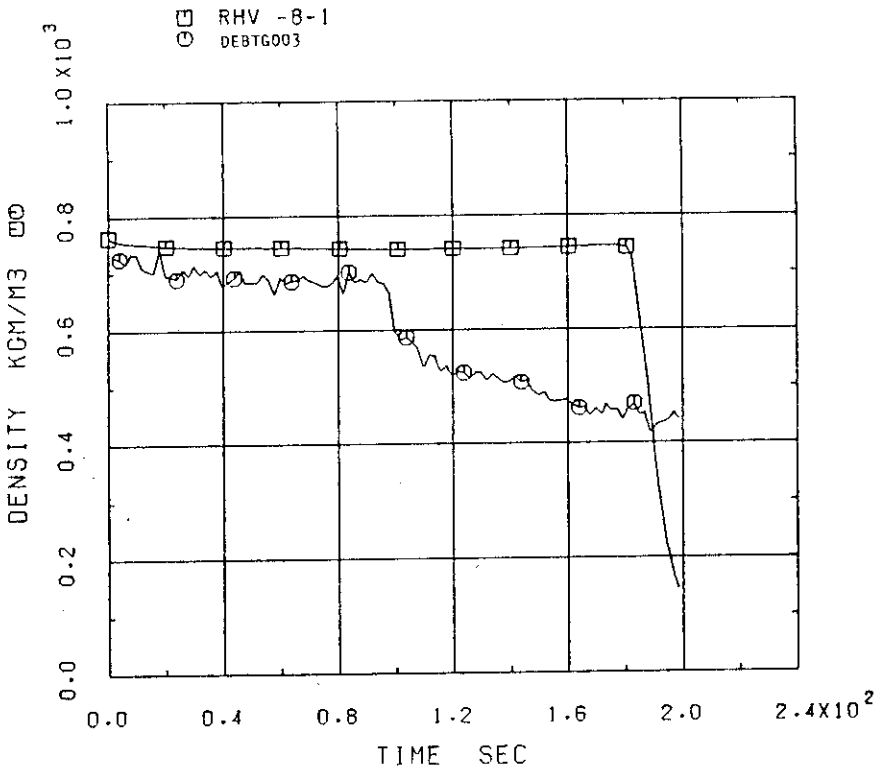

Fig.6.9 Coolant density at broken loop cold leg (short range)

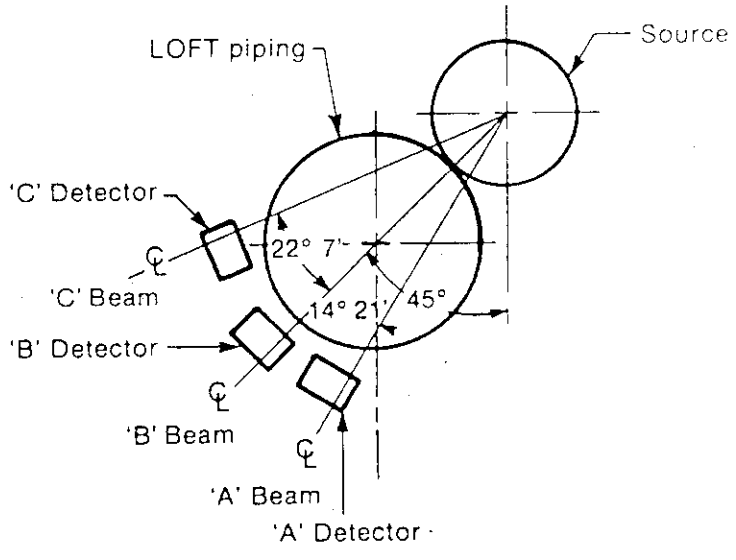

Fig.6.10 Relation of source and detectors to pipe for typical densitometers

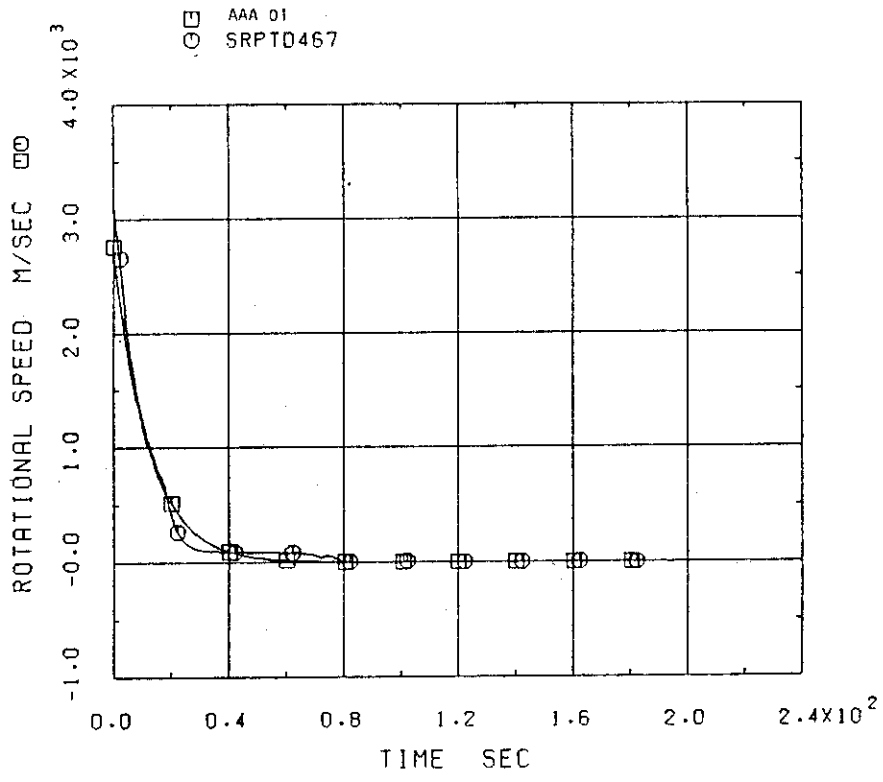

Fig.6.11 Pump rotational speed

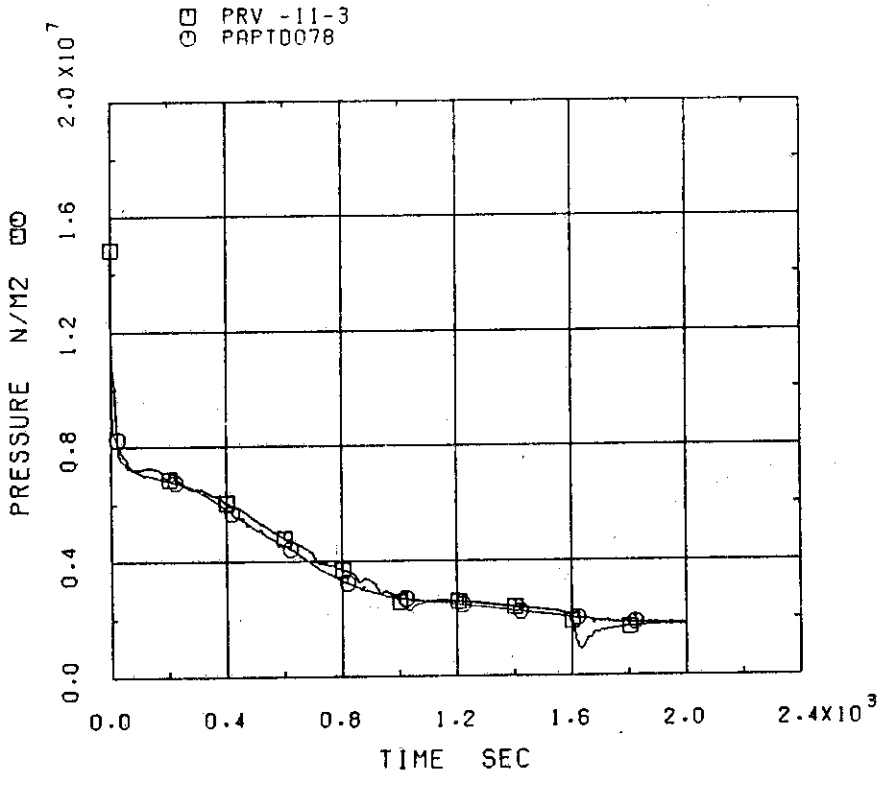

Fig.6.12 Intact loop hot leg pressure

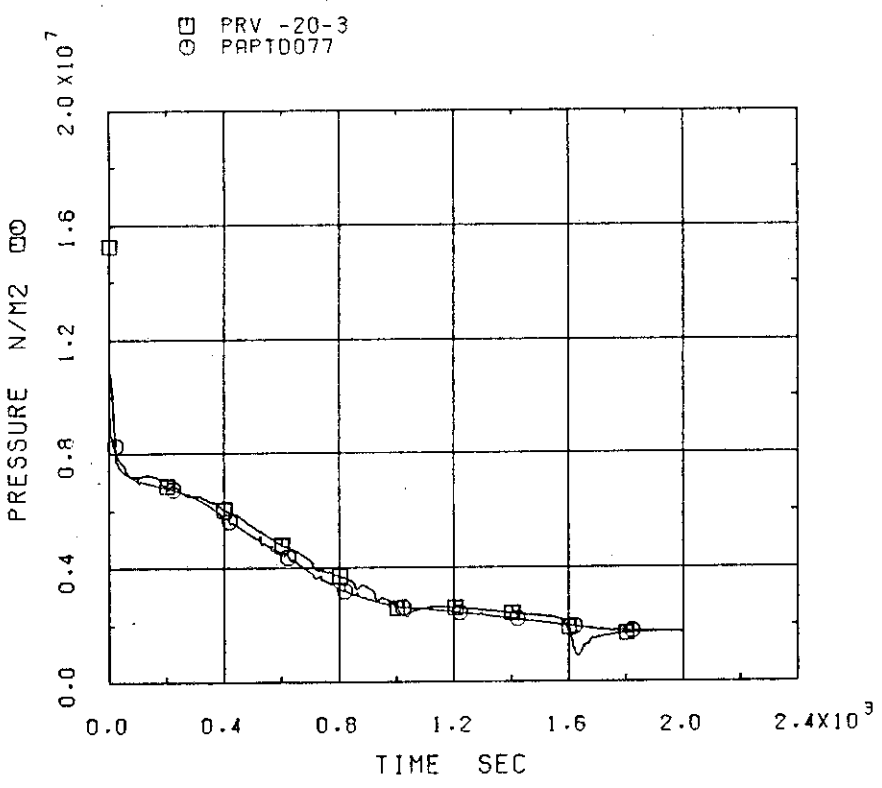

Fig.6.13 Intact loop cold leg pressure

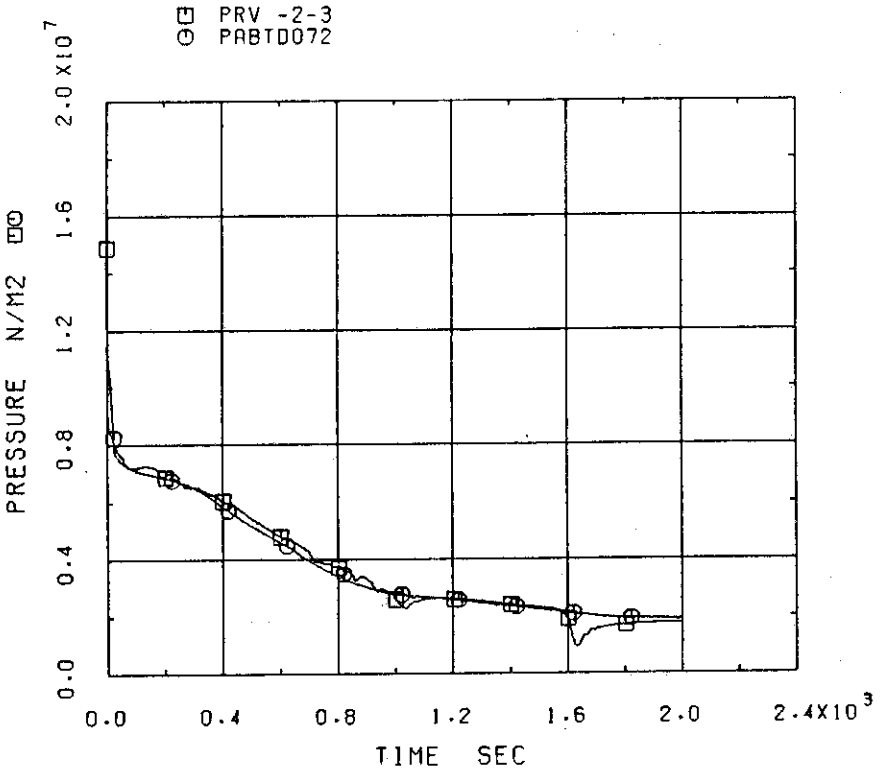

Fig.6.14 Broken loop hot leg pressure

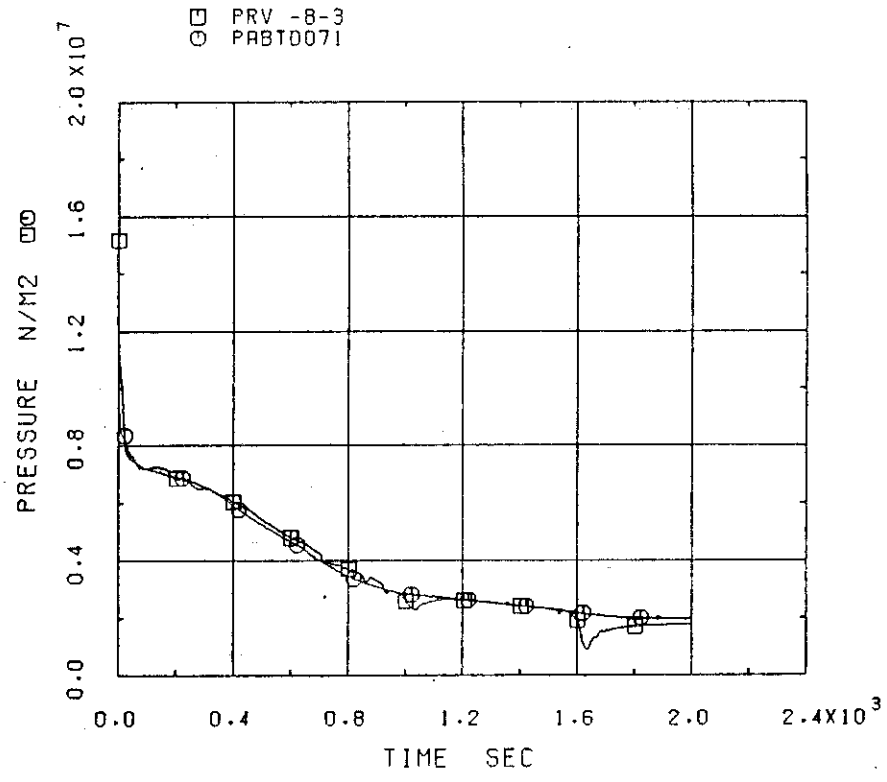

Fig.6.15 Broken loop cold leg pressure

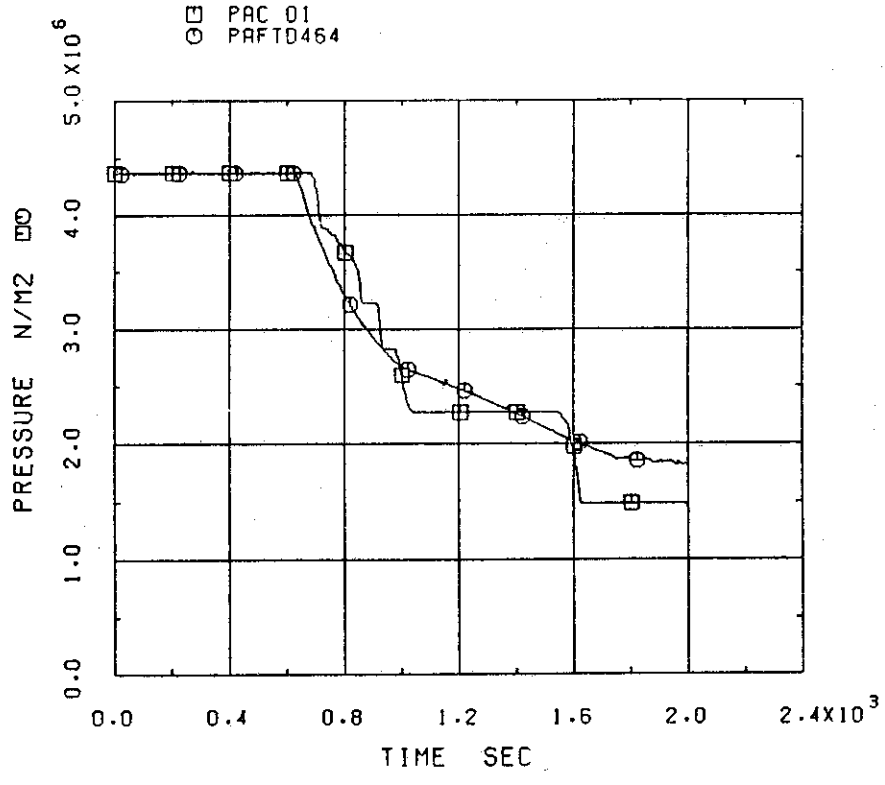

Fig.6.16 Accumulator pressure

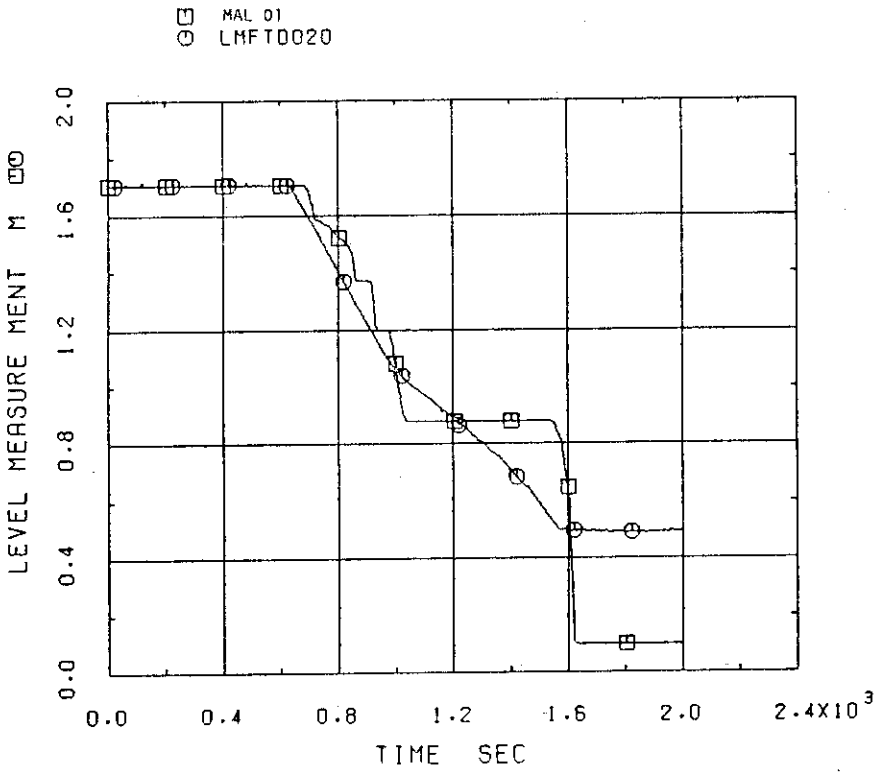

Fig.6.17 Accumulator liquid level

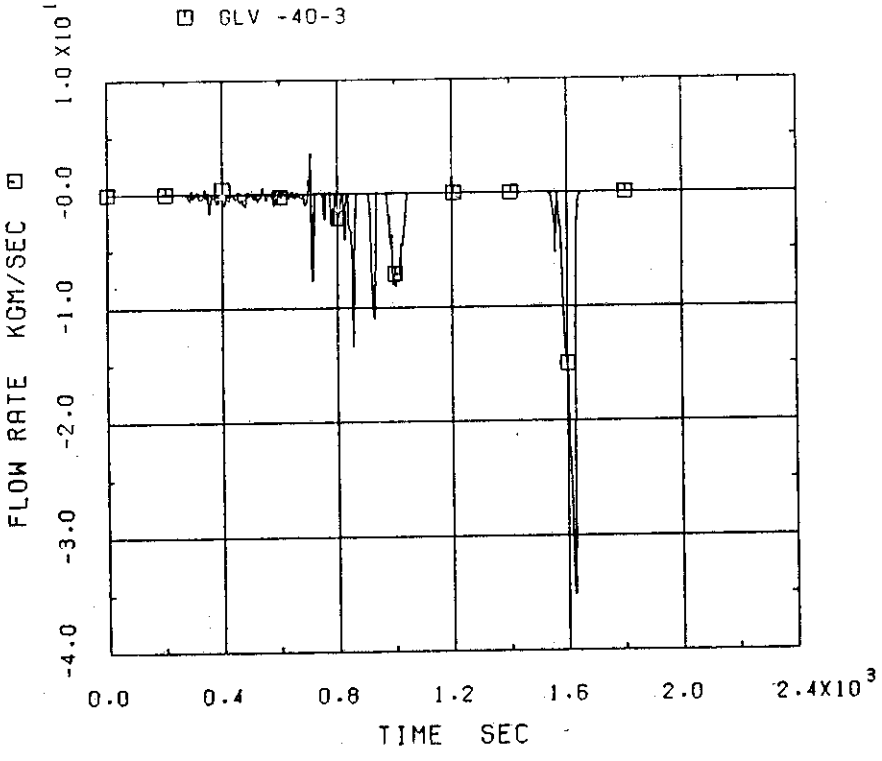

Fig.6.18 Accumulator injection mass flow rate

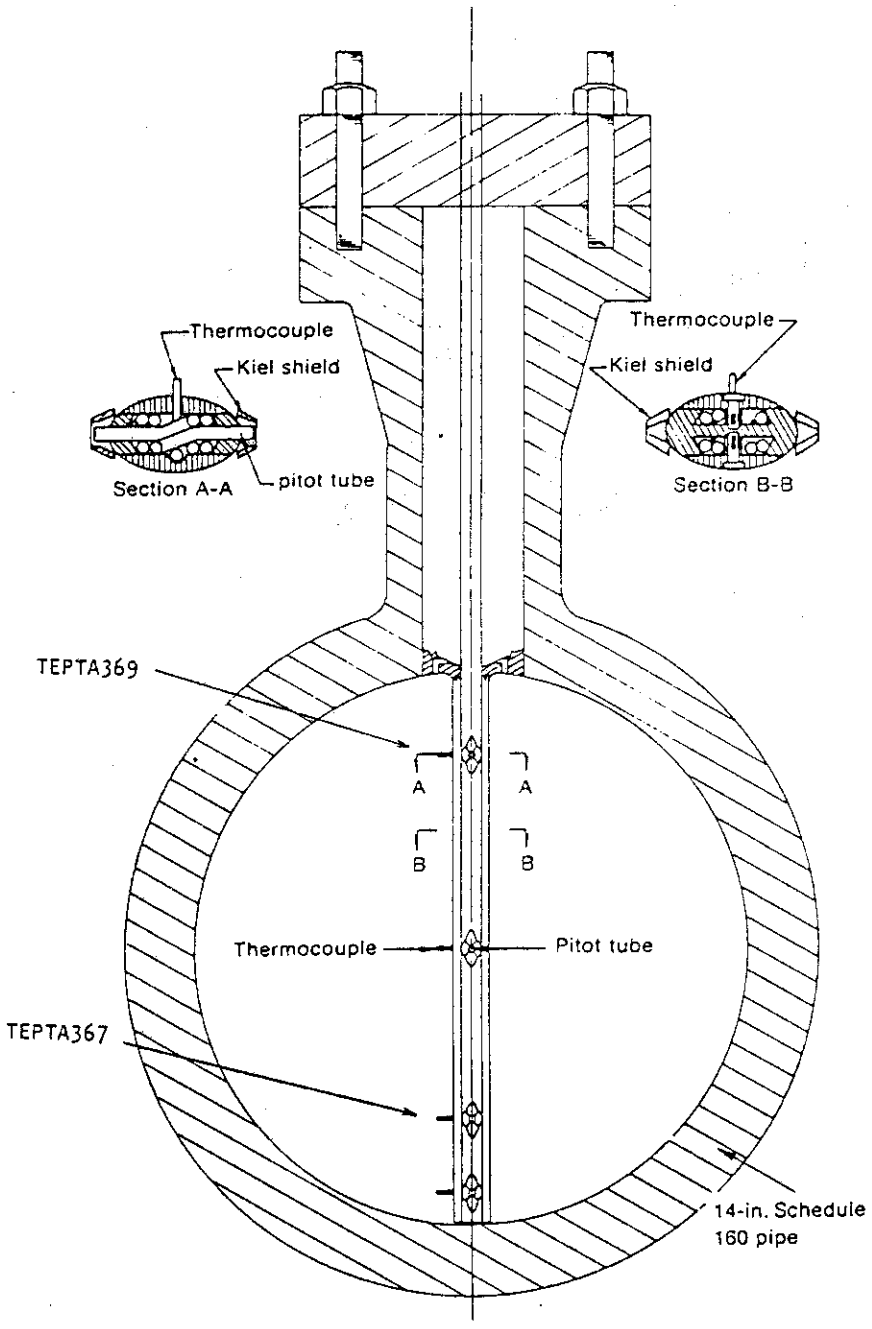

Fig.6.19 ECC Pitot tube rake in pipe

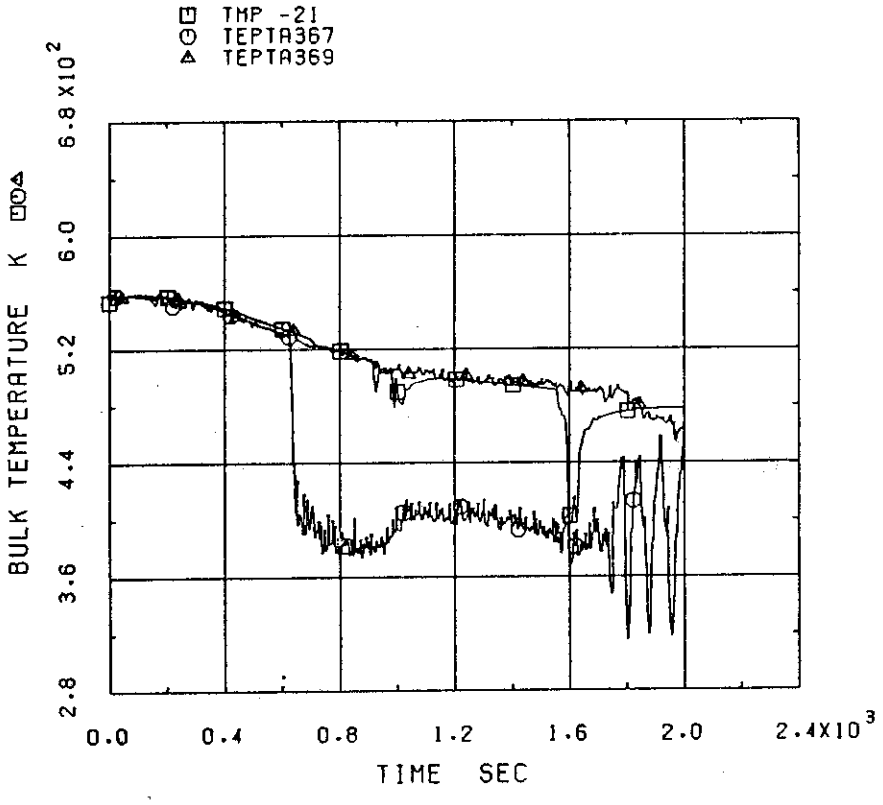

Fig.6.20 Coolant temperature at intact loop cold leg

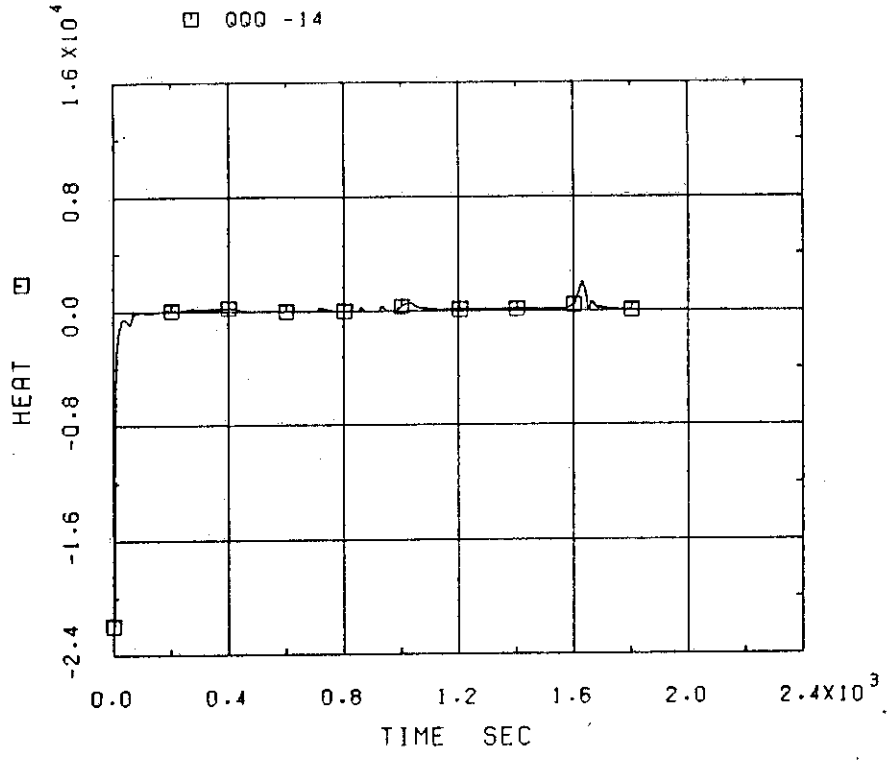

(a) Node 14

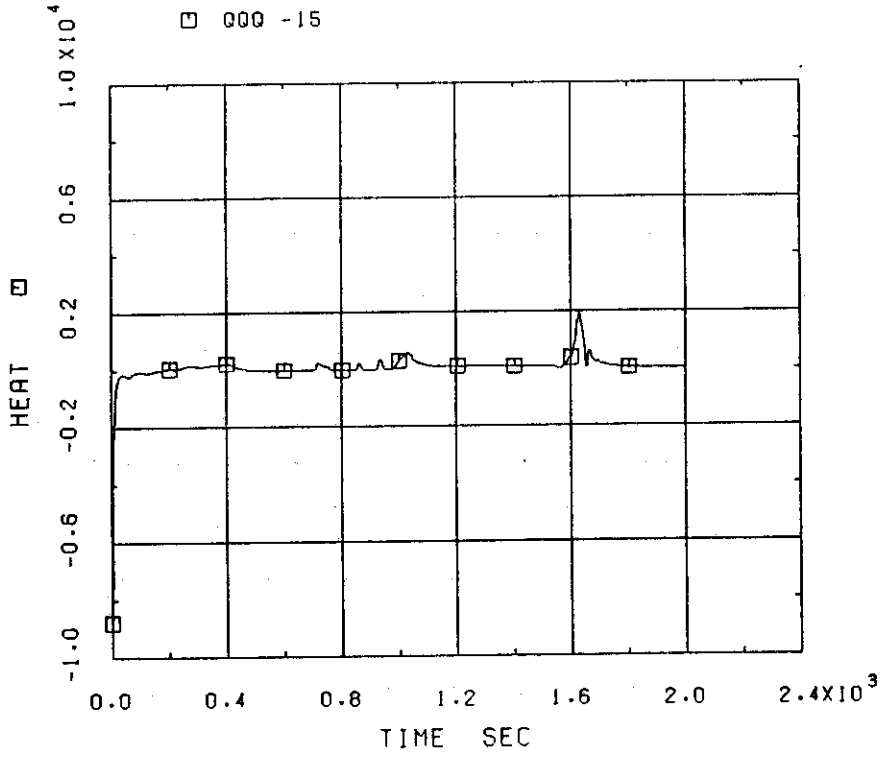

(b) Node 15

Fig.6.21 Heat from SG secondary system

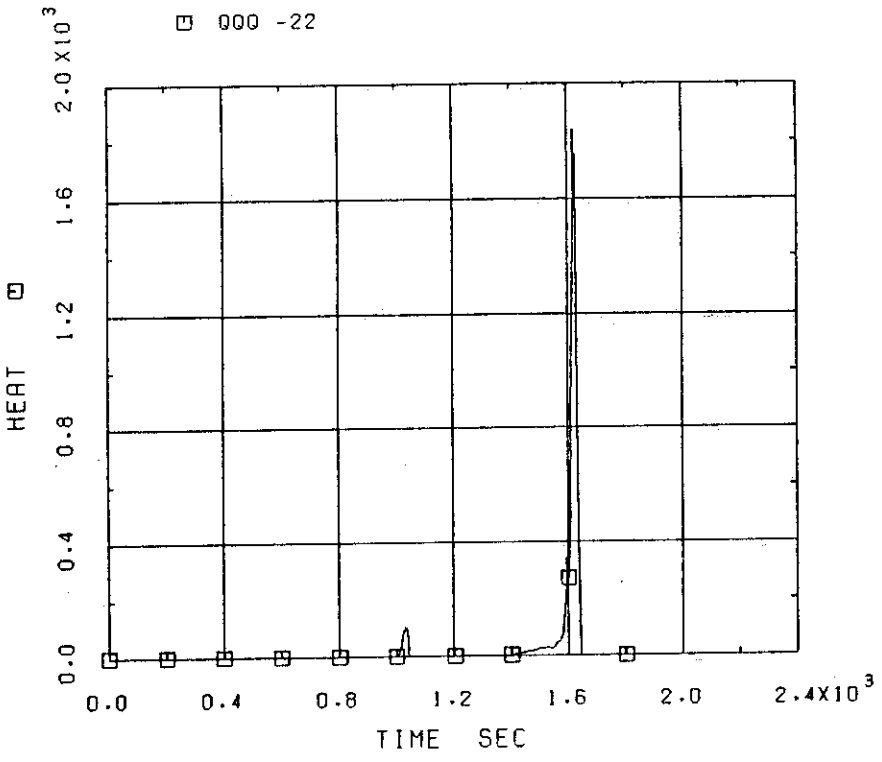

Fig.6.22 Heat addition from structure at downcomer

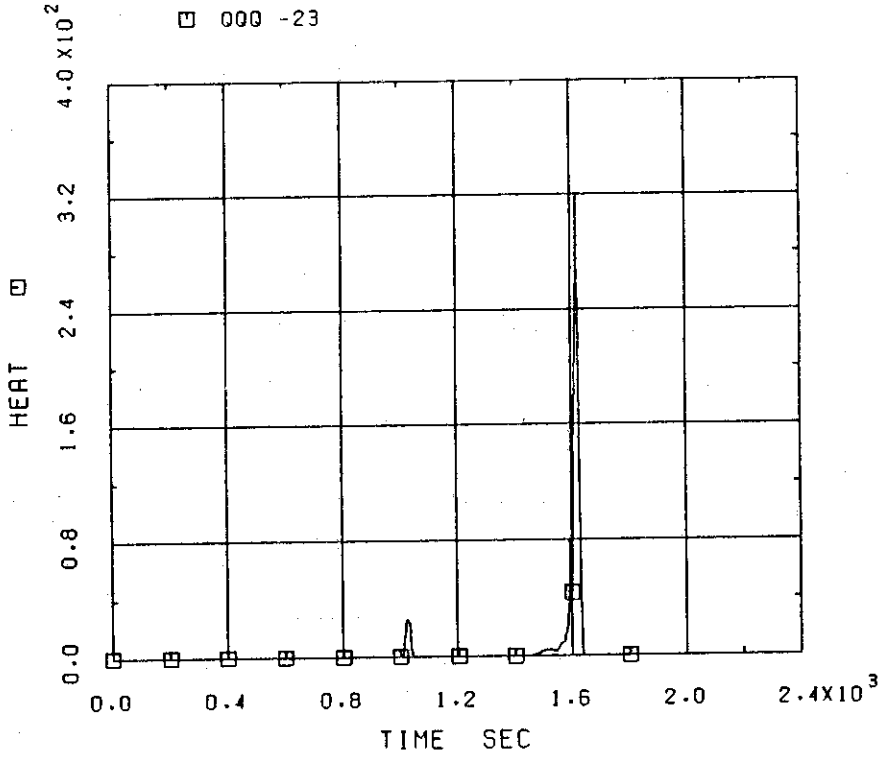

Fig.6.23 Heat addition from structure at lower plenum

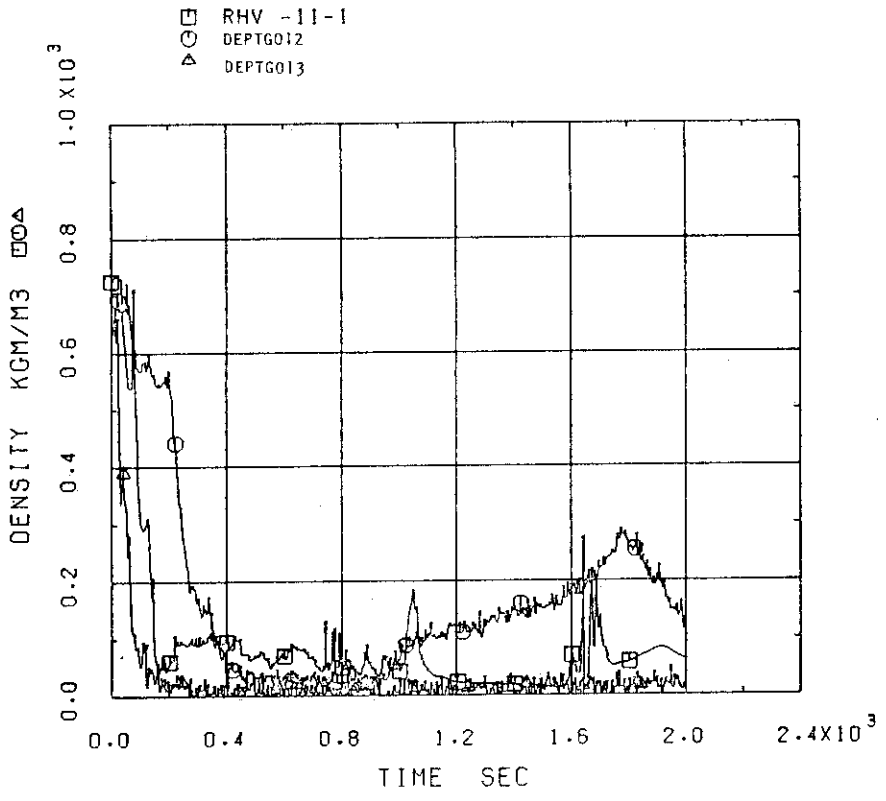

Fig.6.24 Coolant density at intact loop hot leg

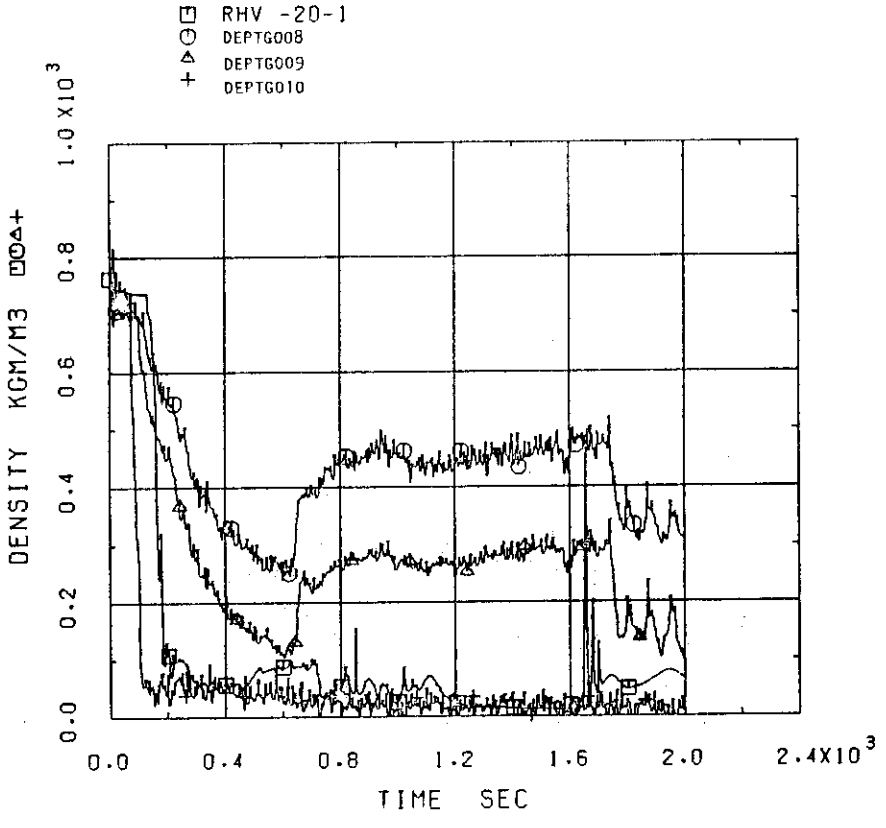

Fig.6.25 Cooland density at intact loop cold leg

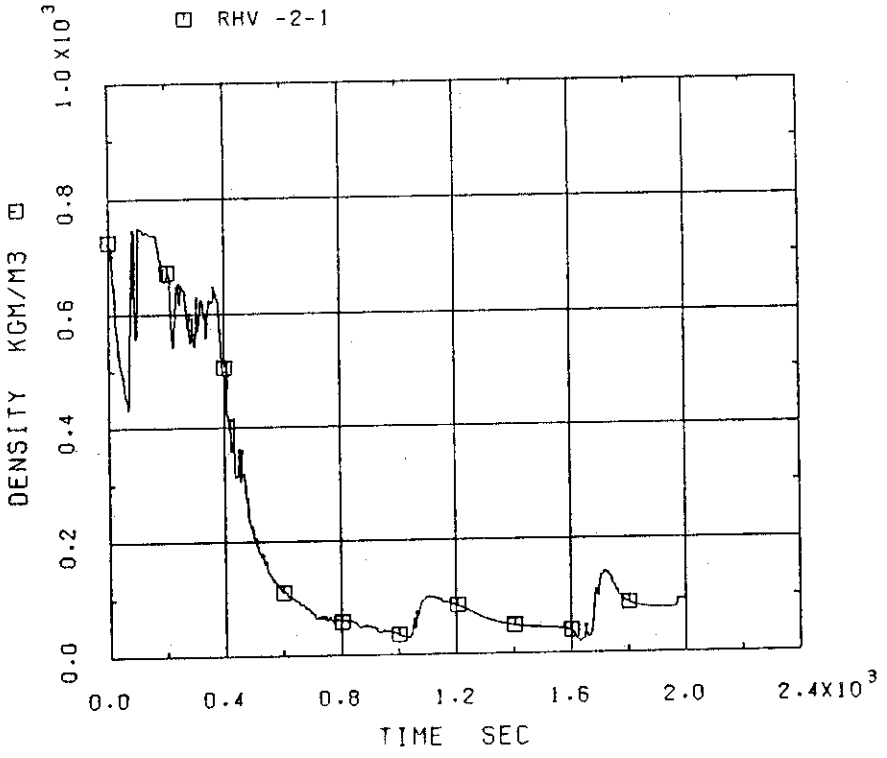

Fig.6.26 Coolant density at broken loop hot leg

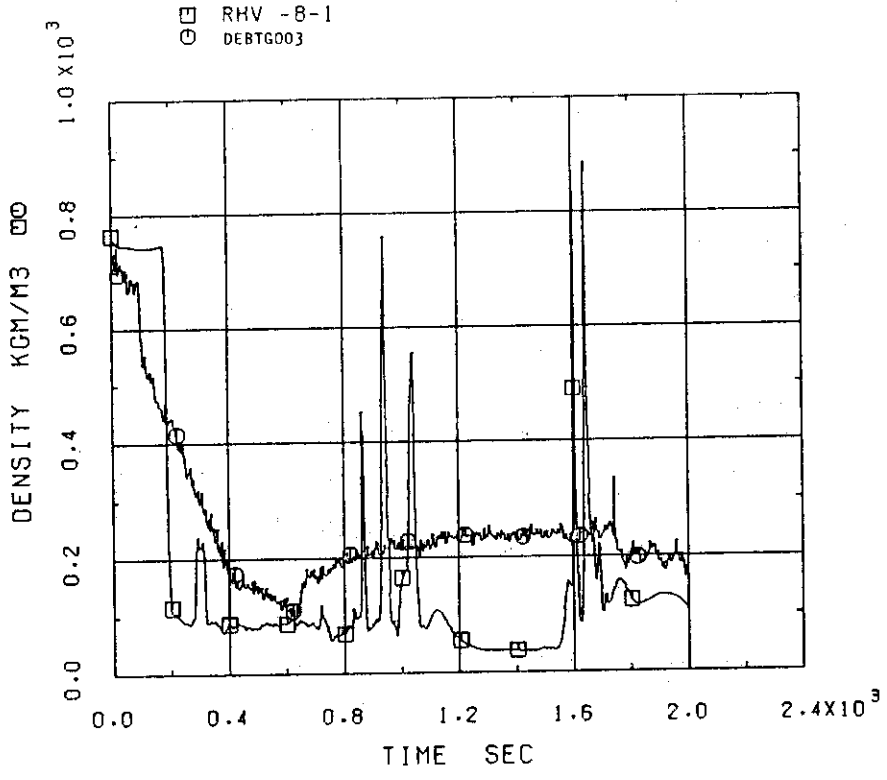

Fig.6.27 Coolant density at broken loop cold leg

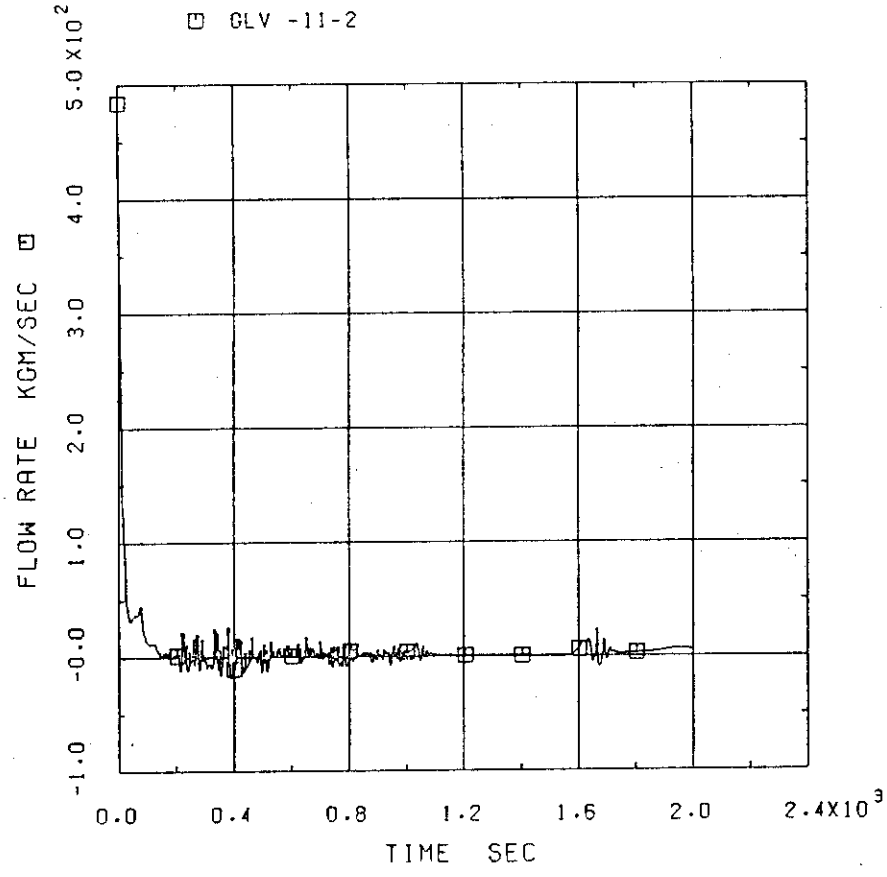

Fig.6.28 Mass flow rate at intact loop hot leg

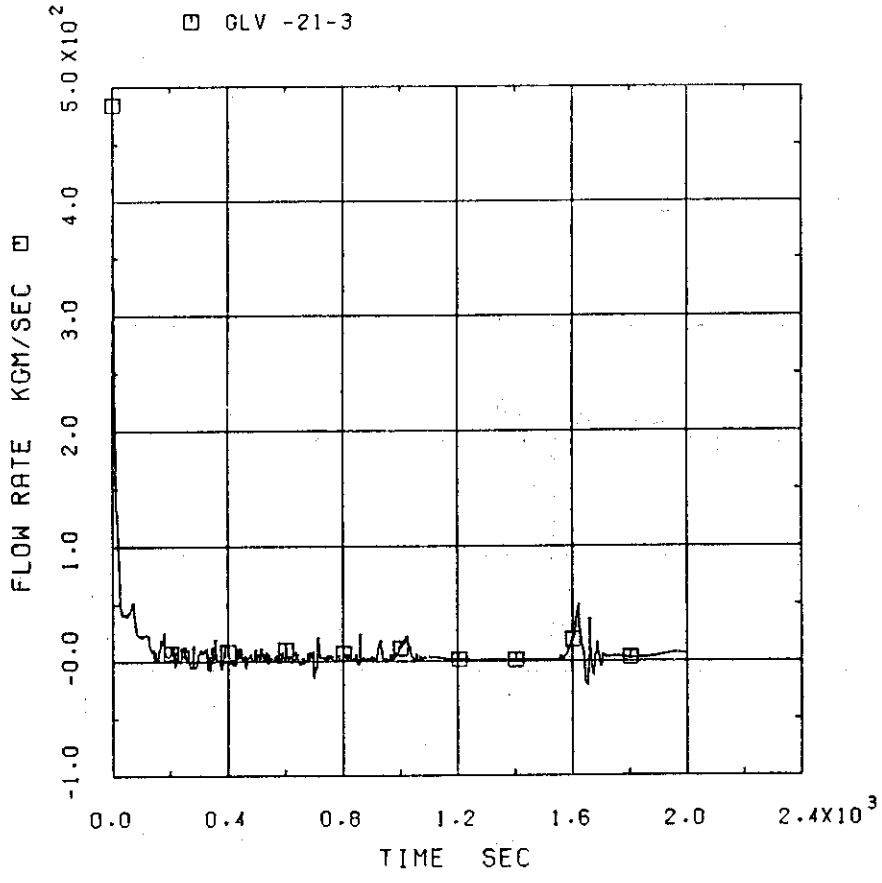

Fig.6.29 Mass flow rate at intact loop cold leg

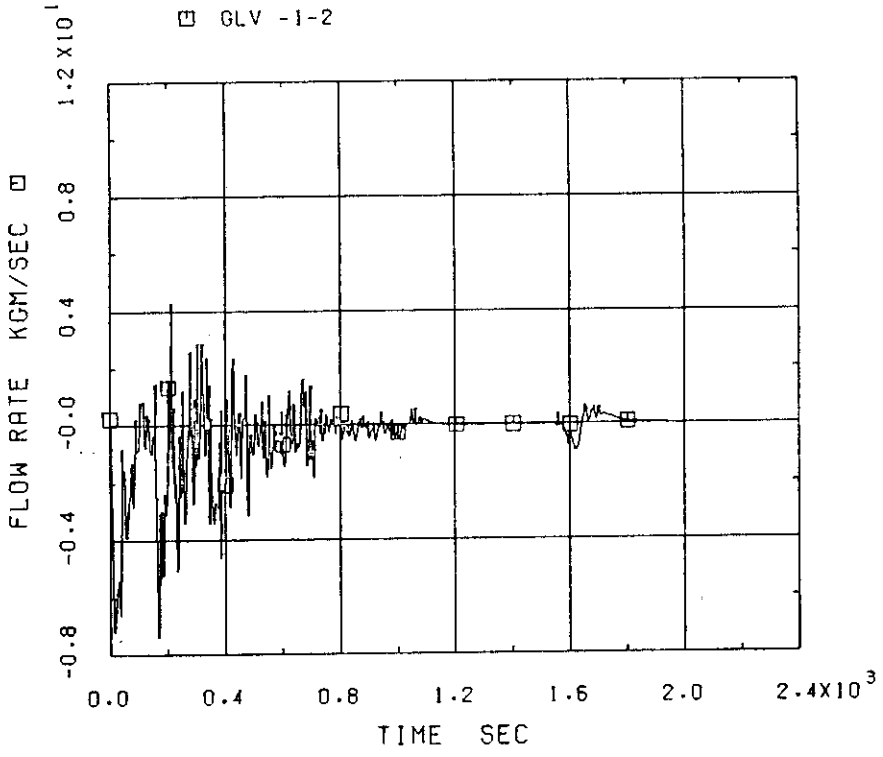

Fig.6.30 Mass flow rate at broken loop hot leg

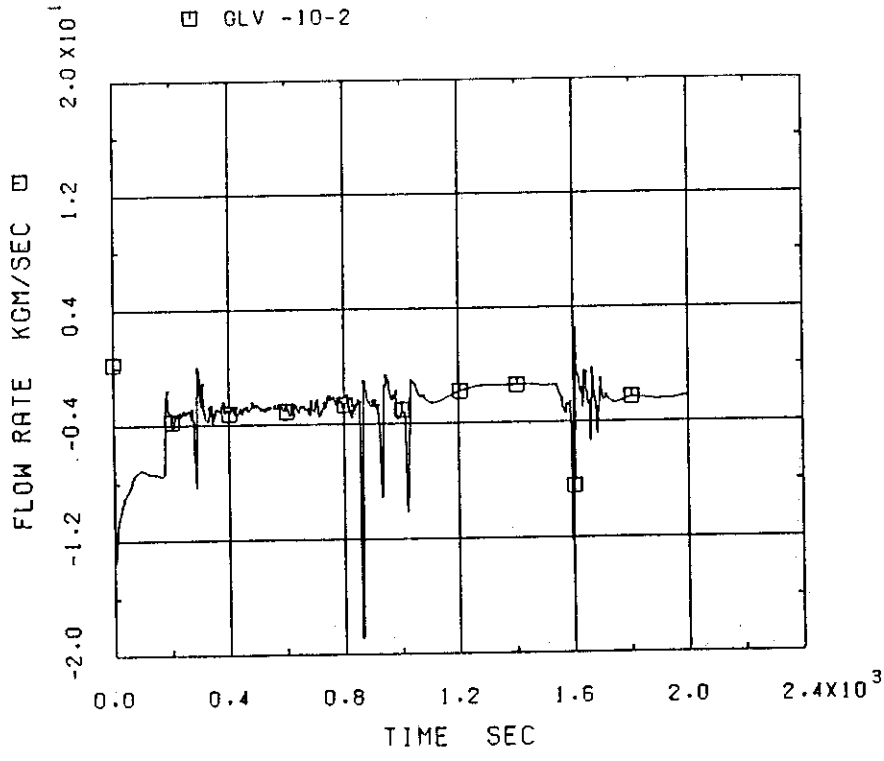

Fig.6.31 Mass flow rate at broken loop cold leg

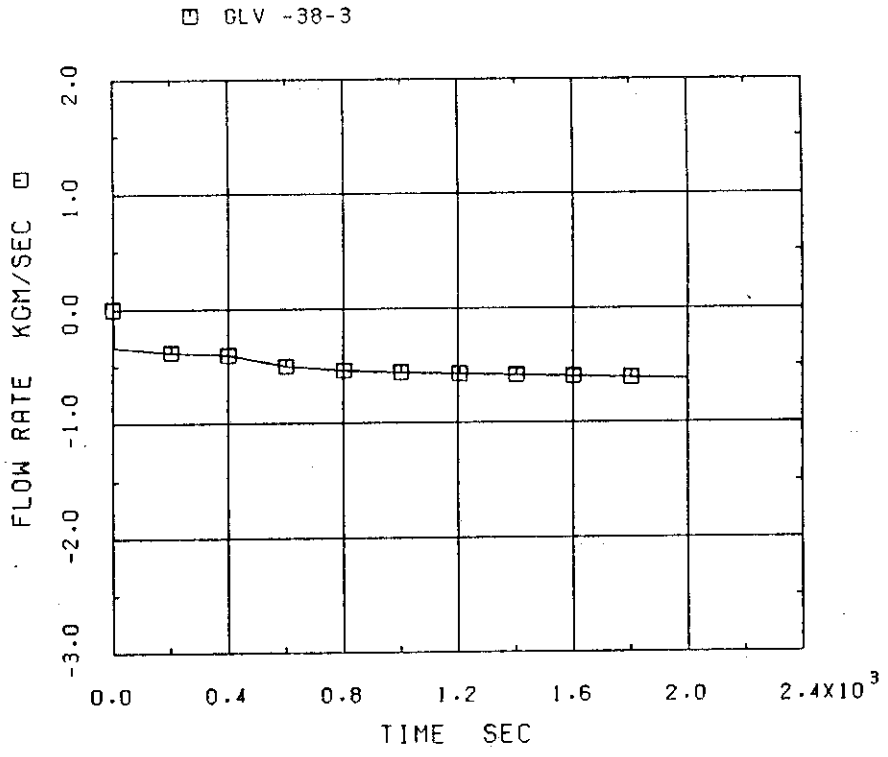

Fig.6.32 HPIS injection mass flow rate

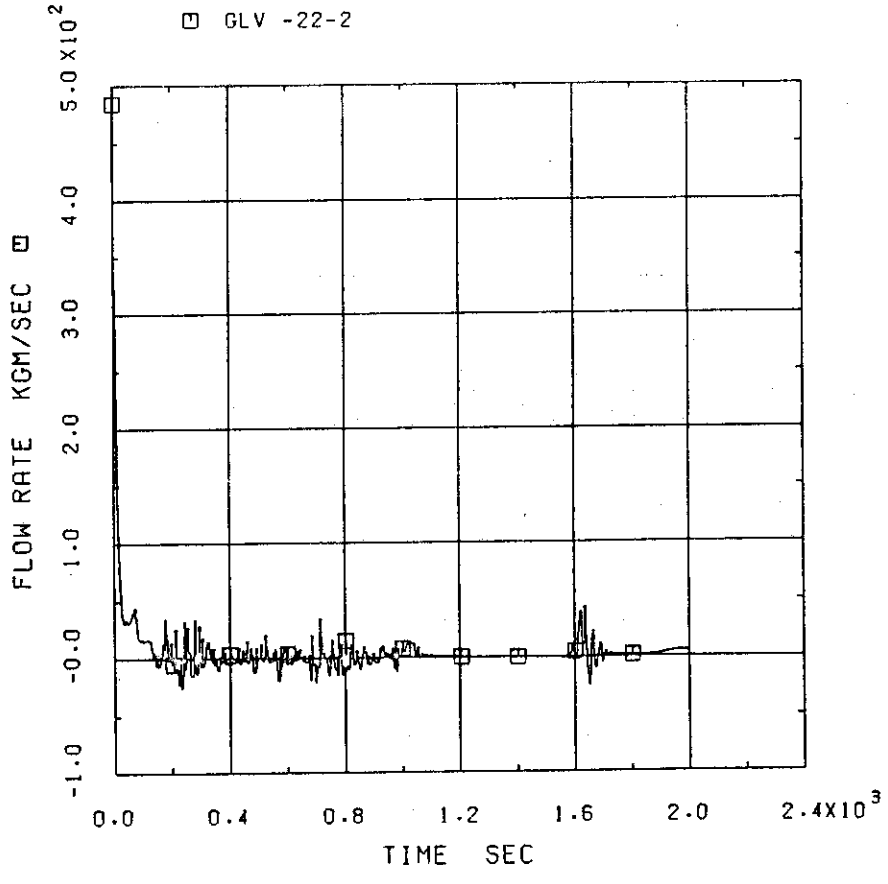

Fig.6.33 Mass flow rate at downcomer inlet

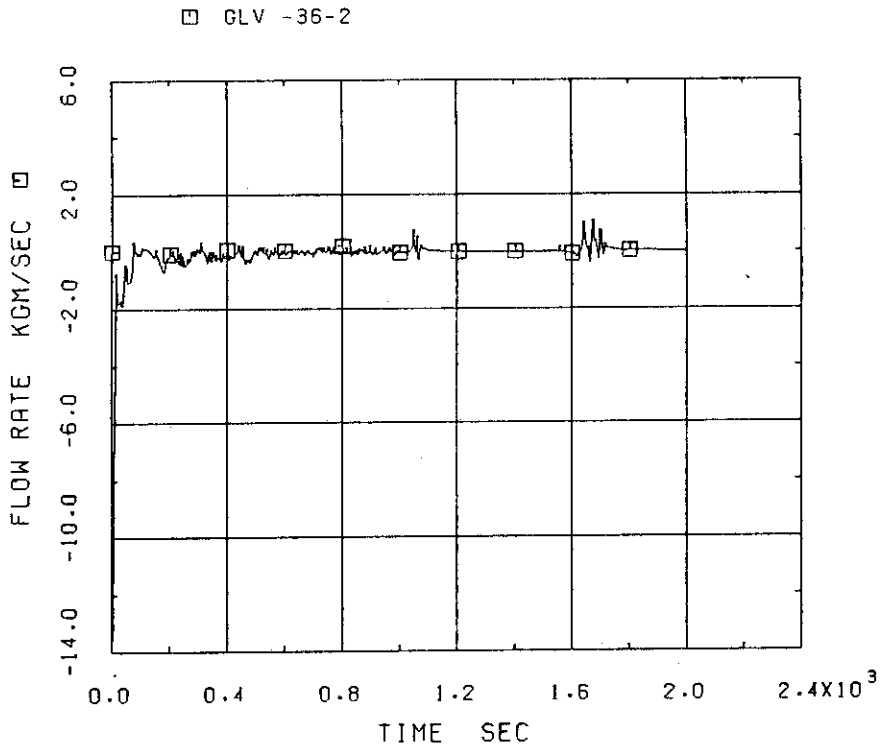

Fig.6.34 Mass flow rate at pressurizer surge line

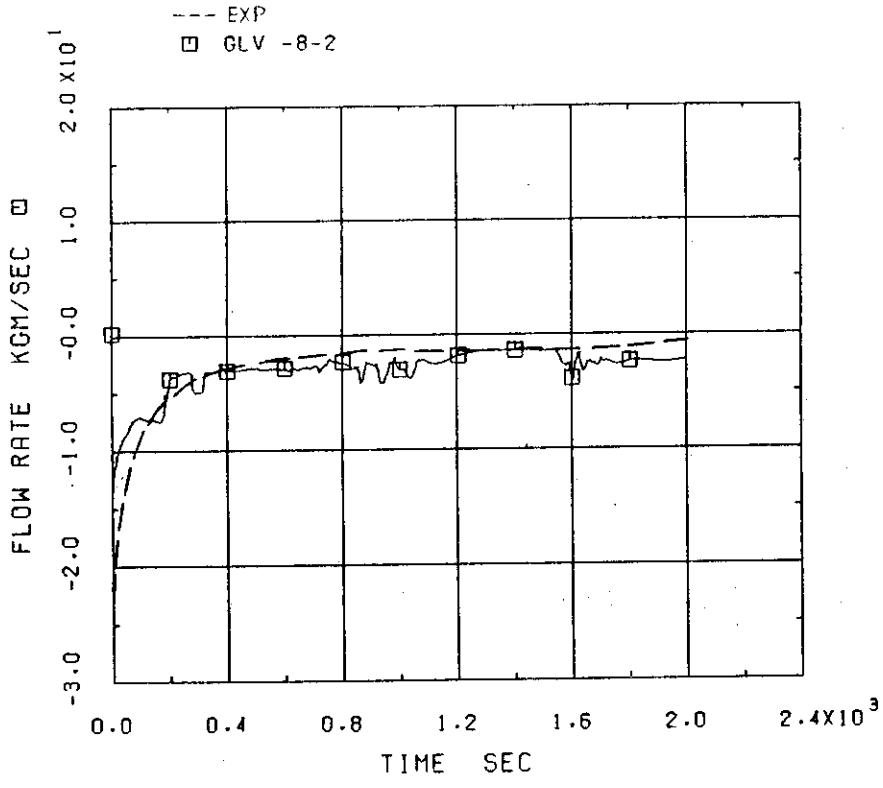

Fig.6.35 Break flow

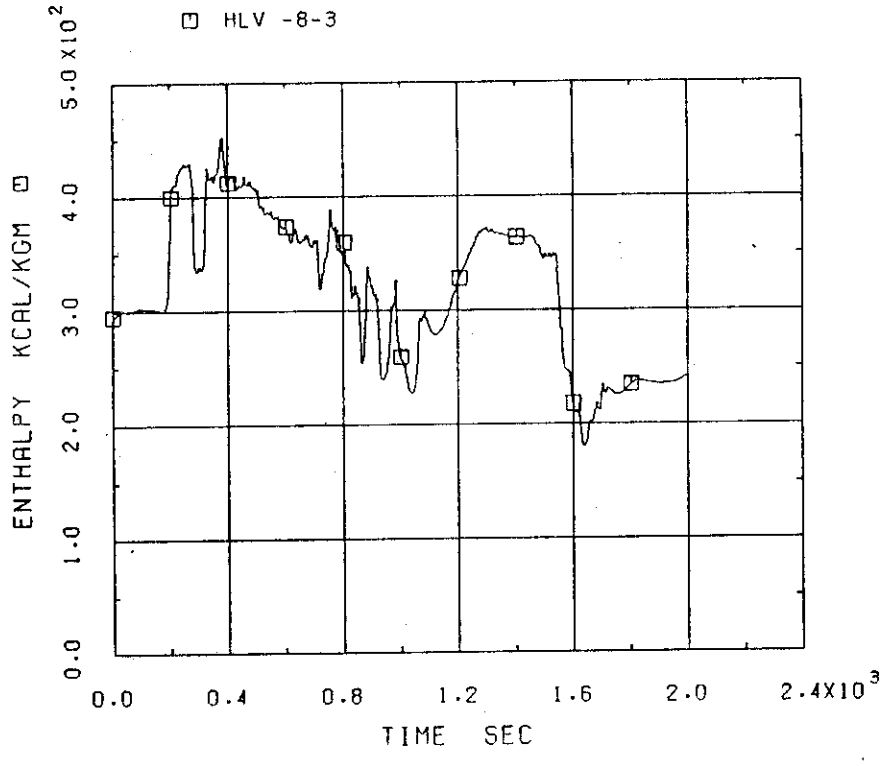

Fig.6.36 Break enthalpy

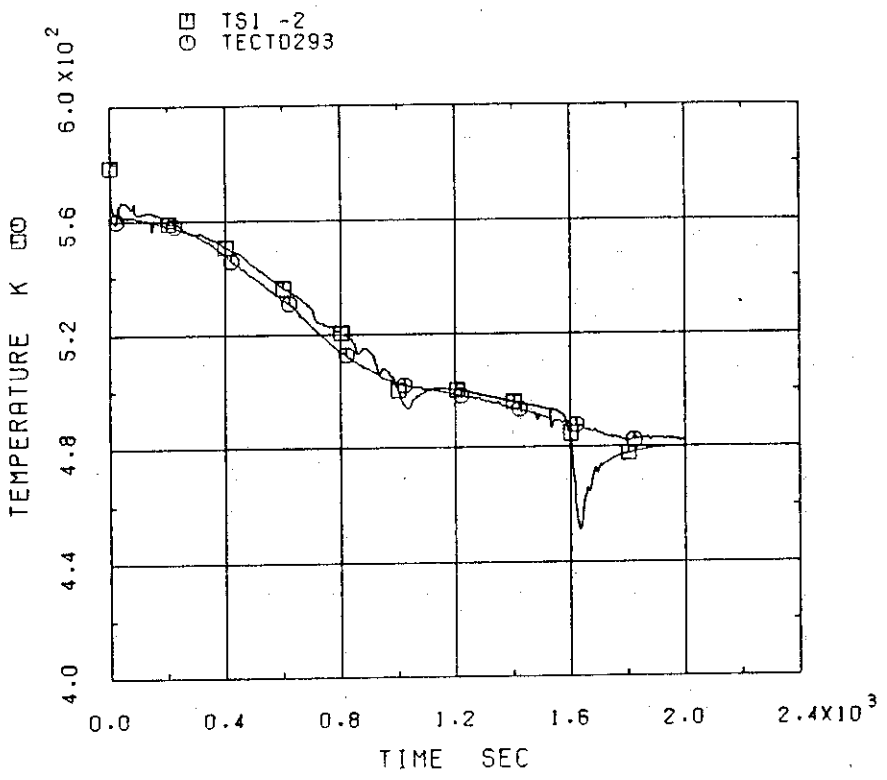

(a) Node 26

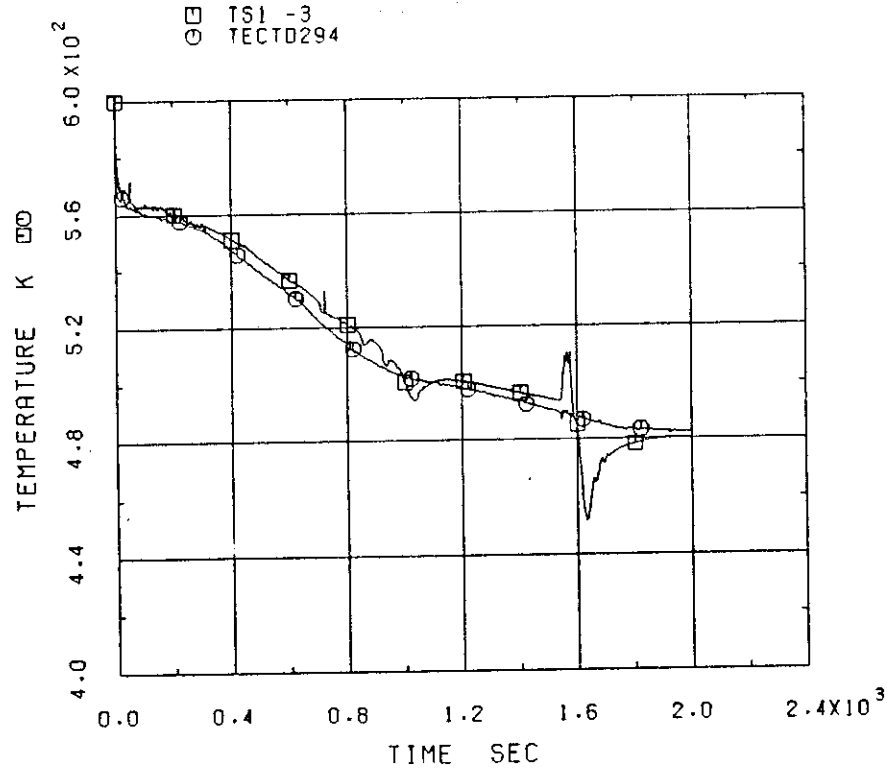

(b) Node 27

Fig.6.37 Cladding surface temperature

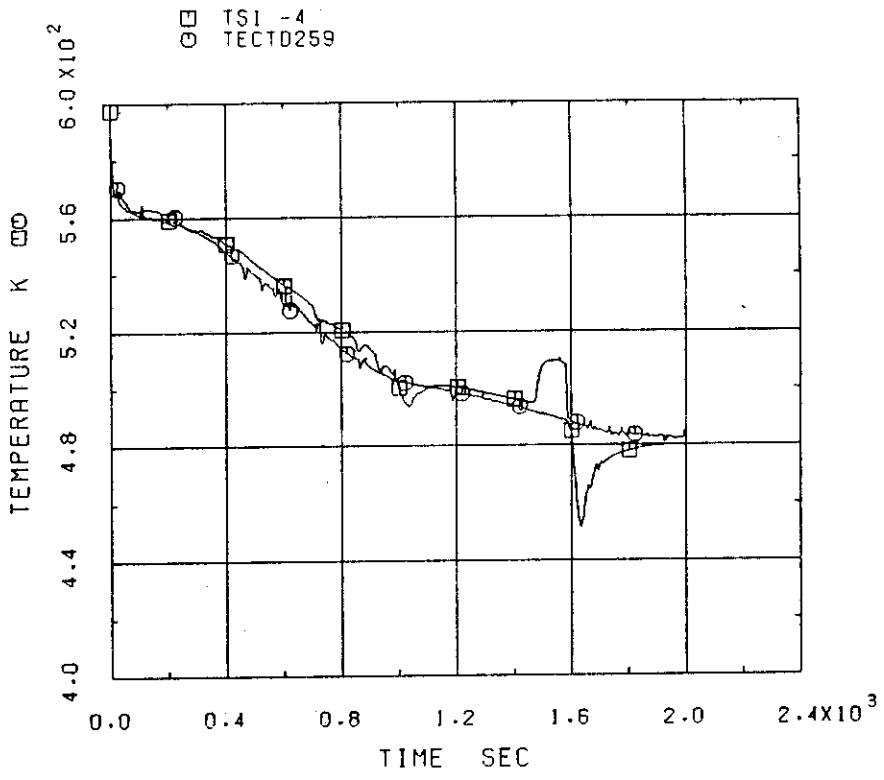

(c) Node 28

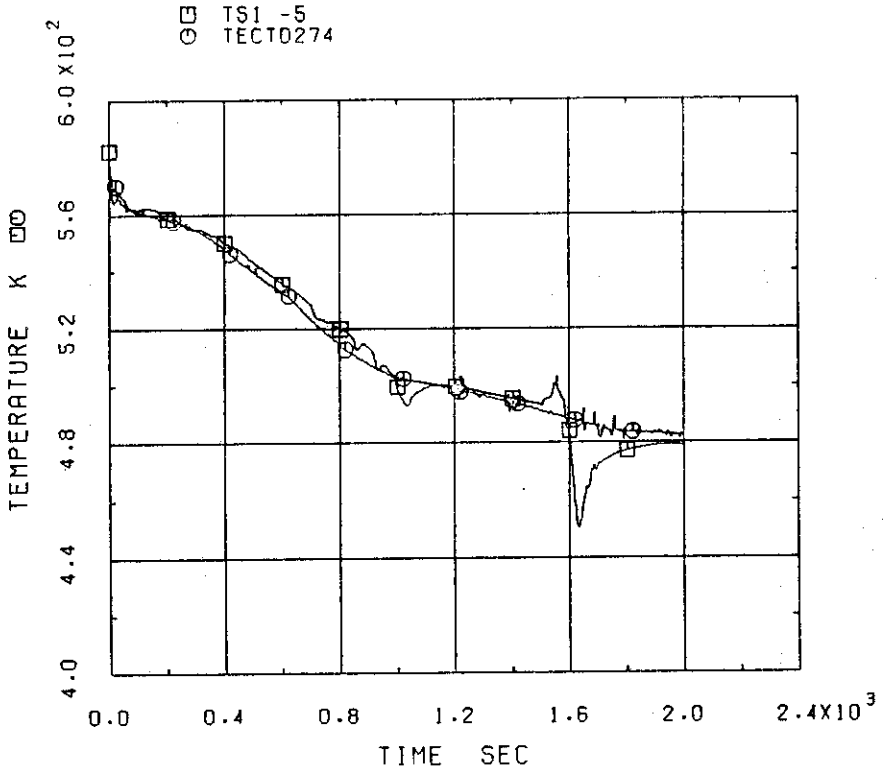

(d) Node 29

Fig.6.37 Cladding surface temperature

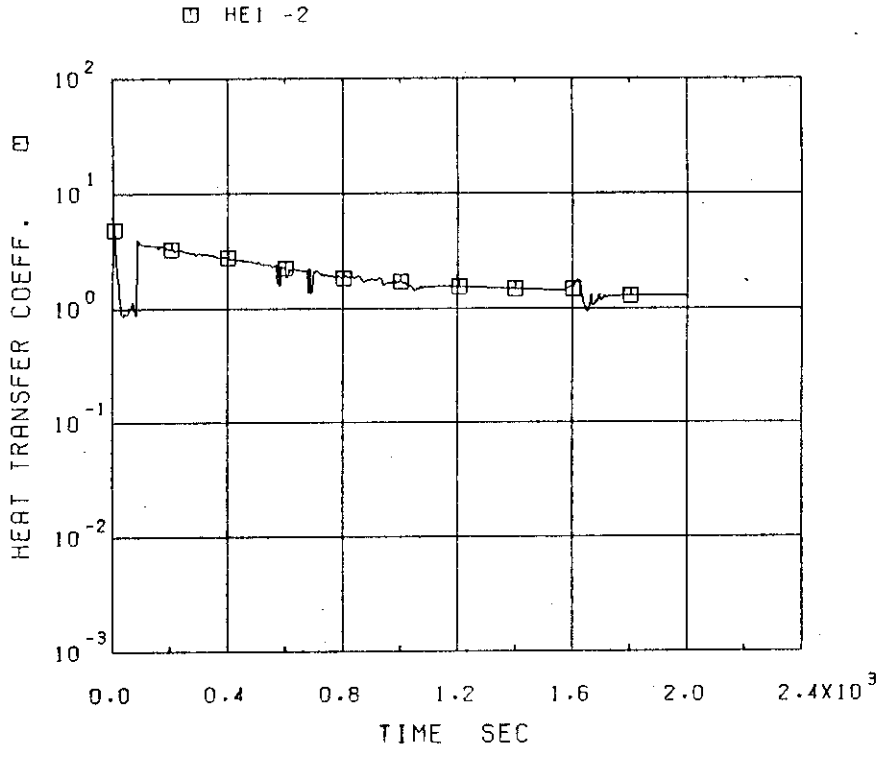

(a) Node 26

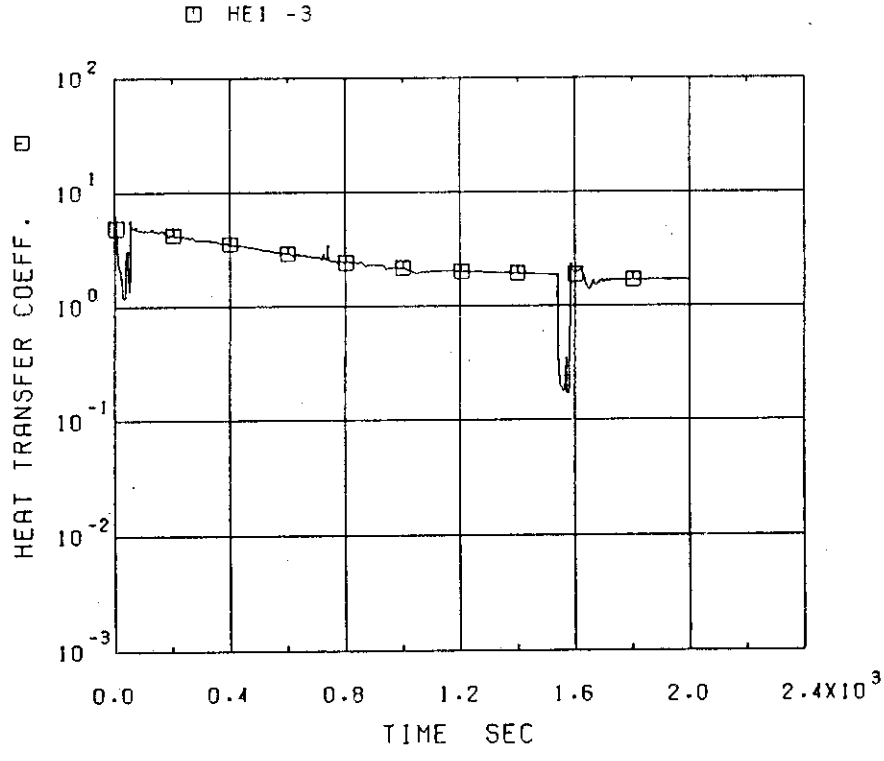

(b) Node 27

Fig.6.38 Heat transfer coefficient

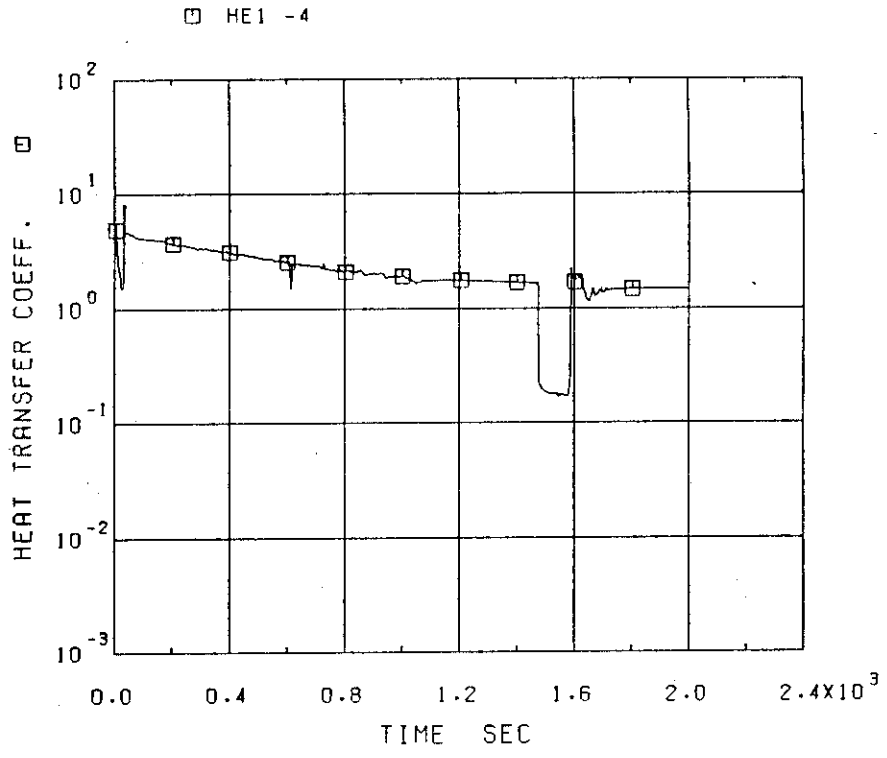

(c) Node 28

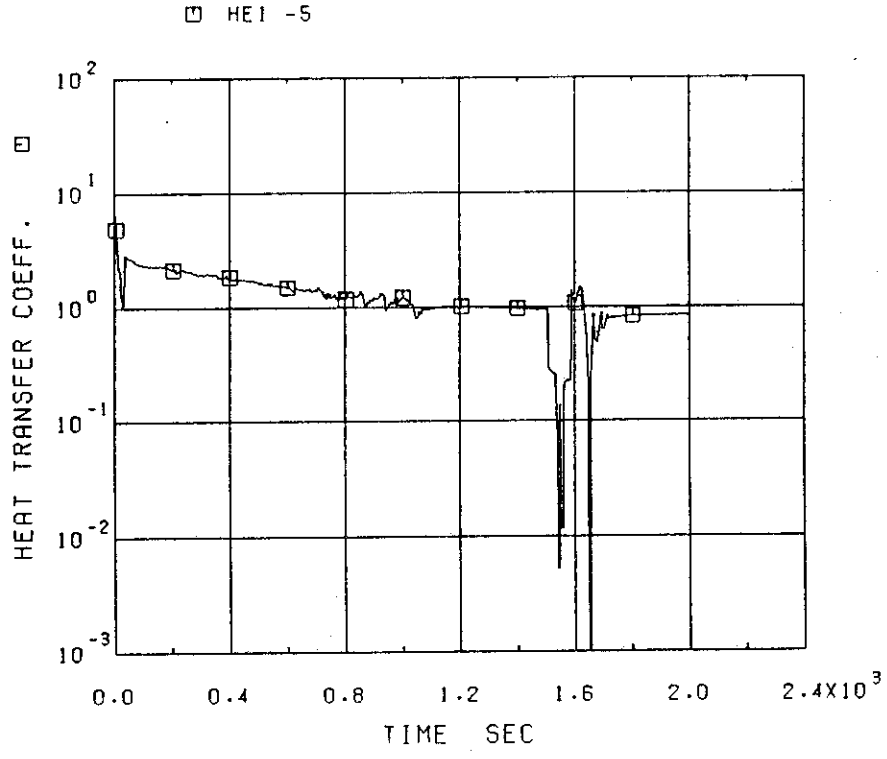

(d) Node 29

Fig.6.38 Heat transfer coefficient

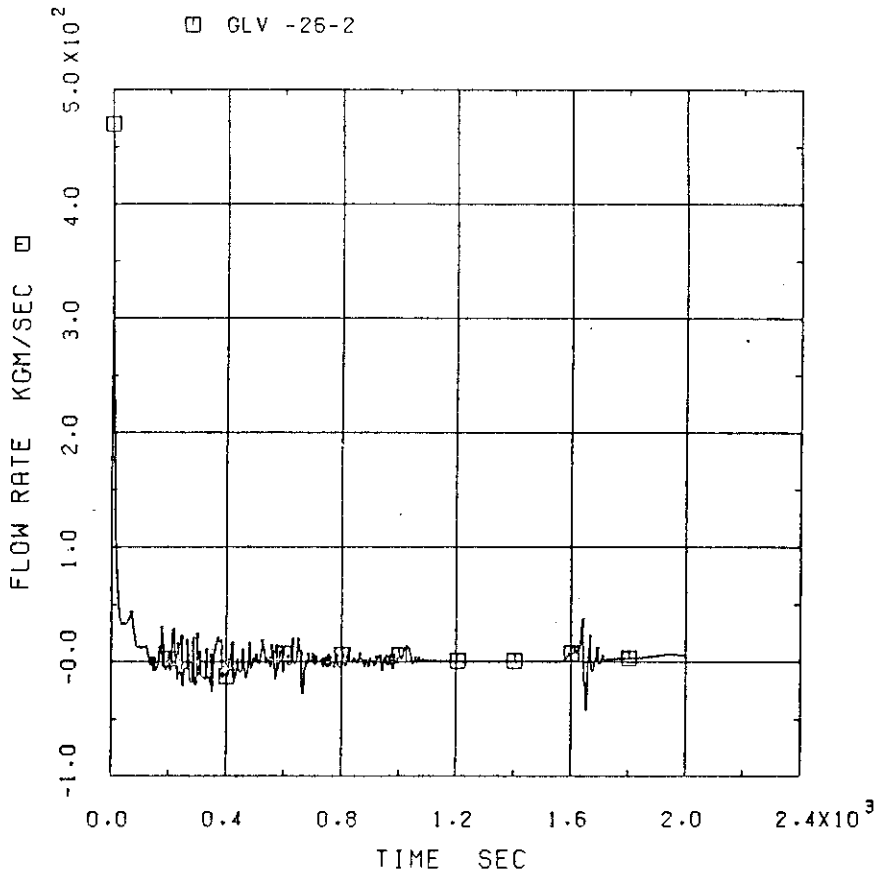

Fig.6.39 Core inlet flow

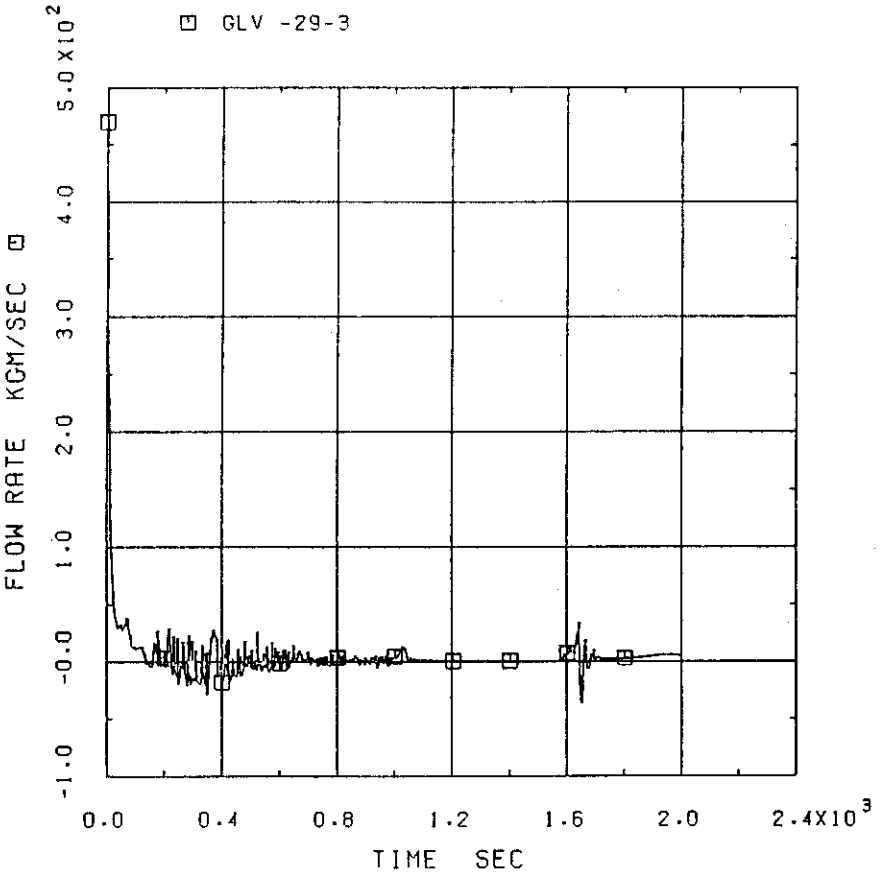

Fig.6.40 Core outlet flow

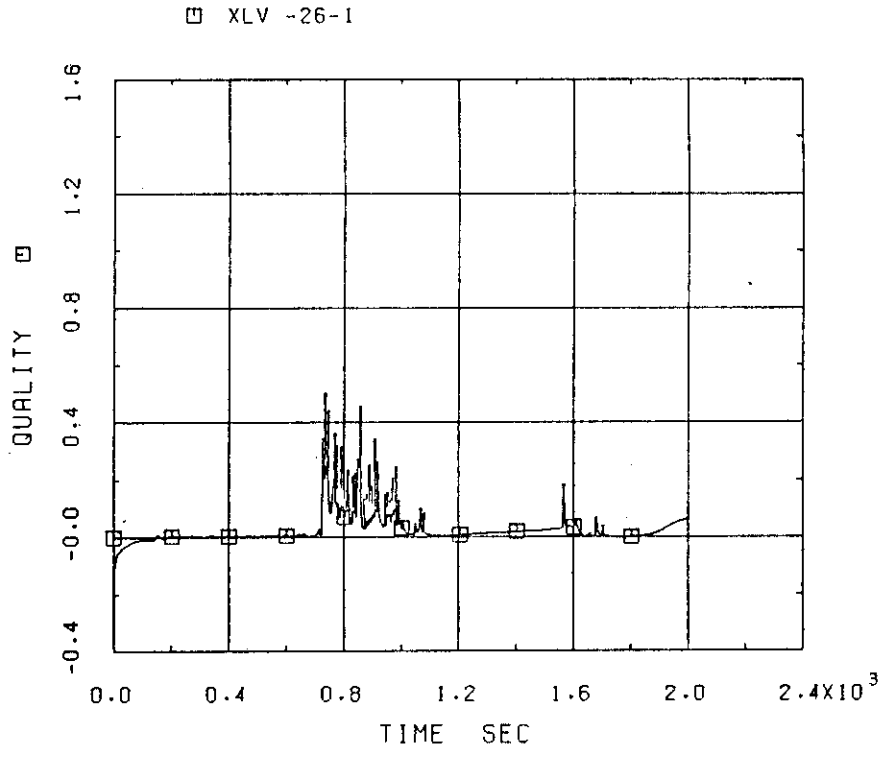

(a) Node 26

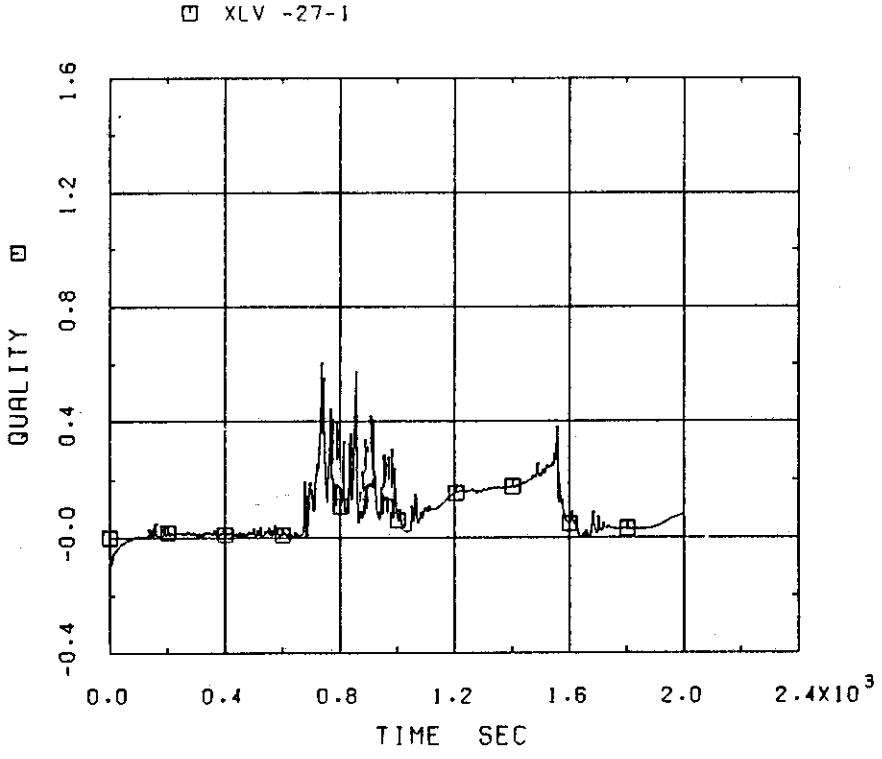

(b) Node 27

Fig.6.41 Core coolant quality

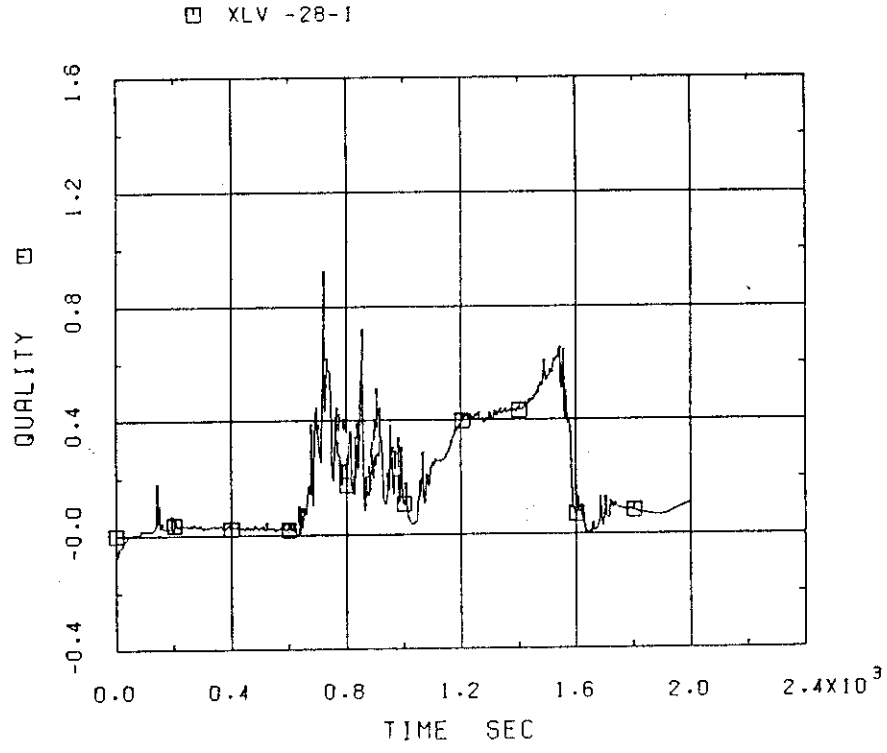

(c) Node 28

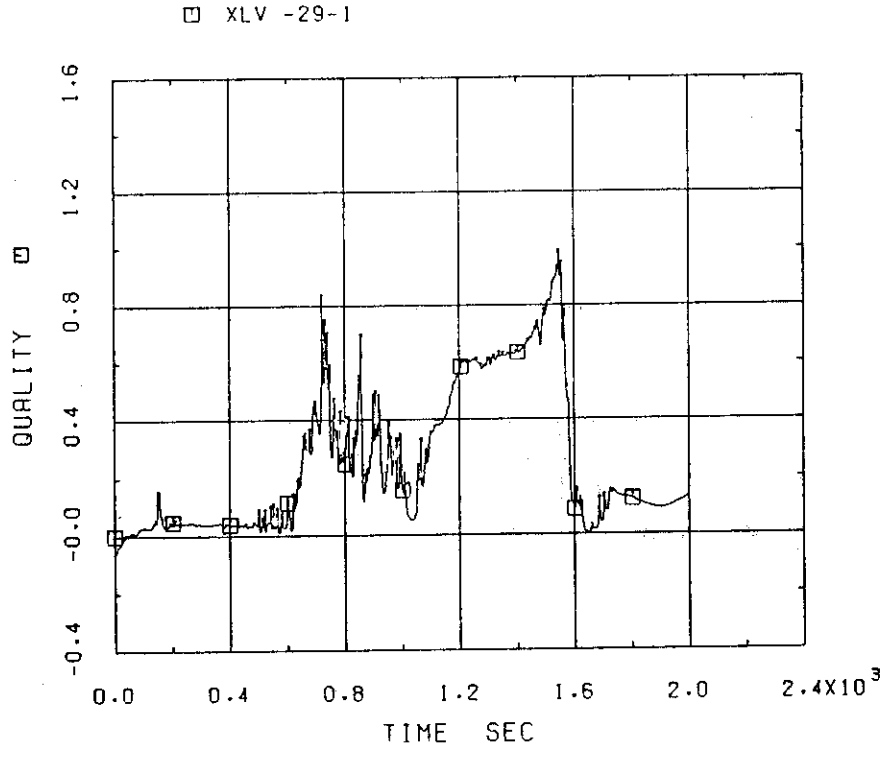

(d) Node 29

Fig.6.41 Core coolant quality

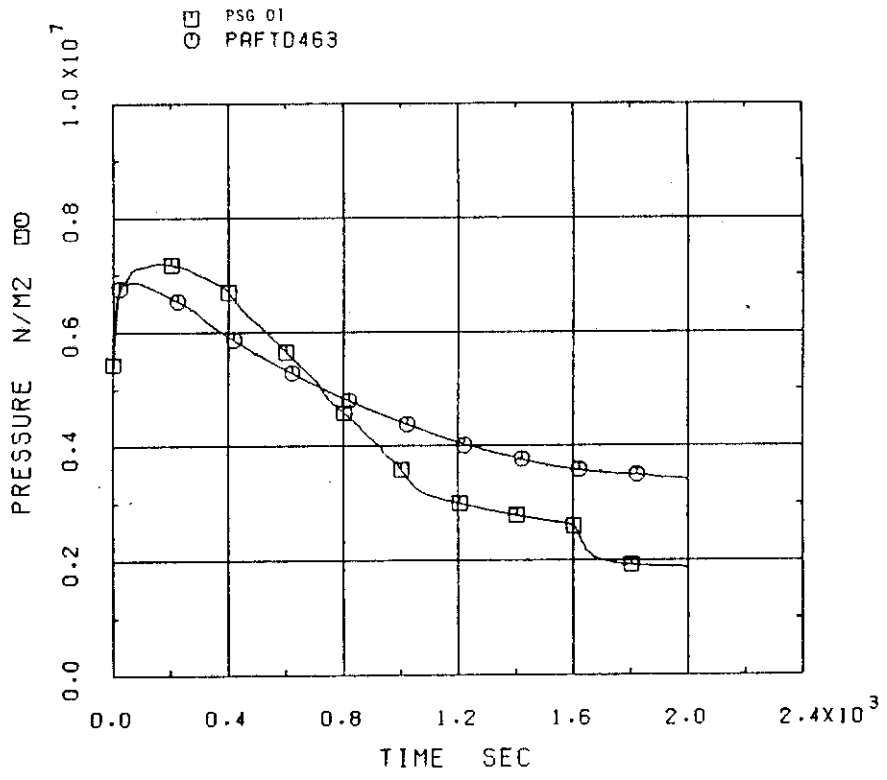

Fig.6.42 SG secondary pressure

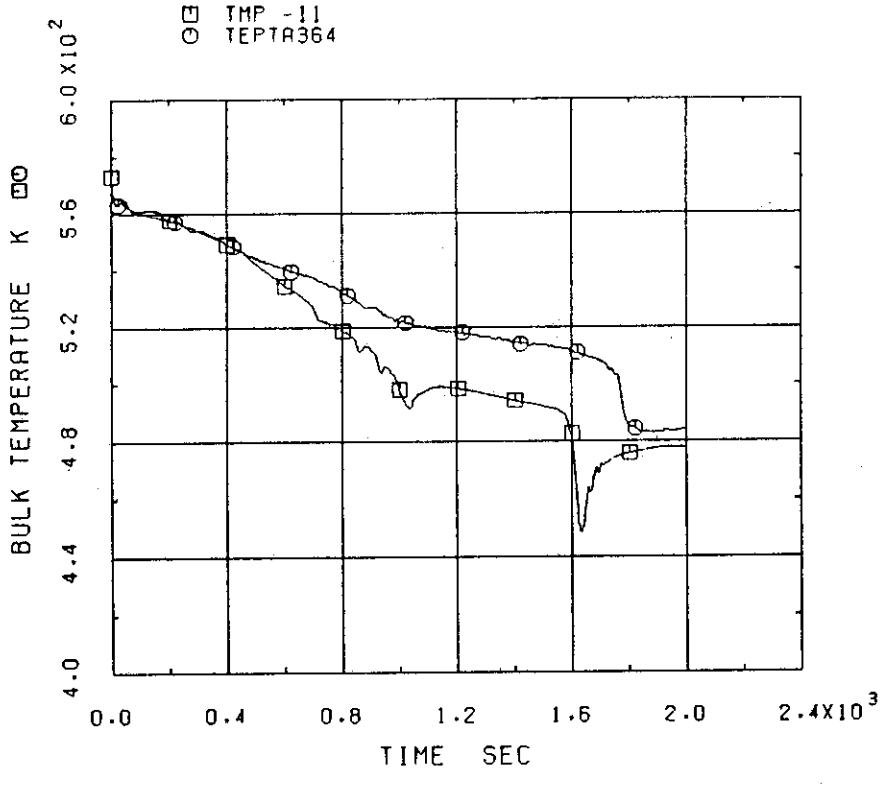

Fig.6.43 Coolant temperature at intact loop hot leg

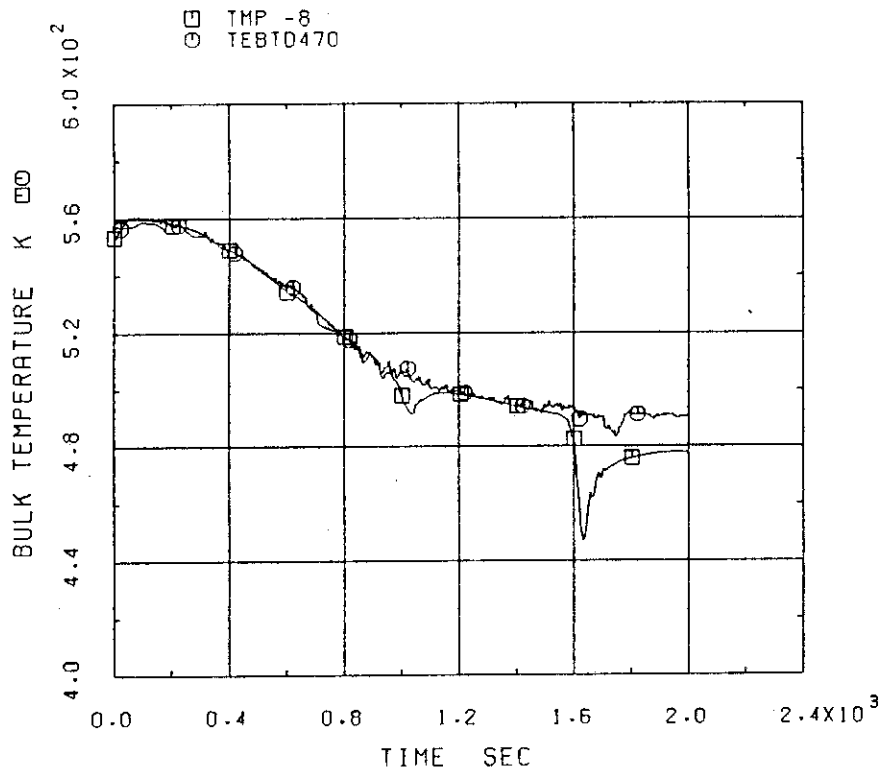

Fig.6.44 Coolant temperature at broken loop hot leg

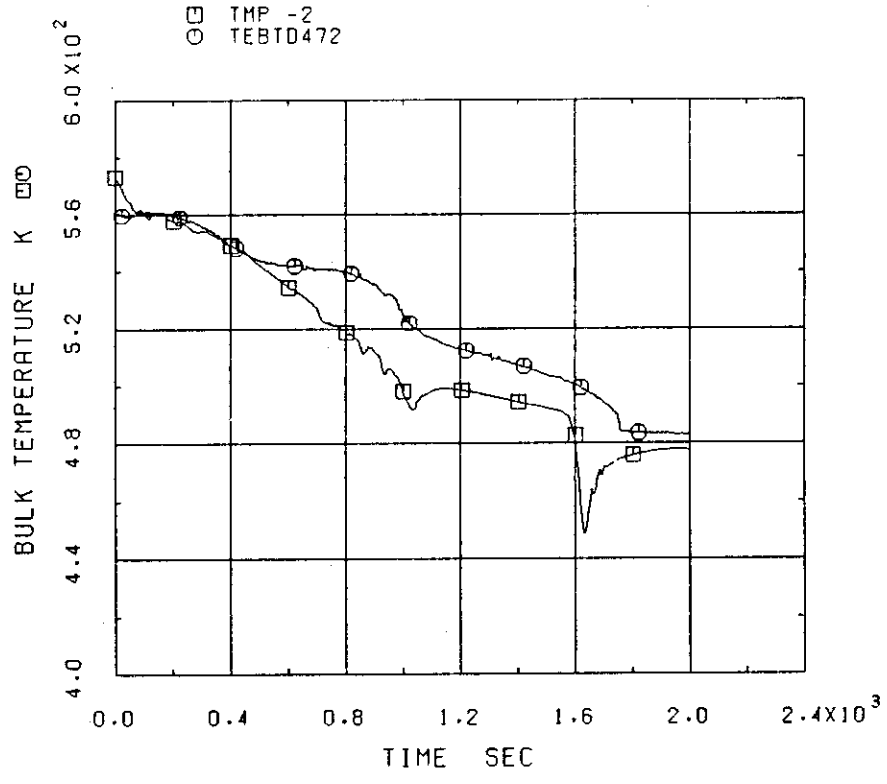

Fig.6.45 Coolant temperature at broken loop cold leg

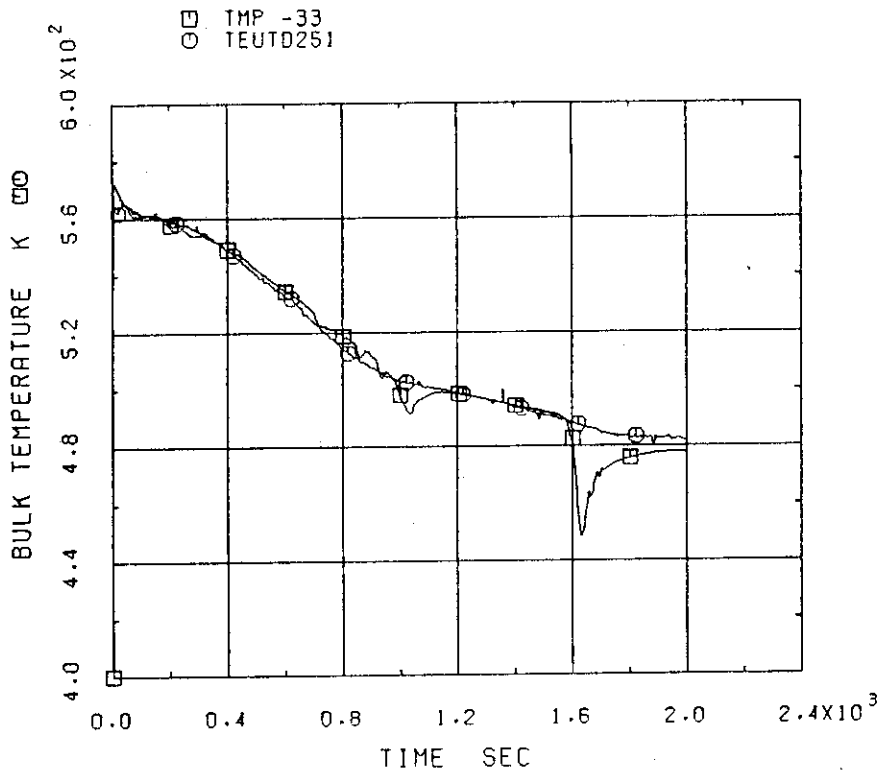

Fig.6.46 Coolant temperature at upper plenum

Appendix A Input Data List

```
 -- LOFT L3-1 ANALYSIS BY THYDE-P CODE --                    80.08.13        00000010
/                                                                           00000011
/  **** DIMENSION DATA ****                                                 00000012
BB01                                                                        00000020
  0  0  9  3  17  43  37  9  2  2  1  1  2  6  5  3                        00000030
/                                                                           00000040
/  **** MINOR EDIT DATA ****                                                00000050
BB02                                                                        00000060
PRE-30  PRA-08  PRA-07  GLA-21  GLE-07  GLA-08  GLE-35  GLA-23  GLA-23      00000070
/                                                                           00000080
/  **** TIME STEP CONTROL DATA ****                                         00000090
BB03                                                                        00000100
SB0301                                                                      00000110
    0.4  0.4  100.                                                          00000120
SB0304                                                                      00000130
    10  2  50   0  8.0E-3  1.0E-4   20.   0.1                              00000140
SB0305                                                                      00000150
    30  3  50   0  1.6E-2  1.0E-4  1000.  0.1                              00000160
SB0308                                                                      00000170
    30  3  50   0  1.6E-2  1.0E-4  2000.  0.1                              00000180
/                                                                           00000190
/  **** TRIP CONTROLL DATA ****                                             00000200
BB04                                                                        00000210
SB0480                                                                      00000220
  1  0  1  0      1.E4      0.0                                            00000230
SB0481                                                                      00000240
  5 42  1  0      1.E-5     0.0                                            00000250
SB0482                                                                      00000260
  2 18  1  0      0.04      0.0                                            00000270
SB0483                                                                      00000280
  2 19  1  0      0.04      0.0                                            00000290
SB0484                                                                      00000300
  3  0  1  0      1.E-5     0.0                                            00000310
SB0485                                                                      00000320
  4  1  1  0      4.5       0.0                                            00000330
SB0486                                                                      00000340
  4  2  1  0      1.E4      0.0                                            00000350
SB0487                                                                      00000360
 -4  1  1  0      1.E4      0.0                                            00000370
SB0488                                                                      00000380
  -4  2   1  0   1.E4  0.0                                                 00000390
SB0489                                                                      00000400
   6  1  -3  1  240.0  0.005                                               00000410
SB0490                                                                      00000460
   6  2  -3  1  250.0  0.0                                                 00000470
SB0491                                                                      00000480
   6  3  -3  1  360.0  0.0                                                 00000490
SB0492                                                                      00000500
  -6  1   3  1  350.0  0.0                                                 00000510
SB0493                                                                      00000520
  -6  2   3  1  305.0  0.0                                                 00000530
SB0494                                                                      00000540
  -6  3   3  1  380.0  0.0                                                 00000550
SB0495                                                                      00000560
   6  2  -2  1  160.0  0.0                                                 00000570
SB0496                                                                      00000572
  -6  2   2  1  190.0  0.0                                                 00000574
/                                                                           00000580
```

```
/  **** FLOW AJUST DATA ****                                                    00000590
BB05                                                                          00000600
  1    3.818  320.0                                                           00000610
/                                                                             00000620
/  **** NODE DATA ****                                                        00000630
BB06                                                                          00000640
SB0601                                                                        00000650
 1  1 22 29  0 146.56          0.2842    0.0      1.332      0.0              00000660
                               0.4       0.8      0.0        0.0              00000662
SB0602                                                                        00000670
 2  1 29  1  0 146.837507482   0.2842    0.0      0.6965     0.0              00000680
                               0.0       0.0     -1.0       -1.0              00000682
SB0603                                                                        00000690
 3  1  1  2  0 146.837499636   0.1032    0.0      1.517      0.7174           00000700
                              -1.0      -1.0      1.52       1.09             00000710
SB0604                                                                        00000712
 4  1  2  3  0 146.787187778   0.3485    0.0      3.228      2.705            00000720
                               0.0       0.0    189.0      189.0              00000722
SB0605                                                                        00000730
 5  1  3  4  0 146.597499855   0.3485    0.0      3.228     -2.705            00000740
                               0.0       0.0    142.0      198.0              00000742
SB0606                                                                        00000750
 6  1  4  5  0 146.787170796   0.1272    0.0      2.423     -2.0394           00000760
                               0.0       0.0     20.0       20.0              00000762
SB0607                                                                        00000770
 7  1  5  6  0 146.930128676   0.1032    0.0      1.883      1.322            00000780
                               0.0       0.0 -4.9338328905E5      0.0        00000782
SB0608                                                                        00000790
 8  1  6  7  0 149.652473350   0.1032    0.0      0.4877     0.0              00000800
                               0.0       0.0     -1.0       -1.0              00000802
SB0609                                                                        00000810
 9  1  7 30  0 149.652473691   0.2842    0.0      0.6965     0.0              00000820
                              -1.0      -1.0      0.0        0.0              00000822
SB0610                                                                        00000830
10  1 30 27  0 149.652473683   0.2842    0.0      0.9510     0.0              00000840
                               0.0       0.0      3.58       3.0              00000842
SB0611                                                                        00000850
11  1 22 23  0 146.56          0.2842    0.0      2.616      0.0              00000860
                               0.4       0.8      0.0        0.0              00000862
SB0612                                                                        00000870
12  1 23  8  0 146.25234       0.2832    0.0      2.643      0.2432           00000880
                               0.0       0.0     -1.0       -1.0              00000882
SB0613                                                                        00000890
13  1  8  9  0 146.28074       0.9084    0.0      0.5175     0.5175           00000900
                              -1.0      -1.0     -1.0       -1.0              00000902
SB0614                                                                        00000910
14  7  9 10  1 146.15415       0.01021   0.0      2.568      2.483            00000920
                              -1.0      -1.0     -1.0       -1.0              00000922
SB0615                                                                        00000930
15  7 10 11  1 145.75345       0.01021   0.0      2.568     -2.483            00000940
                              -1.0      -1.0     -1.0       -1.0              00000942
SB0616                                                                        00000950
16  1 11 12  0 145.74068       0.9084    0.0      0.5175    -0.5175           00000960
                              -1.0      -1.0     -1.0       -1.0              00000962
SB0617                                                                        00000970
17  1 12 24  0 145.32114       0.2941    0.0      2.426     -1.523            00000980
                              -1.0      -1.0      0.0        0.0              00000982
SB0618                                                                        00000990
```

```
18  8 24 25  0 145.687          0.3468     0.0      1.867      1.2807      00001000
                                0.0        0.0      0.0        0.0         00001002
SB0619                                                                     00001010
19  8 24 25  0 145.687          0.3043     0.0      3.111      1.2807      00001020
                                0.0        0.0      0.0        0.0         00001022
SB0620                                                                     00001030
20  1 25 26  0 150.6054         0.2757     0.0      1.399      0.0         00001040
                                0.0        0.0      0.0        0.0         00001042
SB0621                                                                     00001050
21  1 26 27  0 150.6356         0.2842     0.0      0.5313     0.0         00001060
                                0.0        0.0      3.58       3.0         00001062
SB0622                                                                     00001070
22  4 27 13  0 149.5569         0.45190    0.0426   4.256     -4.256       00001080
                                0.62       0.62     3.5        3.5         00001082
SB0623                                                                     00001090
23  5 13 28  0 149.6645         1.004      0.0      0.7318     0.0         00001100
                                0.0        0.0      0.0        0.0         00001102
SB0624                                                                     00001110
24  1 28 14  0 149.6064         0.4417     0.0      0.4285     0.4285      00001120
                                0.0        0.0     -1.0       -1.0         00001122
SB0625                                                                     00001130
25  2 14 15  0 148.94           1.0        0.0      0.09423    0.09423     00001140
                               -1.0       -1.0      0.0        0.0         00001142
SB0626                                                                     00001150
26  2 15 16  1 148.69           1.0        0.0      0.4191     0.4191      00001160
                                0.0        0.0      0.0        0.0         00001162
SB0627                                                                     00001170
27  2 16 17  1 148.41           1.0        0.0      0.4191     0.4191      00001180
                                0.0        0.0      0.0        0.0         00001182
SB0628                                                                     00001190
28  2 17 18  1 148.13           1.0        0.0      0.4191     0.4191      00001200
                                0.0        0.0      0.0        0.0         00001202
SB0629                                                                     00001210
29  2 18 19  1 147.85           1.0        0.0      0.4191     0.4191      00001220
                                0.0        0.0      0.0        0.0         00001222
SB0630                                                                     00001230
30  2 19 20  0 147.57           1.0        0.0      0.01753    0.01753     00001240
                                0.0        0.0     -1.0       -1.0         00001242
SB0631                                                                     00001250
31  1 20 22  0 147.32           0.5513     0.05486  1.668      1.668       00001260
                               -1.0       -1.0      0.0        0.0         00001262
SB0632                                                                     00001270
32  1 28 22  0 149.6064         0.0779     0.0      4.164      4.164       00001280
                                0.0        0.0      0.0        0.0         00001282
SB0633                                                                     00001290
33 13 22 37  0   0.1   0.5419  0.0   0.9144  0.9144 0.0  0.0  0.0  0.0    00001300
SB0634                                                                     00001310
34 13 29 35  0   0.1   0.222   0.0   4.048   0.8620 0.4  0.8  0.0  0.0    00001320
SB0635                                                                     00001330
35 13 30 36  0   0.1   0.222   0.0   4.840   0.6075 0.4  0.8  0.0  0.0    00001340
SB0636                                                                     00001350
36 13 23 21  0  10.0   0.043   0.0   4.592   0.4255 0.4  0.8  9.0  9.0    00001360
SB0637                                                                     00001370
37 13 21 34  0  10.0   0.043   0.0  -4.767   0.7678 0.0  0.0  0.0  0.0    00001380
SB0638                                                                     00001390
38 13 26 31  0  10.0   0.089   0.0   5.5     0.0    0.4  0.8  0.0  0.0    00001400
SB0639                                                                     00001410
39 13 26 32  0  10.0   0.089   0.0   5.5     0.0    0.4  0.8  0.0  0.0    00001420
```

```
SB0640                                                                  00001430
40 13 26 33  0  10.0   0.089    0.0   58.0    0.0    0.4  0.8  0.0  0.0 00001440
/                                                                       00001450
/  **** JUNCTION DATA ****                                              00001460
BB07                                                                    00001470
    1   1   0.0                                                         00001480
    2   1   0.0                                                         00001490
    3   1   0.0                                                         00001500
    4   1   0.0                                                         00001510
    5   1   0.0                                                         00001520
    6   1   0.0                                                         00001530
    7   1   0.0                                                         00001540
    8   1   0.0                                                         00001550
    9   1   0.0                                                         00001560
   10   1   0.0                                                         00001570
   11   1   0.0                                                         00001580
   12   1   0.0                                                         00001590
   13   1   0.0                                                         00001600
   14   1   0.0                                                         00001610
   15   1   0.0                                                         00001620
   16   1   0.0                                                         00001630
   17   1   0.0                                                         00001640
   18   1   0.0                                                         00001650
   19   1   0.0                                                         00001660
   20   1   0.0                                                         00001670
   21   1   0.0                                                         00001680
   22   4   0.1937                                                      00001690
   23   4   0.04149                                                     00001700
   24   4   0.05040                                                     00001710
   25   4   0.04644                                                     00001720
   26   4   0.08948                                                     00001730
   27   4   0.18                                                        00001740
   28   4   0.064                                                       00001750
   29   4   0.04474                                                     00001760
   30   4   0.04474                                                     00001770
   31   7   0.0                                                         00001780
   32   7   0.0                                                         00001790
   33   5   0.0                                                         00001800
   34   6   0.0                                                         00001810
   35   8   0.0                                                         00001820
   36   8   0.0                                                         00001830
   37   8   0.0                                                         00001840
/                                                                       00001861
/  **** MIXING JUNCTION DATA ****                                       00001862
BB08                                                                    00001870
SB0801                                                                  00001880
   22   3    1  11  33   0   0.0005 0.9995  0.    0.                  00001890
SB0802                                                                  00001900
   23   2   12  36   0   0   1.0    0.0     0.    0.                  00001910
SB0803                                                                  00001920
   24   2   18  19   0   0   0.5    0.5     0.    0.                  00001930
SB0804                                                                  00001940
   25   1   20   0   0   0   1.0    0.0     0.    0.                  00001950
SB0805                                                                  00001951
   26   4   21  38  39  40   1.0    0.0     0.    0.                  00001952
SB0806                                                                  00001953
   27   1   22   0   0   0   1.0    0.0     0.    0.                  00001954
SB0807                                                                  00001955
```

```
   28   2   24   32   0   0   0.97  0.03    0.    0.                          00001956
SB0808                                                                       00001957
   29   2    2   34   0   0   1.0   0.0     0.    0.                          00001958
SB0809                                                                       00001959
   30   2   10   35   0   0   1.0   0.0     0.    0.                          00001960
/                                                                            00001971
/  **** PUMPED INJECTION DATA ****                                           00001972
BB09                                                                         00001980
SB0901                                                                       00001990
    1   31    24.0                                                           00002000
    9                                                                        00002010
   0.0   0.00   1.0   0.33   2.E2  0.38    4.E2  0.40      6.E2  0.50       00002020
   8.E2  0.54   1.E3  0.56   2.E3  0.62    4.E3  0.65                       00002021
SB0902                                                                       00002030
    2   32    24.0                                                           00002040
    2                                                                        00002050
     0.0   0.00     0.0   0.00                                              00002060
/                                                                            00002101
/  **** PUMP DATA ****                                                       00002102
BB10                                                                         00002110
SB1001                                                                       00002120
 18 1 0 3530. .3155  500.24  108.1 613.73  3140. 1.4328 .0 .0 0.08333        00002130
SB1002                                                                       00002140
 19 1 0 3530. .3155  500.24  108.1 613.73  3140. 1.4328 .0 .0 0.08333        00002150
/                                                                            00002151
/  **** PUMP DATA TABLE ****                                                 00002152
BB11                                                                         00002160
SB1101                                                                       00002170
 1                                                                           00002180
 12                                                                          00002190
 -1.0        2.4722                  -0.80574   2.0474                       00002200
 -0.6096     1.831                   -0.40683   1.624                        00002210
 -0.200171   1.4705                   0.0       1.4036                       00002220
  0.19061    1.3636                   0.38963   1.3186                       00002230
  0.4118     1.3                      0.59396   1.2328                       00002231
  0.7902     1.1336                   1.0       1.0078                       00002232
 12                                                                          00002240
 -1.0                -1.0            -0.80574            -0.6               00002242
 -0.6096             -0.3            -0.40683            -0.05              00002244
 -0.200171            0.13            0.0                 0.25              00002246
  0.19061             0.28            0.38963             0.34              00002248
  0.4118              0.2768          0.59396             0.46              00002250
  0.7902              0.70            1.0                 0.9465            00002252
 17                                                                          00002258
 -1.0       -1.0                     -0.82297  -0.98                        00002259
 -0.63332   -0.95                    -0.45534  -0.90                        00002260
 -0.27109   -0.82                    -0.17716  -0.78                        00002270
 -0.09073   -0.72                     0.0      -0.67                        00002271
  0.091099  -0.60                     0.186509 -0.52                        00002272
  0.271762  -0.42                     0.45582  -0.21                        00002273
  0.574406  -0.02                     0.740576  0.26                        00002274
  0.766619   0.36                     0.871471  0.63                        00002275
  1.0        1.0078                                                         00002276
 17                                                                          00002278
 -1.0                2.4722          -0.82297            1.9968           00002280
 -0.63332            1.5897          -0.45534            1.3279           00002282
 -0.27109            1.1949          -0.17716            1.0605           00002284
 -0.09073            1.0156           0.0                0.934279         00002286
```

```
 0.091099          0.9229          0.186509          0.8963          00002288
 0.271762          0.875           0.45582           0.8433          00002290
 0.574406          0.8355          0.740576          0.8466          00002292
 0.766619          0.8469          0.871471          0.8838          00002294
 1.0               0.9465                                            00002296
14                                                                   00002298
-1.0       1.9843                 -0.80096   1.394                   00002299
-0.60638   1.0975                 -0.40686   0.822                   00002300
-0.30      0.71                   -0.19928   0.6648                  00002310
-0.10      0.61                    0.0       0.6032                  00002312
 0.1930    0.6325                  0.393     0.7369                  00002320
 0.50      0.79                    0.59552   0.8381                  00002321
 0.79782   0.9229                  1.0       0.9672                  00002322
14                                                                   00002324
-1.0               -1.0            -0.80096          -0.98           00002326
-0.60638           -0.94           -0.40686          -0.91           00002328
-0.30              -0.90           -0.19928          -0.70           00002330
-0.10              -0.51            0.0              -0.45           00002332
 0.1930            -0.37            0.393            -0.26           00002334
 0.50              -0.01            0.59552           0.06           00002336
 0.79782            0.21            1.0               0.3569         00002338
17                                                                   00002348
-1.0       -1.0                   -0.82234  -0.98                    00002349
-0.63371   -0.94                  -0.45853  -0.92                    00002350
-0.267023  -0.91                  -0.176107 -0.85                    00002360
-0.089310  -0.80                   0.0      -0.67                    00002370
 0.090643  -0.59                   0.188569 -0.50                    00002371
 0.27347   -0.40                   0.455869 -0.05                    00002372
 0.57448    0.28                   0.73816   0.52                    00002373
 0.76852    0.61                   0.870057  0.74                    00002374
 1.0        0.9672                                                   00002375
17                                                                   00002376
-1.0               1.9843          -0.82234          1.8308          00002378
-0.63371           1.6824          -0.45853          1.557           00002380
-0.267023          1.4362          -0.176107         1.3879          00002382
-0.089310          1.3481           0.0              0.23361         00002384
 0.090643          1.1965           0.188569         1.1096          00002386
 0.27347           1.0416           0.455869         0.8958          00002388
 0.57448           0.7807           0.73816          0.6137          00002390
 0.76852           0.5849           0.870057         0.4877          00002392
 1.0               0.3569                                            00002393
12                                                                   00002394
-1.0   -1.15      -0.9   -1.24      -0.6   -2.8      -0.5   -2.9     00002395
-0.4   -2.7        0.0    0.0        0.12   0.85       0.2    1.1     00002396
 0.5    1.02       0.7    1.0        0.9    0.95       1.0    1.0     00002397
4                                                                    00002398
-1.0    0.0        0.0    0.0        0.5   -0.8        1.0   -1.46    00002399
7                                                                    00002400
-1.0    0.0        0.0    0.0        0.1   -0.02       0.2    0.0     00002402
 0.3    0.1        0.9    0.78       1.0    1.0                       00002403
12                                                                   00002404
-1.0   -1.15      -0.8   -0.5       -0.6   -0.2      -0.4    0.03     00002405
-0.2    0.04       0.0    0.1        0.2    0.15       0.4    0.12     00002406
 0.6    0.05       0.8   -0.5        0.9   -0.9        1.0   -1.46     00002407
0                                                                    00002408
0                                                                    00002409
0                                                                    00002410
0                                                                    00002411
```

```
 13                                                                                                  00002439
  0.0  0.0     0.05 0.0       0.1  0.025      0.15  0.075   0.2  0.18                              00002441
  0.3    0.475       0.4     0.625      0.5     0.74         0.6      0.82                          00002442
  0.7    0.87        0.8     0.84       0.9     0.72         1.0      0.08                          00002443
 11                                                                                                  00002444
  0.0    0.0         0.1     0.0        0.20    0.13         0.3      0.24                          00002445
  0.4    0.31        0.5     0.33       0.6     0.3          0.7      0.23                          00002446
  0.8    0.16        0.9     0.08       1.0     0.0                                                00002447
  6  6                                                                                                00002456
  0.0  0.2  0.4  0.6  0.8  1.0                                                                        00002457
  0.0  0.0  0.0  0.0  0.0  0.0  0.0                                                                  00002458
  0.2  0.0  3.0650E-5  7.7239E-5  1.3263E-4  1.9460E-4  2.6207E-4                                    00002459
  0.4  0.0  4.8660E-5  1.2261E-4  2.1053E-4  3.0996E-4  4.1602E-4                                    00002460
  0.6  0.0  6.3760E-5  1.6066E-4  2.7587E-4  4.0485E-4  5.4514E-4                                    00002470
  0.8  0.0  7.7239E-5  1.9463E-4  3.3419E-4  4.9044E-4  6.6037E-4                                    00002480
  1.0  0.0  8.9628E-5  2.2585E-4  3.8780E-4  5.6910E-4  7.6631E-4                                    00002490
/                                                                                                    00002491
/  **** ACCUMLATOR DATA ****                                                                         00002492
BB12                                                                                                 00002500
SB1201                                                                                               00002510
   43   33    1.71   1.39   30.    43.13     0.9      0.1                                           00002520
/                                                                                                    00002561
/  **** BREAK POINT DATA ****                                                                        00002562
BB13                                                                                                 00002570
   6   0.000    0.500  0.800 0.8   0.6   0.800 0.8   0.6                                            00002580
   2                                                                                                 00002590
  0.0     1.0          100.0    1.0                                                                 00002600
/                                                                                                    00002601
/  **** PRESSURIZER DATA ****                                                                        00002602
BB14                                                                                                 00002610
   41     34       1      0.557    1.7235      1.1        0.99        0.01                          00002620
   1.0   1.0    1.0      1.0      1.0         0.0737     0.0737      0.0737                        00002630
   0.313 0.313  0.313    1.0      1.0        1.0                                                    00002640
   2                                                                                                 00002660
   0.     1.0    1.0      1.0        1000.      1.0       1.0      1.0                             00002670
/                                                                                                    00002671
/  **** STEAM GENERATOR DATA ****                                                                    00002672
BB15                                                                                                 00002680
SB1501                                                                                               00002690
 42     1845     14     15      2       1                                                           00002700
 1.589  4.188  1.0    1.0  0.01905   0.005105  4.469  1.00  190.0  25.0                            00002710
 0.300  0.990 53.6                                                                                  00002720
       -20.0    -8.0                                                                               00002730
   0.001    80.  0.5  0.5  0.5                                                                      00002740
   3                                                                                                 00002750
   0.0  1.0  1.0  1.0  1.0  1.0  1.0  1.0  1000.0  1.0  1.0  0.0                                     00002760
/                                                                                                    00002841
/  **** CORE DATA ****                                                                               00002842
BB16                                                                                                 00002850
  1300    25       30          0          9000.                                                     00002860
  5.359E-3 6.172E-4   4.647E-3  1.43E-2   0.6     19.52E-6                                          00002870
  0.0124   2.395E-4   0.0305    1.5897E-3 0.111   1.423E-3                                          00002880
  0.301    2.869E-3   1.14      8.347E-4  3.01    3.048E-3                                          00002882
  5.0      0.6        4.91E-04  3.41E-06  1.2      1.54E03                                          00002910
  0.0    148.06     249.64    190.32     62.88     0.0                                             00002920
1.0000E-07  1.00E-07  1.00E-07  1.00E-07  1.000E-07  1.0E-7                                         00002930
1.0000E-07  1.00E-07  1.00E-07  1.00E-07  1.000E-07  1.0E-7                                         00002940
1.0000E-07  1.00E-07  1.00E-07  1.00E-07  1.000E-07  1.0E-7                                         00002950
```

```
1.0000E-07  1.00E-07  1.00E-07  1.00E-07  1.000E-07  1.0E-7                00002960
/                                                                          00002961
/  **** SG RELIEF VALVE DATA ****                                          00002962
BB17                                                                       00002970
    6                                                                      00002980
  0.  0.  0.1  -14.   0.18  -32.  0.34  -62.  0.5  -94.  0.58  -179.       00002990
    4                                                                      00003000
 50. -0.00030  380.  -0.00022  1200. -0.00015  2280.  -0.00008             00003010
    9                                                                      00003020
  0.0  0.0  0.2   -0.2  0.4   -0.4    0.6   -1.4   0.8    -2.6            00003029
  1.0 -5.6  1.2  -12.6  1.4  -15.4  200.0  -15.6                           00003030
/                                                                          00003031
/   ****                      ****                                         00003032
BB18                                                                       00003040
    1.54E03      0.775E-04     2.29E04                                     00003050
/                                                                          00003051
/  **** FUEL GAP DATA ****                                                 00003052
BB19                                                                       00003060
 5.7E-4  0.0      5.493E-6  0.0     0.0                                    00003070
 0.0     0.0      0.9       0.75    0.0                                    00003072
 0.887   0.0355   0.0063    0.0     0.0712                                 00003074
 0.0     0.0                                                               00003080
/                                                                          00003081
/  ****                     ****                                          00003082
BB21                                                                       00003090
2  2  5.00E7    6.96E-08  2.87E4   2.86E-03  1.15E0  1.528E0               00003100
      1.49E-07  2.0E-08  1.25E-16  1.85E-01  8.0E09  3.3E-03               00003110
/                                                                          00003111
/  **** OTHER DATA ****                                                    00003112
BB22                                                                       00003120
   0. 1.4  1.4  0.                                                         00003130
BEND                                                                       00003140
5                                                                          00003150
  0  0     0  0  0  0.                                                    00003160
  0. 1.E-5 0. 0. 0. 0.                                                    00003170
END                                                                        00003180
```

Appendix B Nomenclature

Nomenclature

Alphabetic Symbols

A	Refers to flow area (m^2)
A_k	Refers to heat transfer area (m^2)
a	Refers to normalized pump speed (-)
a^*	Refers to quantity defined in Subsec 4.2 (-)
c_d	Refers to orifice flow coefficient (=0.61)
c_p	Refers to isobaric specific heat (kcal/kg.c)
G	Refers to mass flux ($kg/m^2.s$)
G_c	Refers to critical flow ($kg/m^2.s$)
G_{min}	Refers to minimum mass flux of forced convection condition (=273 $kg/m^2.s$)
g	Refers to gravitational acceleration (m/s^2)
h_{tc}	Refers to heat transfer coefficient ($kcal/m^2.s.c$)
k	Refers to loss coefficient (-)
P	Refers to pressure (Pa)
P_t	Refers to pressure defined by Eq. 4.2.2 (Pa)
P_{ref}	Refers to reference pressure (Pa)
ΔP	Refers to pressure difference (Pa)
r_1	Refers to quantity defined by Eq. 4.6.1 (m^{-1})
r_2	Refers to quantity defined by Eq. 4.6.1 (-)
Re	Refers to Reynolds number (-)
T	Refers to temperature (c)
$T_{coolant}$	Refers to coolant temperature (c)
T_{sat}	Refers to saturation temperature (c)
T_{wall}	Refers to wall temperature (c)
ΔT_s	Refers to wall superheat (c)
ΔT_{min}	Refers to minimum film boiling wall superheat (c)
Q^*	Refers to heat input to coolant per unit volume ($kcal.m^3.s$)
t	Refers to current time (s)
Δt	Refers to time step width (s)
V	Refers to volume (m^3)
v_{gj}	Refers to drift velocity (m/s)
x	Refers to coolant quality (-)
x_c	Refers to critical quality (=0.01)

Greek Symbols

τ_b	Refers to quantity defined by Eq. 4.2.2 (-)
τ_{pump}	Refers to time constant for pump coastdown (s)
ϕ	Refers to heat flux ($kal/m^2.s.c$)
ϕ_{CHF}	Refers to critical heat flux ($kal/m^2.s.c$)
ϕ_{4-1}	Refers to heat flux calculated by mode 4-1 ($kal/m^2.s.c$)
ϕ_{4-2}	Refers to heat flux calculated by mode 4-2 ($kal/m^2.s.c$)
ρ	Refers to density (kg/m^3)
σ	Refers to surface tension (kg/s^2)

Subscript

ACC	Refers to accumulator
b	Refers to break
fs	Refers to saturated fluid
gs	Refers to saturated steam
n	Refers to node number
o	Refers to orifice
trip	Refers to trip action

Superscript

A	Refers to point A of node
E	Refers to point E of node
f	Refers to forward flow
k	Refers to structure
r	Refers to reverse flow